OKLAHOMA TRANSPORTATION CENTER

ECONOMIC ENHANCEMENT THROUGH INFRASTRUCTURE STEWARDSHIP

INFLUENCE OF BACKFILL MOISTURE CONTENT ON THE PULLOUT CAPACITY OF GEOTEXTILE REINFORCEMENT IN MSE WALLS

KIANOOSH HATAMI, PH.D., P.ENG., M.ASCE
GERALD A. MILLER, PH.D., P.E.
JAIME E. GRANADOS, M.SC.

OTCREOS10.1-18-F

Oklahoma Transportation Center
2601 Liberty Parkway, Suite 110
Midwest City, Oklahoma 73110

Phone: 405.732.6580
Fax: 405.732.6586
www.oktc.org

DISCLAIMER

TECHNICAL REPORT DOCUMENTATION PAGE

1. REPORT NO. OTCREOS10.1-18-F	2. GOVERNMENT ACCESSION NO.	3. RECIPIENTS CATALOG NO.
4. TITLE AND SUBTITLE Influence of Backfill Moisture Content on the Pullout Capacity of Geotextile Reinforcement in MSE Walls		5. REPORT DATE December 31, 2012 6. PERFORMING ORGANIZATION CODE
7. AUTHOR(S) Kianoosh Hatami, Gerald A. Miller and Jaime E. Granados		8. PERFORMING ORGANIZATION REPORT
9. PERFORMING ORGANIZATION NAME AND ADDRESS The University of Oklahoma School of Civil Engineering and Environmental Science Norman, OK 73019		10. WORK UNIT NO. 11. CONTRACT OR GRANT NO. DTRT06-G-0016
12. SPONSORING AGENCY NAME AND ADDRESS Oklahoma Transportation Center (Fiscal) 201 ATRC Stillwater, OK 74078 (Technical) 2601 Liberty Parkway, Suite 110 Midwest City, OK 73110		13. TYPE OF REPORT AND PERIOD COVERED Final October 2010 – September 2012 14. SPONSORING AGENCY CODE
15. SUPPLEMENTARY NOTES University Transportation Center		

16. ABSTRACT

Sources of high-quality soils to meet design standards for the construction of reinforced soil structures are in many cases rare and in short supply. An economical alternative to coarse-grained, free-draining soils consists of using locally available soils of marginal quality (e.g. those containing more than 15% fines). Although this may lead to significant savings, detailed studies are necessary to assess the performance of these materials, including soil-reinforcement interaction. The pullout capacity of the geotextile reinforcement is a main concern in the internal stability analysis of reinforced soil structures constructed with marginal soils. Precipitation, ground water infiltration and seasonal variations of moisture content over the service life of the structure or during its construction process may lead to significant changes in the fill moisture content. The resulting loss in the soil matric suction can reduce the soil-reinforcement interface strength, which could result in unacceptable deformations or even failure of the structure.

In this study, multi-scale pullout tests were carried out to evaluate the pullout resistance of a geotextile reinforcement material in a selected marginal soil. The soil was selected to meet the limiting requirements of the National Concrete Masonry Association (NCMA) guidelines for the construction of segmental retaining walls with respect to the fines content, gradation and plasticity. The soil in different tests was compacted at different moisture contents that included dry and wet sides of the soil Optimum Moisture Content (OMC). The matric suction in each test was measured in order to evaluate its influence on the soil-reinforcement interaction. In addition to pullout resistance, the soil shear strength and soil-geotextile interface strength were evaluated to determine their variation with the soil moisture content. Moisture Reduction Factors (MRF) were calculated to account for the reduction in the reinforcement pullout resistance as a result of the loss in the soil matric suction.

17. KEY WORDS Pullout capacity, marginal soils, soil-geotextile interface strength, unsaturated soils	18. DISTRIBUTION STATEMENT No restrictions. This publication available at www.oktc.org and from the NTIS.		
19. SECURITY CLASSIF. (OF THIS REPORT) Unclassified	20. SECURITY CLASSIF. (OF THIS PAGE) Unclassified	21. NO. OF PAGES 144 + covers	22. PRICE N/A

SI (METRIC) CONVERSION FACTORS

Approximate Conversions to SI Units

Symbol	When you know	Multiply by	To Find	Symbol
		LENGTH		
in	inches	25.40	millimeters	mm
ft	feet	0.3048	meters	m
yd	yards	0.9144	meters	m
mi	miles	1.609	kilometers	km
		AREA		
in^2	square inches	645.2	square millimeters	mm
ft^2	square feet	0.0929	square meters	m^2
yd^2	square yards	0.8361	square meters	m^2
ac	acres	0.4047	hectares	ha
mi^2	square miles	2.590	square kilometers	km^2
		VOLUME		
fl oz	fluid ounces	29.57	milliliters	mL
gal	gallons	3.785	liters	L
ft^3	cubic feet	0.0283	cubic meters	m^3
yd^3	cubic yards	0.7645	cubic meters	m^3
		MASS		
oz	ounces	28.35	grams	g
lb	pounds	0.4536	kilograms	kg
T	short tons (2000 lb)	0.907	megagrams	Mg
		TEMPERATURE (exact)		
°F	degrees Fahrenheit	(°F-32)/1.8	degrees Celsius	°C
		FORCE and PRESSURE or STRESS		
lbf	poundforce	4.448	Newtons	N
lbf/in^2	poundforce per square inch	6.895	kilopascals	kPa

Approximate Conversions from SI Units

Symbol	When you know	Multiply by	To Find	Symbol
		LENGTH		
mm	millimeters	0.0394	inches	in
m	meters	3.281	feet	ft
m	meters	1.094	yards	yd
km	kilometers	0.6214	miles	mi
		AREA		
mm^2	square millimeters	0.00155	square inches	in^2
m^2	square meters	10.764	square feet	ft^2
m^2	square meters	1.196	square yards	yd^2
ha	hectares	2.471	acres	ac
km^2	square kilometers	0.3861	square miles	mi^2
		VOLUME		
mL	milliliters	0.0338	fluid ounces	fl oz
L	liters	0.2642	gallons	gal
m^3	cubic meters	35.315	cubic feet	ft^3
m^3	cubic meters	1.308	cubic yards	yd^3
		MASS		
g	grams	0.0353	ounces	oz
kg	kilograms	2.205	pounds	lb
Mg	megagrams	1.1023	short tons (2000 lb)	T
		TEMPERATURE (exact)		
°C	degrees Celsius	9/5+32	degrees Fahrenheit	°F
		FORCE and PRESSURE or STRESS		
N	Newtons	0.2248	poundforce	lbf
kPa	kilopascals	0.1450	poundforce per square inch	lbf/in^2

ACKNOWLEDGMENTS

The authors would like to acknowledge the funding and support from the Oklahoma Department of Transportation (ODOT), the Oklahoma Transportation Center (OkTC) and TenCate Geosynthetics for the study reported in this paper. Contributions of Mr. Michael Schmitz at the Fears Structural Laboratory, graduate students: Danial Esmaili and Yewei Zheng, and undergraduate students: Brandi Dittrich, Carl Walkup, Carlos Chang, Evan Burns, Christopher Barclay, Thai Dinh, Max Newton, Juan Pereira, Adam Burke, Nick Ibarguen and Jesse Berdis in this project are also acknowledged.

INFLUENCE OF BACKFILL MOISTURE CONTENT ON THE PULLOUT CAPACITY OF GEOTEXTILE REINFORCEMENT IN MSE WALLS

FINAL REPORT

OTCREOS10.1-18

November 2012

Submitted to:

Oklahoma Transportation Center
2601 Liberty Parkway, Suite 110
Midwest City, Oklahoma 73110

Submitted by:

Kianoosh Hatami, Gerarld A. Miller and Jaime E. Granados
School of Civil Engineering and Environmental Science
The University of Oklahoma
202 W. Boyd St., Room 334
Norman, OK 73019

TABLE OF CONTENTS

LIST OF TABLES

LIST OF FIGURES

EXECUTIVE SUMMARY

The objective of this study was to evaluate the effect of moisture content and matric suction on the reinforcement pullout resistance and soil-reinforcement interface shear strength in Mechanically Stabilized Earth (MSE) walls constructed with marginal quality soils.

The study involved a multi-scale testing program that included large-scale pullout tests, small-scale pullout tests, small-scale interface shear tests, direct shear tests and triaxial tests. The pullout response and interface shear strength of a woven geotextile in a marginal soil were evaluated over a range of moisture contents that included both the dry and wet sides of the soil Optimum Moisture Content (OMC) and overburden pressures that varied between 10 kPa and 50 kPa. In all these tests, the soil matric suction was either directly measured using different sensors or determined using the soil gravitational water content (GWC) and the soil water characteristic curve (SWCC).

The marginal soil used in the study was prepared using a blend of an Oklahoma natural soil and sand to meet the limiting National Concrete Masonry Association requirements for the backfill of Segmental Retaining Walls (NCMA 2002).

A series of Moisture Reduction Factors (MRFs) was determined to account for the loss of matric suction as a result of an increase in the soil moisture content. The MRFs were calculated based on the measured suction in the soil compacted at OMC-2%, as a recommended GWC value for the compaction of reinforced soil structures.

Results of the study indicate that the shear strength of the soil and the soil-reinforcement interface can be significantly reduced as a result of an increase in the GWC of the backfill. The pullout capacity of the reinforcement in large-scale tests was approximately 37% lower when the soil was compacted at OMC+2% as compared to that for the soil compacted at OMC-2%. The amount of this reduction was approximately 47% in small-scale pullout tests. The corresponding differences in the shear strength of the soil and that of the soil-geotextile interface were 32% and 23%, respectively.

These results indicate that for soils with significant fines content which meet the NCMA design requirements, the reduction in the reinforcement pullout capacity and the soil-reinforcement interface shear strength as a result of an increase in the moisture content could be significant and needs to be considered in design. The moisture reduction factors calculated in this study demonstrate the magnitude of reduction that could be expected in similar backfill and reinforcement materials for their interface shear strength and pullout capacity in the internal stability analysis and design of MSE walls. It is also concluded that Small-scale pullout tests hold promise as a faster and more economical alternative to the large-scale tests to help determine coefficients of interaction for geotextiles and marginal quality soils. However, further research is underway to better understand the extent of scale effects and boundary conditions in the corresponding test results.

1. INTRODUCTION

1.1 Background

The advent of the modern reinforced soil technology is commonly attributed to the French engineer and architect, Henri Vidal in 1966. However, it was only after 1972 that the Federal Highway Administration (FHWA) brought Vidal's technology to solve landslide problems in the United States (Anderson and Brabandt 2005). The success of this technology motivated its rapid growth and the generic name Mechanically Stabilized Earth (MSE) was coined. Reinforced soil structures such as MSE walls have been increasingly used as retaining structures during the last decades. MSE technology is used for highway, industrial, military, forestry, commercial and residential applications.

MSE walls have been constructed to retain fills of significant height and to support vertical and lateral loads as cost-effective structures. Due to their inherent structural flexibility, properly designed MSE walls can tolerate differential settlements in difficult foundation soil conditions better than their conventional counterparts and have demonstrated good seismic performance (Berg et al. 2009). Among other advantages, the equipment used is commonly available, site preparation is often not as extensive, construction time is relatively short and these structures blend well with the environment. Due to these advantages, reinforced soil walls are desirable cost-effective alternatives to conventional retaining structures such as traditional gravity and reinforced concrete retaining walls. **Figure 1** shows the aesthetic design of an MSE wall constructed with concrete panel system by the Oklahoma Department of Transportation (ODOT) in Oklahoma City, OK.

Figure 1. Concrete panel system MSE wall, ODOT I-40 Crosstown on Western Avenue, Oklahoma City, OK (Courtesy of The Reinforced Earth Company, 2012)

1.2 Problem Statement

A key factor in the construction of reinforced soil structures is the quality of the backfill material. Coarse-grained, free-draining soils are preferred over marginal quality soils (i.e. soils that have significant fines content) due to the high shear strength, hydraulic conductivity and that they are fairly easy to place and compact. However, in Oklahoma and many other places across the United States, sources of high-quality soils for the construction of MSE walls are relatively scarce. A viable solution is to use soils with a sizable amount of fines.

In the public sector, soils with significant fines contents are not recommended for construction of MSE walls. Design guidelines such as the Federal Highway Administration (FHWA) and American Association of State Highway and Transportation Officials (AASHTO) recommend that the backfill for MSE walls should contain up to 15% fines and the Plasticity Index (PI) should be limited to 6 (e.g. Berg et al. 2009, AASHTO 2003). On the other hand, guidelines by the private sector (e.g. the National Concrete Masonry Association, NCMA 2002) allow up to 35 percent of fines and a PI value of up to 20. Therefore, in the discussion of backfill quality for MSE walls in this study, such soils with more than 15% fines and a PI greater than 6 are referred to as marginal soils.

Marginal quality soils have been used successfully for the construction of MSE walls as an alternative to granular materials and its use could lead to significant savings by avoiding high transportation costs (e.g. Keller 2005). However, properties of the materials and their interaction must be carefully evaluated (Berg et al. 2009).

Regarding the soil moisture content, FHWA/AASHTO and NCMA guidelines recommend that the backfill should be compacted within a range in the proximity of the soil Optimum Moisture Content (OMC). For instance, FHWA and AASHTO recommend the moisture content within a range of ±2% of the OMC. The NCMA recommends the compaction of low-quality soils within the range of -3% to +1% of the OMC. With respect to the compaction effort, the backfill unit weight is usually targeted at 95% of the maximum standard Proctor (AASHTO T-99, ASTM D698) or 90% of maximum modified Proctor values (AASHTO T-180, ASTM D1557). Compaction moisture contents dry of optimum are recommended during the construction process. However, materials for soil structures are typically tested at moisture content values near optimum.

In actual construction, several factors such as precipitation, ground water infiltration and seasonal variations of moisture content could cause the fill moisture content to deviate from the design value. These factors can measurably reduce the strength of the soil and the soil-reinforcement interface and lead to excessive deformation or failure of the earthen structure.

From the point of view of internal stability, reinforcement pullout capacity is an important factor in the design of MSE walls. Therefore, it is necessary to understand and account for the influence of moisture content on the soil-reinforcement interface shear strength, especially in the case of marginal-quality backfill soils. Due to low permeability and poor drainage of marginal soils, the loss of matric suction as a result of increase in the soil moisture content (e.g. during construction or service life) could have critical consequences for the serviceability and stability of these MSE walls.

1.3 Purpose of the Study

This research was aimed at developing a better understanding of the influence of moisture content (i.e. gravimetric water content) and matric suction on the pullout resistance and interface interaction of geotextile reinforcement for construction of MSE walls using marginal soils. This study is complementary to recently completed projects which focused on the construction of Reinforced Soil Slopes (RSS) in marginal quality soils (Hatami et al. 2010, 2011a,b).

The soil used in this study represents the most critical scenario according to the NCMA guidelines; i.e. approximately 35% fines and a PI value equal to 20. These properties represent the lowest quality soil that can still be allowed for use as backfills of MSE walls as per the NCMA guidelines, in which the influence of soil suction on the soil-reinforcement interface strength (e.g. on the reinforcement pullout capacity) would be the greatest.

1.4 Scope of the Study

The scope of this study included experimental and numerical components. The experimental phase of the study included a series of large-scale pullout tests, in addition to pullout tests, interface shear tests and direct shear tests at small scale. Furthermore, the soil suction was determined in both large-scale and small-scale soil specimens using different instruments to evaluate its influence on the soil-geotextile interface shear strength properties. The tests were carried out over a range of moisture content and overburden pressures that varied from OMC-2% to OMC+2% and from 10 kPa to 50 kPa.

A numerical model was developed to simulate the pullout response of geotextile reinforcement in the tested soil and compare its predicted performance with the measured results from the experimental phase of the study. The finite difference method (FDM)-based computer program Fast Lagrangian Analysis of Continua (FLAC, Itasca 2011) was used to develop the numerical model. Soil elastic parameters were obtained from direct shear and triaxial tests on saturated and unsaturated samples.

1.5 Objectives of the Study

The primary objective of this study was to determine the influence of moisture content on the pullout resistance of geotextile reinforcement in MSE walls constructed using marginal quality soils. A moisture reduction factor (MRF) was developed based on the experimental test results to account for the reduction in the geotextile pullout capacity at soil moisture contents greater than the as-placed value. This MRF could be included in the reinforcement pullout capacity equation found in the design guidelines (e.g. NCMA 2002, Berg et al. 2009).

The experimental program in this study included multi-scale testing of soil-geotextile interfaces with an objective to determine pullout capacity of geotextile reinforcement in marginal soils using commonly available equipment (i.e. a small-scale direct shear test apparatus). The influence of the moisture content on the soil shear strength and soil-reinforcement interface shear strength was also evaluated to determine the corresponding MRFs. The term moisture content in this study corresponds to the gravimetric water content of the soil.

This page is intentionally blank

2. THEORY

2.1 Main Failure Mechanisms of the Geotextile Reinforcement

Figure 2 shows the potential pullout (P_r) and shear (τ_S) failure mechanisms along the soil-reinforcement interface. In both cases, it is expected that moisture content variations in the vicinity of the soil-reinforcement interface affects the response of the structure. Shear and pullout failure mechanisms are described in more detail in **Section 2.1.1** and **Section 2.1.2**, respectively.

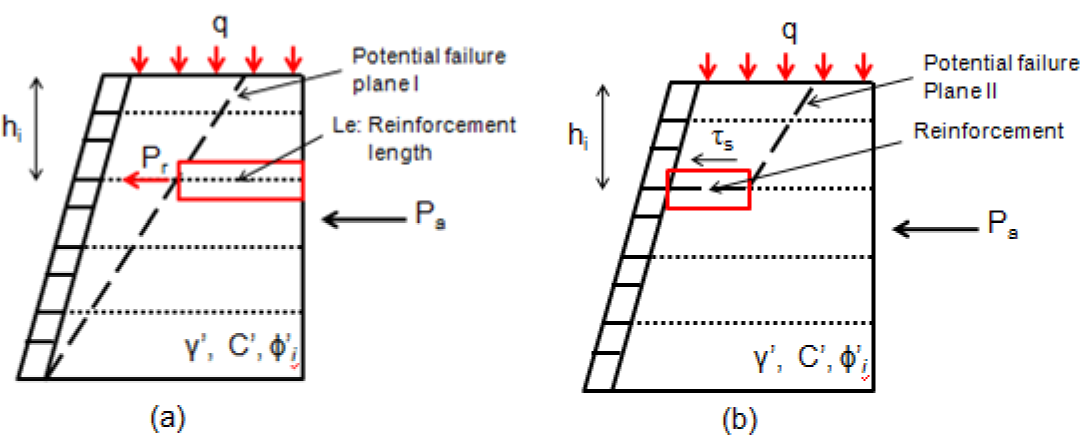

Figure 2. Potential failure mechanisms in MSE walls: (a) Pullout and (b) shear failures

2.1.1 Shear type

The shear type mechanism represents the frictional behavior of the soil-geotextile interface. The interface shear strength between soil and geotextile is developed due the horizontal movement imposed on the structure as a result of vertical and horizontal loads. The resulting soil-geotextile shear strength parameters, i.e. adhesion and interface friction angle, are obtained using a form of the Mohr-Coulomb failure criterion (**Equation** 1):

$$\tau = c_a + \sigma'_n \tan\delta \qquad [1]$$

Where,

τ = shear strength (between soil and geotextile)

σ'_n = effective normal stress on the shear plane

c_a = adhesion (of the geotextile to the soil)

δ = interface friction angle (between soil and geotextile)

2.1.2 Anchorage type

The anchorage type mechanism refers to pullout movement of the reinforcement. Geotextiles are often required to develop pullout resistance for many applications within the reinforcement function. Anchorage reinforcement is similar to the shear type, but now the soil acts on both sides of the geosynthetic as a tensile force tends to pull it out from the soil. The resistance can be represented in the laboratory by means of pullout tests and is a function of the normal stress applied to the soil-interface. Shearing resistances are developed on both surfaces of the geotextile.

Some authors consider that a possible design strategy to calculate the geosynthetic pullout capacity is to take interface shear test results for both sides of the reinforcement and use these values for pullout design purposes. **Equation** 2, as presented by Koerner (2005), is the basic form of the equation to determine the pullout capacity of geosynthetics. **Equation** 2 is also used by the NMCA (2002) guidelines to define the pullout capacity of geosynthetics.

$$P_r = 2C_i L_e \sigma'_n \tan\phi' \qquad [2]$$

Where,

P_r = pullout capacity per unit width (kN/m)

C_i = interaction coefficient (dimensionless, obtained from experimental data)

L_e = geosynthetic embedment length (m)

σ'_n = effective normal stress on the geosynthetic (kPa)

ϕ' = effective soil friction angle (degrees)

Recent studies (e.g. Berg et al. 2009) have shown that the use of this equation by itself is not a conservative practice and soil-reinforcement interface parameters need to be addressed. In all cases, pullout test resistances are less than the sum of the interface shear test resistances. This is due to the large (and non-linear) deformation of the geotextile under pullout loads, which in turn induces the soil particles to reorient themselves into a reduced shear strength mode. Koerner (2005) points out the complexity of the stress state mobilized in this mechanism and the large number of technical references on this topic.

2.2 Unsaturated Soils

Soil (apart from conditions involving frozen soils and presence of contaminants) is considered a three-phase porous medium comprised of solid grains, water and air (**Figure 3**). In traditional soil mechanics, the soil is typically studied at dry or saturated conditions, ignoring the air-water interface (i.e. contractile skin) generated in unsaturated conditions. The most distinctive property of the contractile skin is its ability to exert a tensile pull, which behaves like an elastic membrane under tension interwoven throughout the soil structure (Fredlund and Rahardo, 1993). Soil suction depends primarily on the soil type, density and water content. The understanding of soil suction and its effect on the soil strength is studied within the unsaturated branch of soil mechanics.

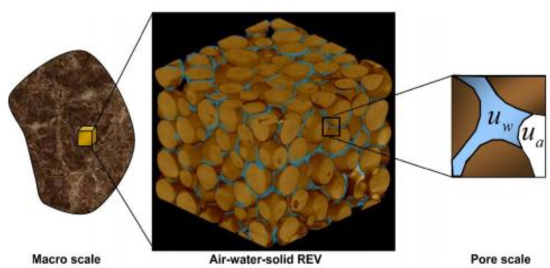

Figure 3. Soil as a three-phase porous medium (After Razavi 2008)

The effect of suction in high-quality, coarse-grained soils is usually negligible. However, it can be very significant in marginal soils. This in turn affects the internal stability of MSE structures because soil-reinforcement interaction could be affected by the soil suction.

Soil matric suction is defined as the difference between the air pressure and pore water pressure (u_a-u_w) within the soil and is a function of the moisture content. As the moisture content increases, the matric suction decreases as shown using the Soil Water Characteristic Curve (SWCC) in **Figure 4**.

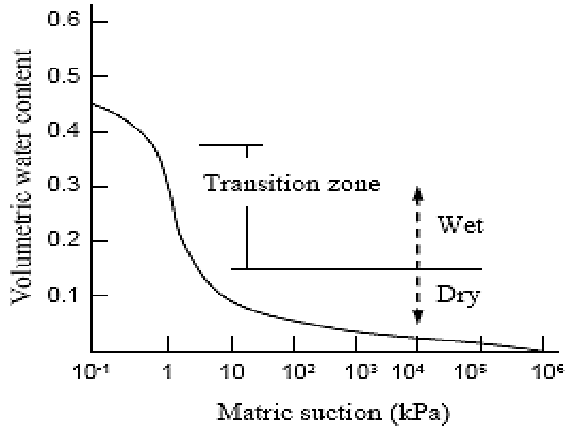

Figure 4. Example of Soil Water Characteristic Curve (After Zollinger et al. 2008)

Fredlund et al. (1978) proposed an expression to represent the shear strength of unsaturated soils as a function of the net normal stress (i.e. the difference between the total stress and the pore air pressure, σ_n - u_a) and the soil matric suction (i.e. the difference between the pore air and pore water pressures, u_a - u_w). Based on this approach, Miller and Hamid (2005) proposed the following **Equation** 3 to determine the shear strength of unsaturated soil-structure interfaces:

$$\tau_{ff} = C_a' + (\sigma_f - u_a)_f \tan\delta' + (u_a - u_w)_f \tan\delta^b \qquad [3]$$

where,

C_a' = intercept adhesion of the extended Mohr-Coulomb failure envelope

$(\sigma_f - u_a)_f$ = net normal stress state on the failure plane

u_{af} and u_{wf} = pore-air and pore water pressure on the failure plane, respectively

δ' = angle of soil-reinforcement interface friction

$(\sigma_f - u_a)_f = \psi$ = matric suction on the failure plane

δ^b = angle indicating the rate of increase in interface shear strength relative to the matric suction

The effect of the soil matric suction on the soil shear strength is accounted for in the analysis by extending the Mohr-Coulomb envelope to a 3-dimensional plane, called the extended Mohr-Coulomb envelope (**Figure 5**).

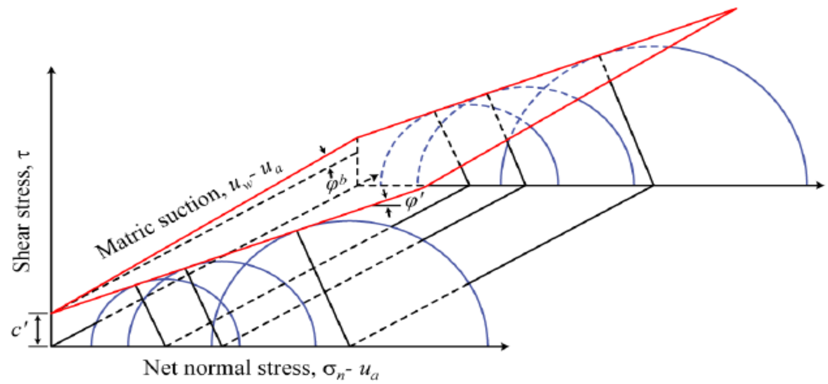

Figure 5. Extended Mohr-Coulomb envelope for unsaturated soils (from Hatami et al. 2010)

2.3 Pullout Capacity Equation for the Reinforcement

The pullout resistance of the reinforcement is defined as the ultimate tensile load required to generate outward sliding of the reinforcement through the reinforced soil zone. Several approaches and design equations have been developed and are currently used to estimate the pullout resistance by considering frictional resistance, passive resistance, or a combination of both. The design equations use different interaction parameters. Therefore, it is sometimes difficult to compare the pullout performance of different reinforcement materials for a specific application. For design and comparison purposes, a normalized definition of pullout resistance has been developed which is promoted by the FHWA (e.g. Berg et al. 2009). The pullout resistance, P_r, at each of the reinforcement levels per unit width of the reinforcement is given by **Equation** 4.

$$P_r = F^* \alpha\, \sigma'_v\, L_e\, C \qquad [4]$$

Where:

F* = the pullout resistance (or friction-bearing-interaction) factor

α = a scale correction factor to account for a nonlinear stress reduction over the embedded length of highly extensible reinforcements. Based on laboratory data, α is 1.0 for non-extensible reinforcements and in between 0.6 to 1.0 for geosynthetic reinforcements.

σ'_v = the effective vertical stress at the soil-reinforcement interfaces

L_e = the embedment or adherence length in the resisting zone behind the failure surface

C = the reinforcement effective unit perimeter, C = 2 for strips and grids

L_eC = the total surface area per unit width of the reinforcement in the resistive zone behind the failure surface

The deformation of the reinforcement within the soil in pullout tests is used to determine the pullout resistance factor (F*) and the scale correction factor (α) in **Equation** 4. The factor F* is calculated as the slope of the P_r – σ_v*L_p curve (**Figure 6**). However, it can also be estimated from empirical procedures or from Interface Shear Tests (IST). The α factor can only be calculated as the normalized pullout resistance factor from pullout tests as shown in **Figure 7**. A recommended value for α for geotextiles is 0.6.

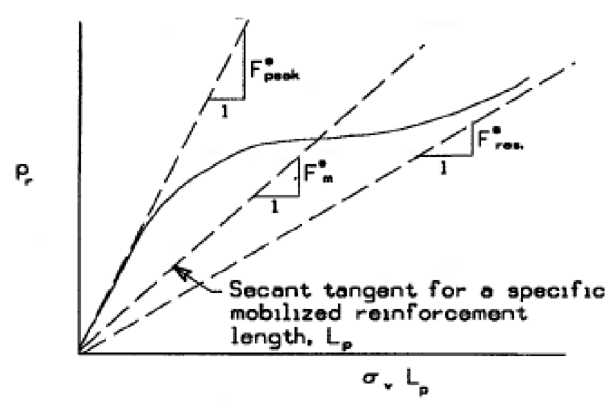

Figure 6. P_r - σ_v*L_p curve (Berg et al. 2009)

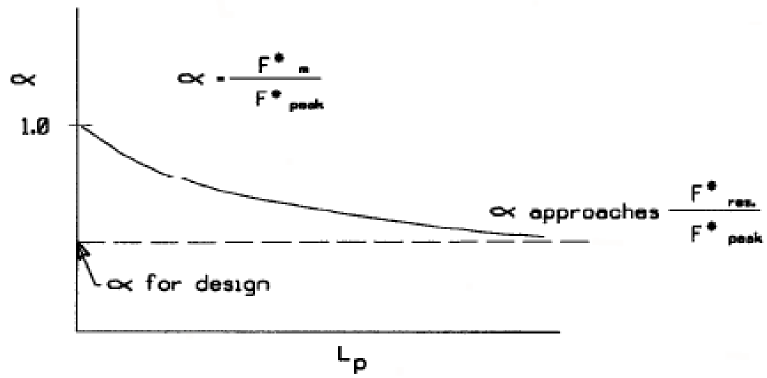

Figure 7. Determination of factor α (Berg et al. 2009)

The pullout resistance is the greater of the peak pullout resistance value prior to, or the value achieved at, a maximum deformation of 5/8 in (15 mm) as measured at the end of the embedded sample for extensible reinforcements. This allowable deflection criterion is based on a need to limit the structure deformations, which are necessary to develop sufficient pullout capacity. For geosynthetic (i.e., geogrid and geotextile) sheet reinforcement, an Interaction Factor, C_i is used as a reduction factor to characterize the pullout resistance in terms of the reduction in the available soil friction. In the absence of test data, the F* value for geosynthetic reinforcement could conservatively be assumed as $F^* = 2/3 \tan\phi$, in which ϕ is the peak friction angle of the soil. For MSE walls constructed with granular backfills, the friction angle of the soil is typically taken as a maximum value of 34° unless project-specific test data indicate higher values.

Pullout test results, as performed following the ASTM D6706 guidelines, provide short-term pullout capacity but does not account for soil or reinforcement creep deformations, which can be significant when using marginal quality soils.

This page is intentionally blank

3. EXPERIMENTAL WORK

3.1 Materials

3.1.1 Soil Properties

As mentioned in the previous sections, the guidelines by the public sector (e.g. Berg et al. 2008 and AASHTO 2003) recommend that soils used as backfill for the construction of MSE walls should contain no more than 15% of fine-grained particles and the PI should not exceed 6. The private sector (e.g. NCMA) is less conservative and allows the use of marginal soils with up to 35% fine-grained particles and PI values up to 20. A soil with the latter properties represents the most critical case for the construction of MSE walls. Therefore, these soil properties were used as target values in this testing program. Two important criteria related to the soil gradation include that the content of fines, i.e. percent of soil passing the #200 sieve, is limited to 35% and the percent of soil passing the sieve #40 is limited to 60% as per gradation shown in **Table 1**.

Table 1. Particle size gradation recommended by NCMA (2002) for construction of Segmental Retaining Walls (SRW)

U.S. Sieve	Size (mm)	Percent of Soil Passing
4 in	101.6	100 - 75
No. 4	4.750	100 - 20
No. 40	0.425	0 - 60
No. 200	0.075	0 - 35

During the first stage of the project, several attempts were made to locate sources of suitable soils near Norman, OK. Soil samples from several candidate sites were identified using the Web Soil Survey (WSS) online utility, available through the Natural Resources Conservation Service website (NRCS 2010). The WSS provides soil data for more than 95% of the counties in the United States including maps, suitability and limitation of use, soil quality and properties and soil reports. The selected samples were tested for their properties but none of them completely satisfied the above requirements of gradation and plasticity. Consequently, it was decided to blend different soil types to obtain the target fill material for the pullout tests near the most critical conditions of gradation and PI. A high-plasticity fine soil and a commercially available sand were candidates for this purpose. The final soil would be a blend made of the natural Renfrow-Huska Complex soil and two commercial medium and coarse Quikrete sands.

3.1.1.1 Soil classification

Samples of the clay soil identified as Renfrow-Huska Complex on the Web Soil Survey (WSS) were obtained from Northern Cleveland County, near Stanley Draper Lake, in vicinity of Moore, OK. **Figure 8** and **Figure 9** show the soil location and the excavation pit along a county road, respectively.

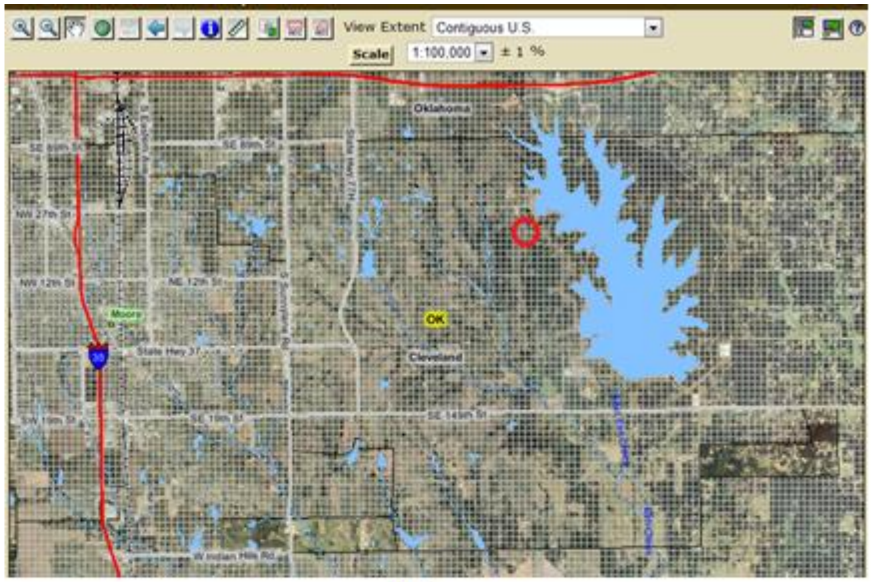

(a)

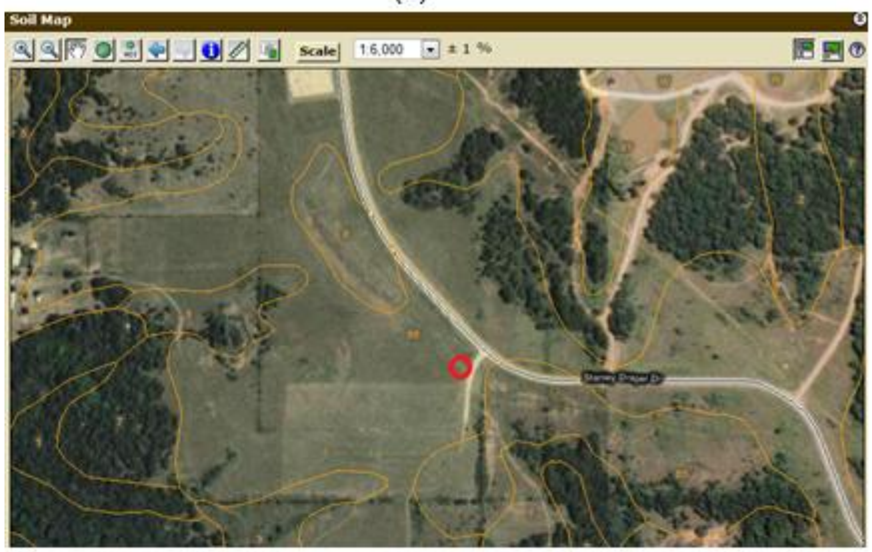

(b)

Figure 8. Location of the Renfrow-Huska soil: (a) overall geographic location and (b) location of the sampling site

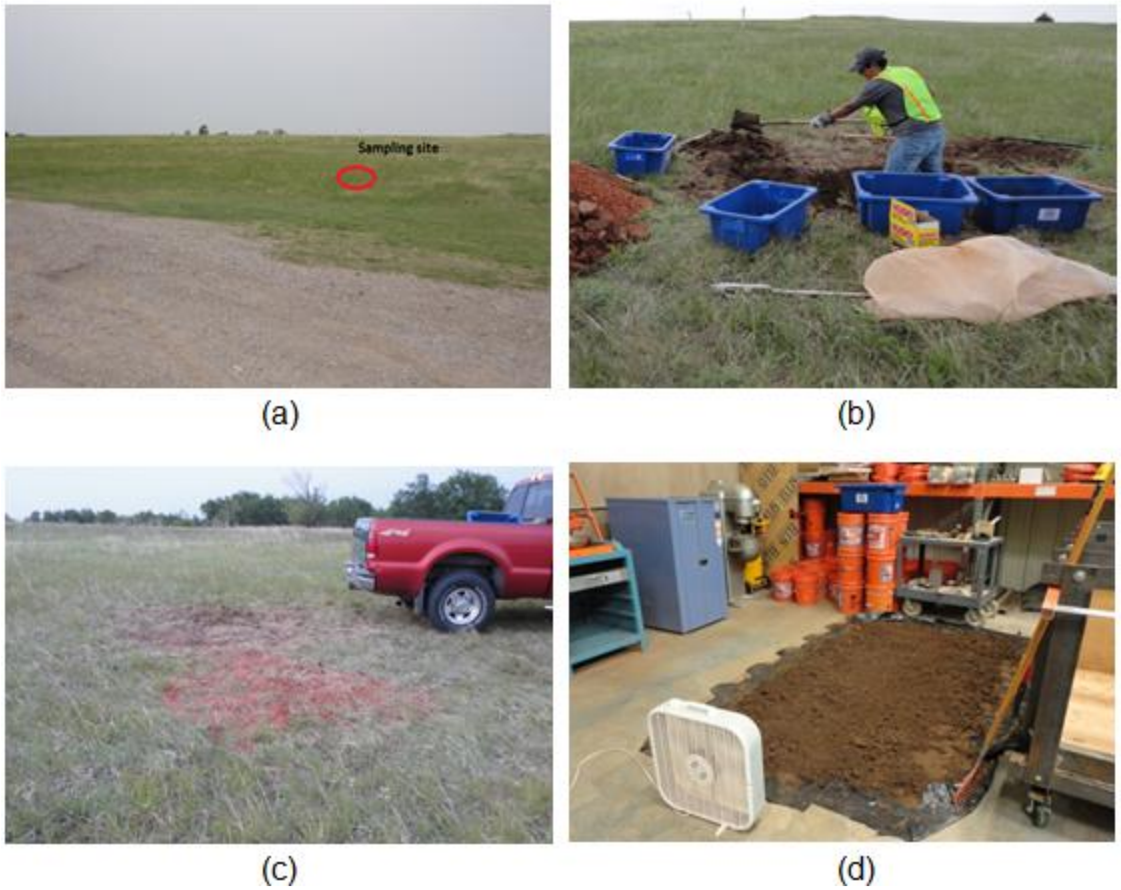

Figure 9. Renfrow-Huska Complex soil: (a) sampling site, (b) excavation pit, (c) site after digging and filling and (d) air-dried process of the soil at Fears Laboratory

Two sizes of the Quikrete commercial grade sand, i.e. medium sand (No. 1962) and coarse sand (No. 1961), which is a high quality silica material, were tested to obtain their gradation. The higher content of the coarse and medium size grains in the sand was desirable to meet the NCMA gradation and the high plasticity of the selected clay would keep the PI value of the blended soil near the limiting and hence, target value of 20. Several tests and trials were needed to achieve the desirable properties and finalized the soil characterization. Soil classification and physical properties of the different soils were carried out following the ASTM test protocols as per required.

3.1.1.2 Sieve analysis and hydrometer tests

Particle size distributions of the soils were obtained by passing air-dried samples through a series of sieves with standard openings as recommended by the ASTM D 422. **Figure 10** shows the sieves and shaker used to determine the gradation of soil particles coarser than the #200 sieve (0.075 mm).

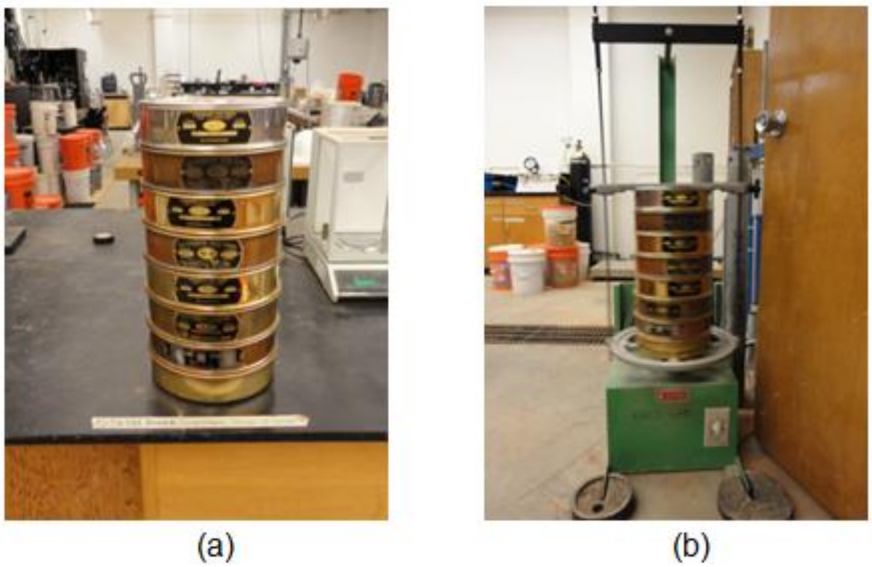

Figure 10. Sieve analysis: (a) ASTM sieves and (b) shaker at the OU Soils Laboratory

Additionally, hydrometer tests were performed on the Renfrow-Huska Complex soil and the final blend. A small amount (approximately 55 g for clays and silts and 115 g for the final clayey sand) of air-dried soil finer than the #10 sieve was selected for the tests. The soil was allowed to soak in 225 mL of a sodium hexametaphosphate solution (40 g/L) for a period of 16 hours and then moved to a sedimentation cylinder where readings were taken with a calibrated hydrometer during 24 hours. The Stockes' Law relating the density and rate of sedimentation of the particles was used to calculate the size and percent of particles in the sample. **Figure 11a** shows the glass cylinders containing three samples of Renfrow-Huska Complex soil (one for each sampling depth) and one sample of the final blend. A cylinder with clean water was used to rinse the hydrometer and another cylinder containing sodium hexametaphosphate solution was used as control to calculate the rate of sedimentation as per the ASTM D422 test protocol (**Figure 11b**). The sieve analysis and hydrometer results carried out on the

Renfrow-Huska Complex soil and the final blend were combined to determine the complete gradation curves for each soil.

(a) (b)

Figure 11. Hydrometer tests: (a) Renfrow-Huska Complex soil and final OUM-NCMA blend (b) rinse and control cylinders with thermometer

Figure 12 shows the gradation curves for the two types of sand tested. For the medium sand, the maximum percentage of particles passing the #40 and #200 sieves were 44% and 0.5%, respectively. The medium sand was classified as poorly graded (SP) with a coefficient of uniformity, C_u = 2.19, and a coefficient of curvature, C_c = 0.83. For the coarse sand, the maximum percentage of particles passing the #40 and #200 sieves were calculated as 0.7% and 0.1%, respectively. The coarse sand was classified as poorly graded (SP) as well. Its coefficient of uniformity was, C_u = 2.64, and the coefficient of curvature, C_c = 0.97. The gradation curves show the percent of soil passing (i.e. finer) selected sieve numbers. The dashed lines indicate important sizes relevant to the NCMA requirements (i.e. #4, #40, and #200 sieves).

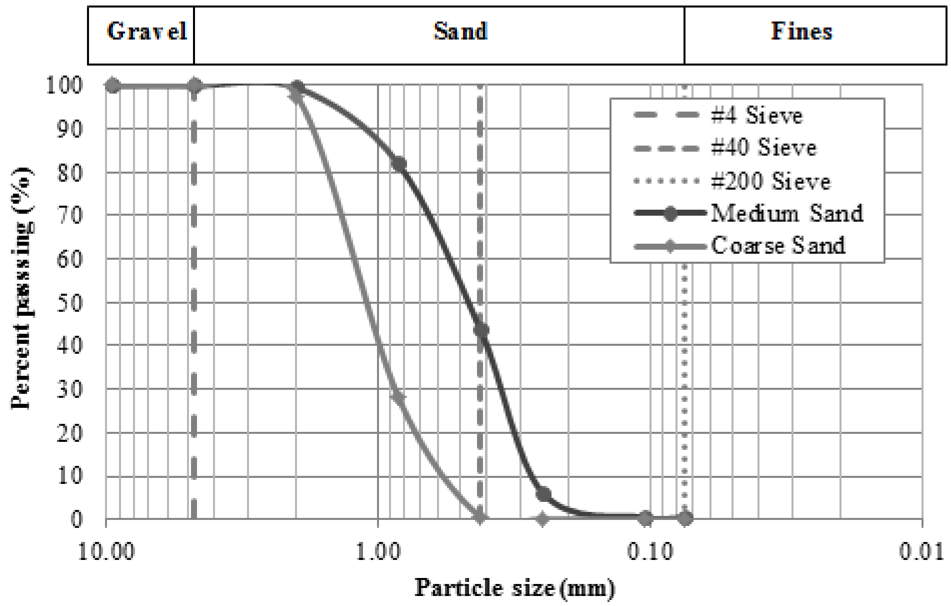

Figure 12. Gradation of the commercial medium and coarse Quikrete sand

The percentage of soil passing the #200 sieve, for the Renfrow-Huska Complex Soil, was approximately 95%. This result was consistent with the WSS data available for the borrow site. Sieve analysis and hydrometer test data for the three depths sampled at the borrow site are plotted in **Figure 13**.

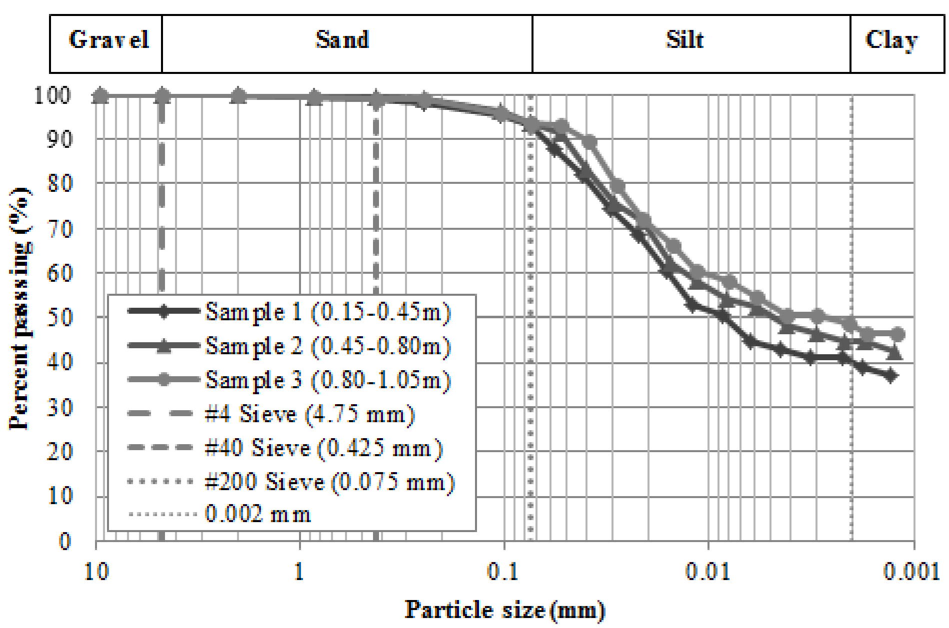

Figure 13. Soil gradation and hydrometer analysis of the Renfrow-Huska Complex soil

3.1.1.3 Atterberg limits

Atterberg Limits were carried out as per the ASTM D4318 test protocol (**Figure 14**). Liquid Limit (LL), Plastic Limit (PL), Plasticity Index (PI) and Shrinkage Limit (SL) were determined for the Renfrow-Huska Complex soil and the final blend. Atterberg limits were performed on the fraction of soil passing the #40 sieve on soils with some plasticity. These tests are not applicable to clean sands. The mean values of LL, PL, PI and SL on the Renfrow-Huska Complex soil were calculated as 52, 23, 29 and 16, respectively.

(a) (b)

Figure 14. Atterberg limits: (a) soil finer than #40 sieve and Casagrande´s cup used to determine the Liquid Limit (LL) and (b) Shrinkage Limit (SL) on three Renfrow-Huska Complex soil samples - left to right - and one OUM-NCMA soil sample

3.1.1.4 Final properties of the soil

The final soil blend used in this study was called the OUM-NCMA marginal soil. Several attempts were necessary to determine the final proportions of the fine soil (Renfrow-Huska Complex) and the sands in the OUM-NCMA blend. The percent of each soil type in the final blend is given in **Table 2**.

Table 2. Final OUM-NCMA blend ratios (by weight)

Soil Type	Percentage (%)
Renfrow-Huska Complex Soil	35
Medium Quikrete Sand	35
Coarse Quikrete Sand	30

As expected, the Atterberg limits of the Renfrow-Huska Complex soil decreased by blending it with the clean sand. The Atterberg limits of the OUM-NCMA marginal soil, i.e. LL, PL, PI and SL, were calculated as 36, 16, 20 and 9, respectively. **Figure 15** shows the sieve analysis and hydrometer test results of the soil. The mean PI value for this blend was 20. The percentages of soil passing the #40 and #200 sieves were calculated as 49% and 33%, respectively. Particle sizes pertaining to the NCMA required gradation, i.e. 4.75 mm (#4), 0.425 mm (#40) and 0.075 mm (#200), are shown as black squares in **Figure 15**.

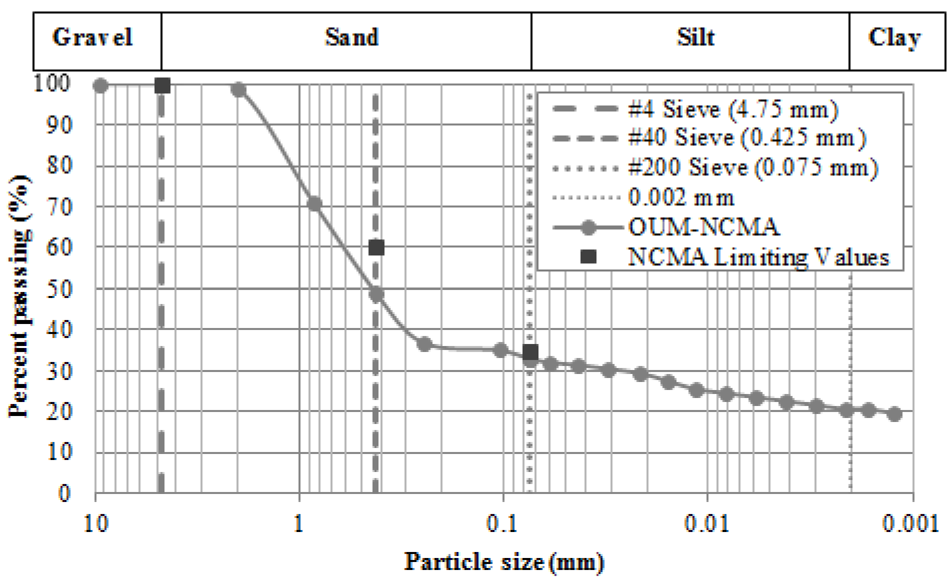

Figure 15. Gradation of the OUM-NCMA soil

The Optimum Moisture Content (OMC) and Maximum Dry Unit Weight ($\gamma_{s\text{-}max}$) of the OUM-NCMA soil were calculated as 12.6% and 18.74 kN/m^3 (119 lbf/ft^3), based on the standard Proctor test as per the ASTM D 698 test protocol. **Figure 16** shows the moisture-density relation curve of the soil. **Table 3** summarizes the properties of each ingredient soil, those of the final blend and the corresponding NCMA requirements.

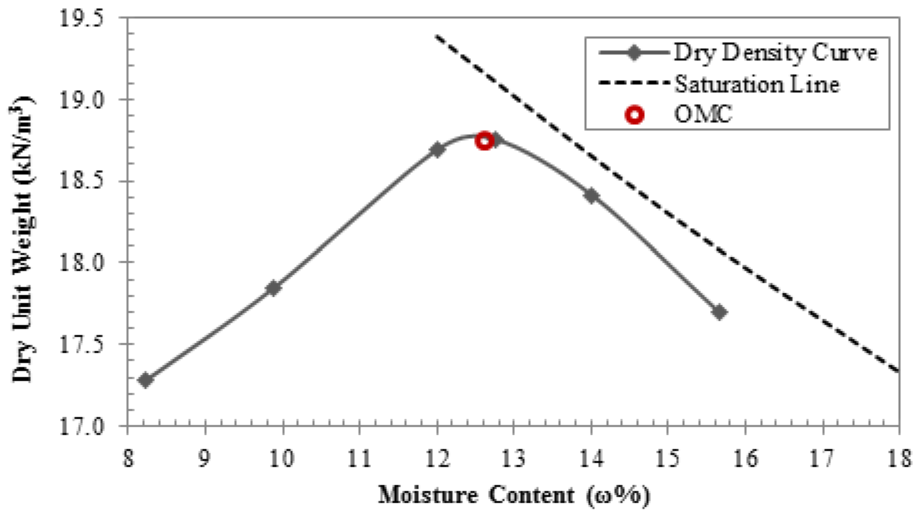

Figure 16. Standard Proctor curve of the OUM-NCMA soil

Table 3. Final soil properties of the OUM-NCMA soil

Soil Properties	**Ingredient Soils**			**OUM-NCMA**	**NCMA Requirements**
	Renfrow-Huska Complex	**Medium Sand**	**Coarse Sand**		
Gravel (%)	0	0	0	0	N/P
Sand (%)	6.5	99.5	99.9	67	N/P
Silt (%)	49.2	0.5	0.1	17	N/P
Clay (%)	44.3	0	0	16	N/P
Passing 4.75 mm (Sieve #4, %)	100	100	100	100	20 – 100
Passing 0.425 mm (Sieve #40, %)	99.2	0.7	44	49	0 – 60
Passing 0.075 mm (Sieve #200, %)	93.5	0.5	0.1	33	0 – 35
Coefficient of Uniformity (C_u)	N/P	2.19	2.64	N/P	N/P
Coefficient of Curvature (C_c)	N/P	0.83	0.97	N/P	N/P
Liquid Limit (LL)	52	NP	NP	36	N/P
Plastic Limit (PL)	23	NP	NP	16	N/P
Plasticity Index (PI)	29	NP	NP	20	20
Specific Gravity (G_s)	2.56	2.6	2.6	2.59	N/P
USCS classification	CH	SP	SP	SC	-
AASHTO classification	A-7-2	A-1-b	A-1-b	A-2-6	-
Optimum Moisture Content (OMC, %)	N/A	N/A	N/A	12.6	N/P
Maximum Dry Density (kN/m^3)	N/A	N/A	N/A	18.74	N/P

Note: N/A: not available; N/P: not provided, (-): depends on soil gradation and plasticity

The OUM-NCMA marginal soil met the requirements on gradation and plasticity established by the NCMA for construction of MSE walls. A total amount of approximately 1000 kg of the OUM-NCMA soil was prepared to carry out the different types of large-scale and small-scale tests in this study. All particles were finer than the #4 sieve.

3.1.2 Geotextile Properties

The reinforcement material used in this research was a TenCate Mirafi HP370 woven geotextile composed of high-tenacity polypropylene yarns. TenCate Mirafi HP series are widely used for stabilization and reinforcement applications as well as separation and filtration. **Figure 17a** shows in detail the yarn orientations in Machine (MD) and Cross-Machine Directions (XD). **Figure 17b** shows that the geotextile is subjected to MD-direction in the pullout tests.

Figure 17. Geotextile reinforcement: (a) detail of yarn orientation of the woven geotextile and (b) geotextile specimen as placed in the pullout system and clamping system

Hatami et al. (2010) evaluated the mechanical response of the geotextile as per the ASTM D4595 test protocol (ASTM 2009) and compared their results with those reported by the manufacturer. **Figure 18** indicates that both the ultimate strength and strength at 5% strain of the tested geotextile are in good agreement with the manufacturer's Minimum Average Roll Value (MARV) data. The ultimate strength in the cross machine direction (XD) was found to be 40.9 kN/m, which is 3.6 % greater than the 39.4 kN/m value in the manufacturer's data. The XD strength at 5% strain was found to be 19.7 kN/m, which is 13.3% lower than the manufacturer's value of 22.8 kN/m.

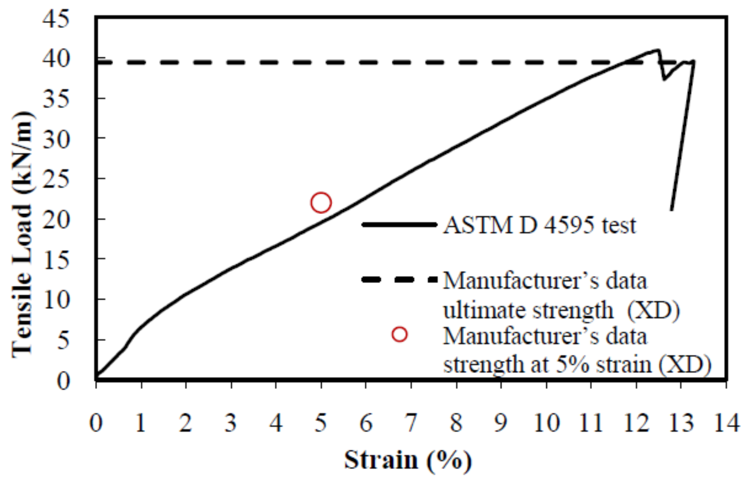

Figure 18. Mechanical response of the woven geotextile as per ASTM D4595

The Young's Modulus of the geotextile at 5% strain was determined to be 396 kN/m. **Table 4** and **Table 5** show the physical and mechanical properties of the geotextile, respectively, as obtained from the manufacture's product specifications (TenCate 2011).

Table 4. Physical properties of Mirafi HP370 geotextile (TenCate 2011)

Physical Properties	Test Method	Unit	Typical Value
Mass/Unit Area	ASTM D5261	g/m^2 (oz/yd^2)	298 (8.8)
Roll Dimensions (width x length)	--	m (ft)	4.5 (15) x 91 (300)
Roll Area	--	m^2 (yd^2)	418 (500)
Estimated Roll Weight	--	kg (lbs)	121 (266)

Table 5. Mechanical properties of Mirafi HP370 geotextile (TenCate 2011)

Mechanical Properties (Mirafi HP370)	Test Method (ASTM)	Units	Minimum Average Roll Value	
			MD	XD
Tensile Strength (ultimate)	D4595	kN/m (lbs/ft)	52.5 (3600)	39.4 (2700)
Tensile Strength (at 2% strain)	D4595	kN/m (lbs/ft)	7.9 (540)	7.9 (540)
Tensile Strength (at 5% strain)	D4595	kN/m (lbs/ft)	21.9 (1500)	22.8 (1560)
Tensile Strength (at 10% strain)	D4595	kN/m (lbs/ft)	35.0 (2400)	35.0 (2400)
Factory Seam Strength	D4884	kN/m (lbs/ft)	24.6 (1688)	24.6 (1688)
Flow Rate	D4491	$l/min/m^2$ ($gal/min/ft^2$)	1630 (40)	1630 (40)
Permeability	D4491	cm/sec	0.05	0.05
Permittivity	D4491	sec^{-1}	0.52	0.52
Apparent Opening Size (AOS)	D4751	mm (U.S. Sieve)	0.6 (30)	0.6 (30)
UV Resistance (at 500 hours)	D4355	% strength retained	80	80

3.2 Large-Scale Testing Program

Figure 19 shows the pullout box used to carry out the large-scale testing program. The pullout box is located at the Fears Laboratory in the University of Oklahoma. Its nominal dimensions are 1800 mm (L) × 900 mm (W) × 750 mm (H). The dimensions of the box and its basic components, e.g. metal sleeves at the front end, are in agreement with the ASTM D6706 test protocol (ASTM 2009). However, only half of the box length was needed to carry out the tests. The pullout load was applied to the geotextile specimen using a 90 kN high-precision servo-controlled hydraulic actuator at a constant speed during the tests. An airbag and a reaction beam assembly were used on the top of the test box to apply overburden pressure on the soil-reinforcement interface.

Figure 19. Large-scale pullout test equipment used in this study

Figure 20 shows a schematic diagram of the pullout system, dimensions and instrumentation. Boundary effects were minimized by lining the sidewalls of the test box with plastic sheets and using a pair of 200 mm-long sleeves in addition to Styrofoam panels to provide a compressible front boundary. The test box also has a 19-mm thick transparent acrylic panel on one side of the box to allow for visual observation of the soil deformation and soil-interface performance over the course of pullout testing.

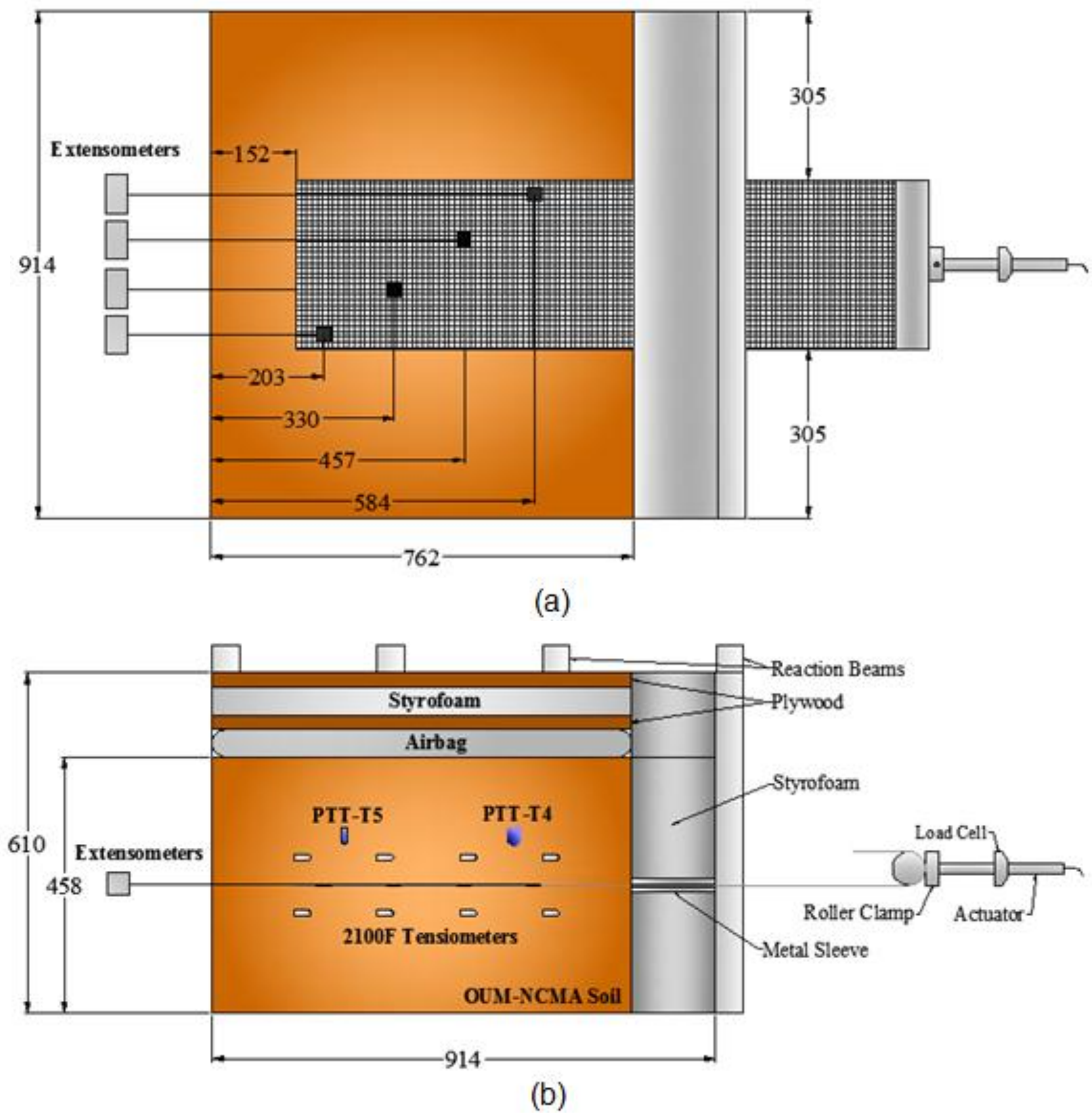

Figure 20. Schematic diagram of the pullout box: (a) plan view and location of extensometers and (b) side view and location of tensiometer cups (2100F, PTT-T4 and PTT-T5), (dimensions are in mm)

The pullout capacity of the geotextile at large-scale was measured at three target moisture contents (i.e. OMC-2%, OMC and OMC+2%) and three different overburden pressures (i.e. 10, 20 and 50 kPa). The soil was compacted at 95% of its maximum dry unit weight (i.e. 17.80 kN/m^3). The soil moisture content was calculated in accordance with the ASTM D2216 (ASTM 2006) test standard. Net normal stresses on the geotextile were calculated as the sum of stresses due to the soil mass on top of the geotextile strip (approximately 4.5 kPa) and the air pressure that was applied to the top of the soil mass.

Figure 21 shows different stages of soil preparation. During the first stage, the soil was air-dried for approximately 24 hours (**Figure 21a**). Soil clumps were processed (**Figure 21b**), sieved over a No. 4 sieve and kept in 25 kg-capacity buckets (**Figure 21c**). The initial moisture content of the soil was calculated and brought to the target value by adding and mixing with water as necessary. The soil was again stored in sealed 25 kg-capacity buckets for its moisture to equilibrate throughout the soil mass (**Figure 21d**). Throughout the process, the soil moisture content was carefully monitored to achieve the least possible variation with respect to the target value.

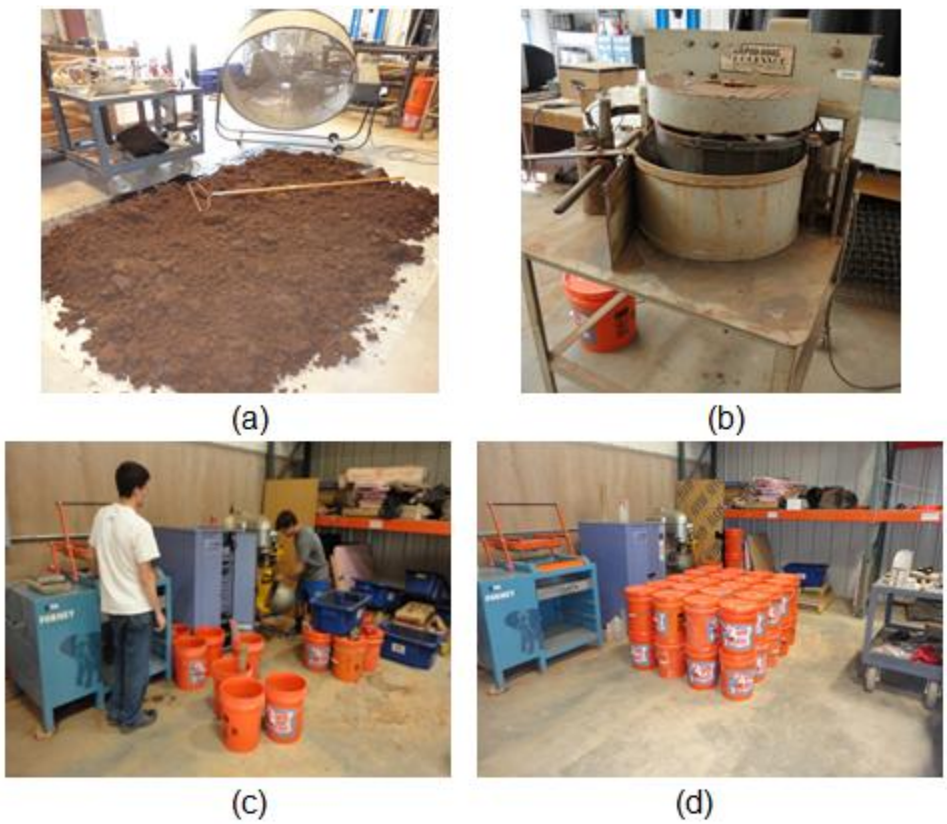

Figure 21. Soil preparation: (a) air-drying soil, (b) soil processor, (c) sieve and mixer and (d) soil storage in 25 kg-capacity buckets

Figure 22 shows different stages of the test setup. The box was filled up with the OUM-NCMA marginal soil in eight (8) or nine (9) 50 mm-lifts layers that were compacted manually using a 6.6 kg, 0.15 m × 0.15 m metallic tamper. The woven geotextile (GT) was installed at mid-height of the box. Four wire-line extensometers were attached to the GT to measure its deformation within the soil. Eight (8) tensiometer cups were placed in the vicinity of the soil-GT interface to determine the soil matric suction. The tensiometers were placed within a range of 25 to 50 mm near the soil-geotextile interface (above and beneath). After compaction of the final layer, the soil was sealed with a plastic sheet to avoid loss of moisture. An Earth Pressure Cell (EPC) and an air-bag were installed on top of the plastic sheet.

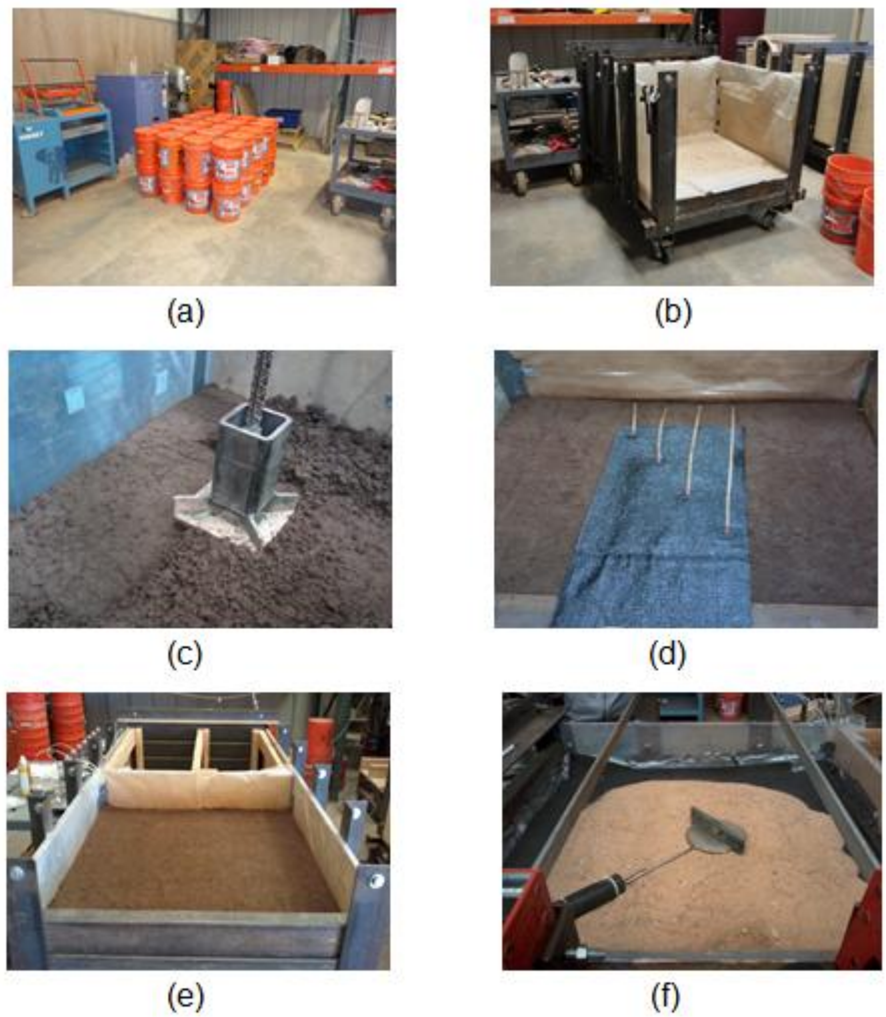

Figure 22. Test preparation: (a) soil in sealed 25-kg plastic buckets, (b) pullout box lined with plastic sheets, (c) manual compaction process, (d) geotextile specimen at the middle soil layer, (e) final soil layer as compacted and (f) EPC

The void between the air-bag and the top Plywood was filled with Styrofoam sheets to facilitate the reaction and uniformity of the vertical stress over the soil. The overburden pressure was applied after the tensiometers reached equilibrium, which typically took between 2 and 4 days. Finally, the geotextile specimen was clamped to the hydraulic actuator before starting the pullout tests (**Figure 23**).

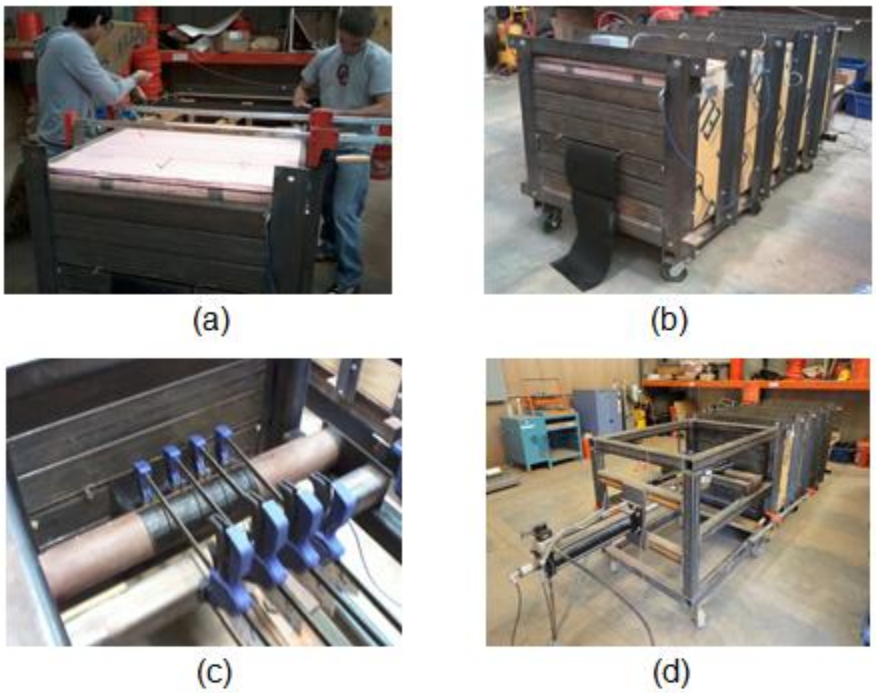

Figure 23. Final test setup: (a) Styrofoam being placed, (b) pullout box, (c) clamping system and (d) complete pullout setup

3.2.1 Pullout System

Figure 24 shows in detail the pullout system and its main components. The geotextile specimen was attached to a roller clamp, which in turn was attached to a 25-kip Lebow load cell. The load cell of the pullout rig hydraulic actuator was calibrated in tensile loading and unloading conditions. A 200-kip Baldwin-Tate-Emery Universal Testing Machine (UTM) was used to calibrate the cell.

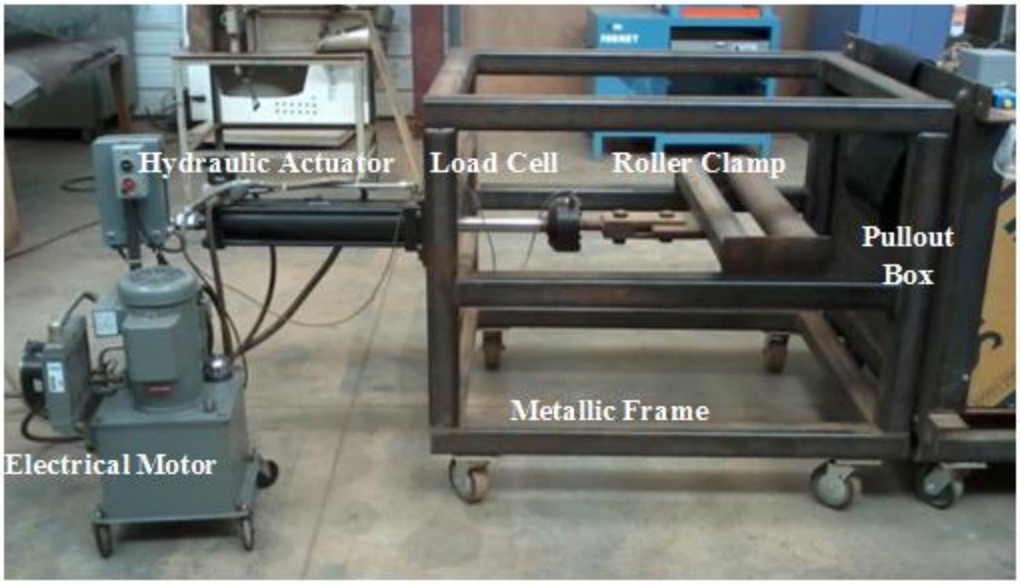

Figure 24. Pullout system

The pullout force on geotextile specimen during the pullout tests was applied at a set displacement rate (i.e. strain-controlled test) using an actuator. The input voltage controls the rate of displacement. However, the actuator was controlled by an open-loop system, which simply uses the input voltage to drive the actuator velocity. This resulted in some variation in the actuator velocity among different tests because the controller was not measuring and responding to feedback from the system. For an input voltage of 0.0089 mV, the average speed of the actuator was 0.016 mm/sec (1 mm/min) but this speed varied slightly depending on the test conditions. It was observed that the speed was stress-dependant, i.e. the displacement rate was faster in tests set up at lower overburden pressures. Nevertheless, the displacement rate was nearly uniform during the period of each pullout test. The actuator is equipped with a Micropulse Linear Variable Differential Transformer (LVDT) to measure the displacement of the clamp.

3.2.2 Deformation of the Geotextile within the Soil

In pullout tests, local movements of geotextile were measured using four (4) Celesco wireline potentiometers (WP) that were attached to the geotextile specimen at four different locations over its length (**Figure 25**). Wires within the soil were protected during compaction using rigid plastic tubes. The displacement of each wire was measured as a voltage and recorded in a data acquisition system using the LabView software. The calibration factor of each WP was determined by measuring the WP output when its wire was pulled out and retracted in ten 25.4 mm (1 in) increments.

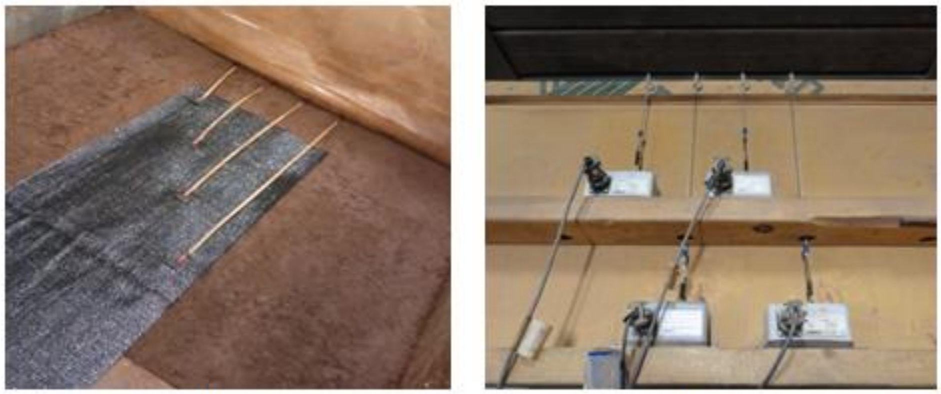

(a) (b)

Figure 25. Extensometers: (a) as attached to the geotextile strip and (b) wire-potentiometers

3.2.3 Overburden Pressure

A Geokon Earth Pressure Cell (EPC) was used to verify the magnitude of the overburden pressure applied by an airbag on the soil during the tests. EPCs use vibrating wire pressure transducers to measure total pressure and thus provide reliable long-term performance and are insensitive to moisture intrusion, which make them suitable for a wide range of construction activities. A layer of sand was placed over a non-woven geotextile at the top layer in order to level the EPC and improve the distribution of vertical stresses when the air-bag was inflated (**Figure 26**).

Figure 26. Earth Cell Pressure (EPC)

3.2.4 Determination of the Soil Water Characteristic Curve (SWCC)

The Soil Water Characteristic Curve (SWCC) shows the relationship between the soil suction and the soil moisture content. During the large-scale pullout testing program, the soil matric suction was measured as a function of the soil moisture content and overburden pressure using a set of eight (8) 2100F probes (i.e. small-tip tensiometers manufactured by Soilmoisture Equipment Corp.). The suction values were verified in selected tests using two models of Pressure Transducer Tensiometers (i.e. PTT, models T4 and T5, manufactured by UMS).

A tensiometer consists of a small ceramic cup made of a high-air entry porous material attached to a tube filled with de-aired water and connected to a pressure measuring device (e.g. a pressure gauge, a transducer or a manometer). The pressure of water contained in the high-air entry porous material will reach equilibrium with the soil water pressure, making it possible to measure negative soil water pressures (i.e. less than atmospheric pressure). The theory of operation, according to the manufacturer, is that the tensiometer measures the force with which water is held in the soil by the soil particles and this force indicates how tightly the water is bound in the soil (Soilmoisture Equipment Corp. 2009).

Tensiometers are suitable to measure relatively low matric soil suction values and are widely used for irrigation systems and research. Due to the water cavitation, the theoretical limit of reading is 100 centibars (≈ 100 kPa). However, the practical reading range is between 0 and 85 kPa at the sea level and it decreases with altitude. The reading range is reduced approximately 3.5 centibars for each 1000 feet increase in elevation. According to the city of Norman, OK website, the elevation of the city is approximately 1200 feet above sea level. Therefore, the range of practical readings can be expected to be between 0 and approximately 81 centibars. When matric suction exceeds 81 centibars, air coming out of solution makes readings inaccurate (Soilmoisture Equipment Corp. 2009). Some specific Pressure Transducer Tensiometer models are capable of measuring suction values exceeding 100 kPa (Umwelt-Monitoring-System 2009).

Measured suction readings values in a finer soil (i.e. Minco silt) in previous studies carried out by Hatami et al. (2010) were reported to be smaller than 32 kPa. Since the OUM-NCMA soil is coarser than Minco silt, its range of suction values was expected to be well within the operating range of the tensiometers.

Factors such as the soil properties (e.g. dry and bulk unit weights), the stress state and instrumentation are critical in determining the SWCC. The unit weight of the OUM-NCMA marginal soil was volumetrically controlled during compaction and was nominally the same across all test cases. The bulk unit weight varied with the target moisture content (i.e. OMC-2%, OMC and OMC+2%).

Figure 27a shows the set of eight (8) 2100F tensiometers in operation and **Figure 27b** shows the installation of the PTT. The PTT (T4 and T5 models) were used to evaluate the accuracy of the 2100F small-tip tensiometers. Due to their small dimensions (i.e. 5 mm diameter), a couple of PTT-T5 tensiometers were placed simultaneously with the 2100F probes in two repeated large-scale pullout tests (i.e. 50 kPa/OMC-2% and 50 kPa/OMC test cases). The PTT-T5s were inserted into the soil through a hole in the test box sidewall during the pullout test setup. Since the PTT-T4 tensiometers were significantly larger (25 mm diameter), they were inserted in the soil after the pullout tests had been completed and the air-bag was removed. The PTT-T5s were installed again to compare with the PTT-T4 readings.

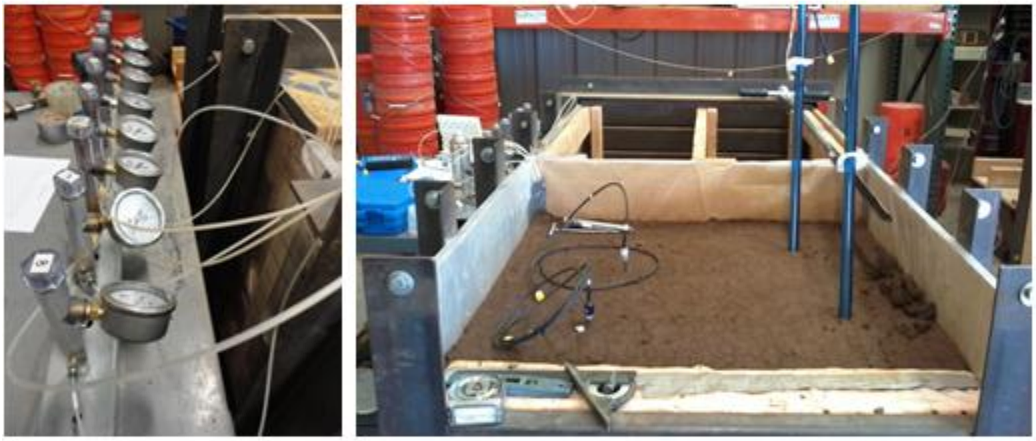

(a) (b)

Figure 27. Suction instrumentation: (a) set of 2100F Soilmoisture tensiometers and (b) Pressure Transducer Tensiometers (PTT-T4 and PTT-T5) in operation

Figure 28 shows the schematic location of the 2100F model tensiometers near the soil-geotextile interface (i.e. ~ 50 mm above and below). The tensiometers were filled with de-aired water before each test to achieve the highest possible level of sensitivity. An electric vacuum pump was also used to apply suction and remove as much of the remaining air as possible from the tensiometer tubes. Although the presence of air in the system is not expected to affect the accuracy of the readings, it increases the response time of the tensiometers. The suction readings were adjusted for the manometer effect when the gauges were not at the same level as the ceramic cups. This correction corresponds to the pressure head and is approximately equal to ±3 centibars (≈ 3 kPa) per foot, depending on whether the ceramic cup was placed above (+) or below (-) the gauge.

The pullout tests were started only after the tensiometers reached equilibrium, which typically took between two and four days. It was observed that the response of the tensiometers was a function of the soil moisture content and loading conditions. Higher moisture content values and overburden pressures (e.g. OMC+2% and 50 kPa, respectively) required longer time to achieve equilibrium. Some suction readings were discarded depending on the performance and availability of the tensiometers.

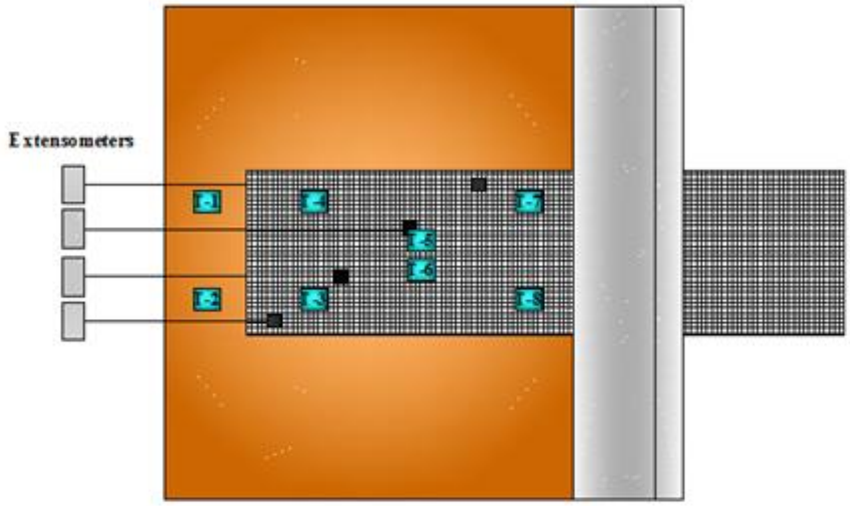

(a)

(b)

Figure 28. Schematic location of tensiometers in the pullout box: (a) plan view and (b) side view

The soil moisture content was calculated in accordance with the ASTM D2216 test standard (ASTM 2006) before and after each pullout test. Three soil samples per layer were taken to determine the moisture content previous compaction. During the excavation stage, two (2) to four (4) samples per layer were taken to determine any change in moisture. The moisture content was especially monitored near the soil-geotextile interface, e.g. within 100 mm (4 in) above and below the geotextile specimen. **Figure 29** shows two undergraduate assistants taking soil samples during the excavation stage to determine the soil moisture content.


Figure 29. Excavation and sampling to determine the soil moisture content

3.3 Small-Scale Testing Program

The pullout capacity of the geosynthetic reinforcement is usually evaluated following the ASTM D6706-01 test protocol (or its counterpart in Europe, the EN 13738:2004). The soil-geosynthetic interface shear strength is performed following the ASTM D5321-08 test protocol (or the EN ISO 12957-1 in Europe). These standards require apparatuses and reinforcement samples of relatively large dimensions and hence, they are considered as large-scale tests. Since only selected laboratories or institutions have the equipment to perform these tests, they can be cost-prohibitive for small to medium budget projects, which are typically candidates to use marginal quality soils as the backfill.

Based on the experience in the current project, performing a single large-scale pullout test required 10-14 days of hands-on activities. The process required several personnel, a significant amount of materials and specialized equipment. Furthermore, the data obtained is valid for specific conditions and are not valid if on-site conditions change with respect to the testing conditions. These concerns motivated the author and colleagues to seek more economical alternatives to evaluate the soil-reinforcement interface properties with a satisfactory level of accuracy. Since particles-size of marginal soils is typically small as compared to that of granular materials, the use of commonly available equipment could be a viable means to evaluate soil-reinforcement interface properties for design. A single operator could carry out these small-scale tests in a much shorter period of time and at a much lower cost and over a wide range of conditions (e.g. moisture contents, overburden pressures and soil types) as compared to the large-scale tests. However, before conducting a wide range of experimental parametric analyses, the results of small-scale tests need to be validated against those from otherwise identical large-scale tests to address any scaling-related issues.

Hatami et al. (2010) carried out a series of small-scale interface shear and pullout tests to evaluate soil-geotextile interface properties for sand and marginal soils as part of a long-term multi-scale research project, in which different types of soils and boundary conditions were studied (Hatami et al. 2010, 2011a,b).

In the present study, a small-scale Direct Shear Testing (DST) machine located at the Unsaturated Soil Mechanics Laboratory at the University of Oklahoma was used to measure the soil strength properties and the soil-geotextile interface strength properties (**Figure 30**). The DST was modified to perform both pullout and interface shear tests using the OUM-NCMA marginal soil.

Figure 30. Direct shear testing (DST) machine at the Unsaturated Soil Mechanics Laboratory in the University of Oklahoma

3.3.1 Small-Scale Test Setup

The small-scale testing program was carried out using a 60 × 60 mm square test cell. Soil samples were compacted at the same target unit weight and moisture content values as in the corresponding large-scale tests.

The DST equipment has two LVDTs to measure horizontal and vertical deformations during the tests. The horizontal force was measured with a 4.45 kN (1 kip) capacity S-shape load cell. Results were collected using a data acquisition system developed by TestNet-GP (GEOTAC 2004). The overburden pressure was applied by placing dead loads on a loading arm with a mechanical advantage of 10. The upper half of the box was stationary and attached to a load cell. The bottom half of the box can be moved in either direction as required.

As a standard procedure, after the soil was mixed with water at a target moisture content, it was placed in a humidity-controlled room for at least 16 hours to promote moisture equilibrium as recommended by the ASTM D3080. The soil moisture content was determined before compaction and after testing. In most cases, the soil was prepared at 0.2% greater moisture content than the target value to account for the expected loss of moisture during compaction and testing procedure. It was observed that the major portion of the moisture loss occurred during sample preparation and compaction inside the test cell as compared to the testing period. Higher variations in the moisture content were found for high moisture contents (e.g. OMC+2%).

In almost all test cases, the strain rate was set at 1 mm/min as recommended by the ASTM D6706 and D5321 test protocols for pullout and interface shear tests, respectively. However, in some test cases, a different displacement rate was used to investigate its influence on the measured shear strength properties of the soil and soil-geotextile interface.

3.3.1.1 Small-scale direct shear tests

The strength properties of the OUM-NCMA marginal soil, i.e. internal friction angle and cohesion, were obtained from two different series of tests at strain rates of 1 mm/min and 0.084 mm/min. The first series of direct shear tests was carried out at four different overburden pressures, i.e. 10, 20, 35 and 50 kPa. The extra data-point at 35 kPa of overburden pressure was included to improve the accuracy of the results. The overburden pressures for the tests at 0.084 mm/min were carried out at 10, 20 and 50 kPa. The soil was mixed and compacted at three different target moisture content values (i.e. OMC-2%, OMC and OMC+2%) to evaluate the influence of matric suction on the soil strength properties. The soil was compacted in three layers of 8 mm at the same unit weight as in large-scale tests, i.e. 17.8 kN/m^3 (95% of the maximum dry unit weight). The total dry mass of soils was approximately 157 g. All soil particles were finer than the #4 sieve as per required by the ASTM D3080 test protocol (ASTM 2004). The bottom half of the cell was subjected to the shearing movement at a constant speed while the upper half was restrained. Tests were stopped at 10% strain, i.e. 6 mm. **Figure 31** shows the DST setup and the shear cell after testing.

Figure 31. Direct shear test machine and test cell

3.3.1.2 Small-scale pullout tests

Small-scale pullout tests were intended to simulate the large-scale conditions and test setup. The DST machine was modified to simulate pullout tests. The size of the shear cell corresponded to the dimensions of the large-scale pullout box scaled down by a factor of 15. Tests were performed at 1 mm/min and 0.074 mm/min. The latter speed corresponds to the mean strain rate of the geotextile at large-scale pullout tests (i.e. 1.1 mm/min) scaled down by a factor of 15.

The main objectives of performing small-scale pullout tests were to evaluate boundary conditions and investigate the relationship between large-scale and small-scale pullout results. The OUM-NCMA marginal soil was prepared at the same target moisture contents (i.e. OMC-2%, OMC and OMC+2%) and subjected to the same vertical stresses as in large scale (i.e. 10, 20 and 50 kPa).

An important consideration in setting up the small-scale tests was to develop boundary conditions that would impose minimum influence on the response of the soil and soil-reinforcement specimens. An important boundary condition is at the front end of the test cell which should consistently represent a similar condition in comparable large-scale tests. To reduce the boundary effects at the front end of the pullout box in large-scale tests, two 152.4 mm-thick Styrofoam blocks were placed above and beneath the sleeves (**Figure 32a**). This is a more accurate representation of the actual on-site conditions in which the active zone in the reinforced mass does not provide a rigid boundary in front of the reinforcement layer under tensile load. A comparison of the large-scale and small-scale front boundaries is shown in **Figure 32b**. A U-shape, 3-mm thick metal spacer was placed to create a gap and prevent contact between the geotextile strip and the box. A pair of metal sleeves was used for the same purpose in large-scale tests as recommended by the ASTM D6706. Several materials, i.e. Styrofoam, cardboard and rubber from *papermate*® eraser, were used at the front end of the shear box to evaluate and compare the resulting interface shear parameters and the repeatability of the tests. A series of pullout tests was also carried out as control with the original rigid front boundary.

(a) (b)

Figure 32. Pullout test front boundary: (a) Styrofoam placed at the front end of the large-scale pullout box and (b) rubber placed at the front of the small-scale shear cell

Small-scale pullout results using Styrofoam were somewhat unexpected for tests performed at 1 mm/min strain rate. For instance, the interface friction angle did not exhibit the expected variation with the soil moisture content. Hatami et al. (2011) found relatively reasonable and consistent results using cardboard plates to reduce boundary conditions in similar tests. However, in this study the use of cardboard did not show satisfactory results because the high compressibility of the material affected the density control of the soil during compaction.

Satisfactory results were obtained for rubber from *papermate®* erasers at a strain rate of 1 mm/min. Results using Styrofoam at a strain rate of 0.074 mm/min led to relatively good results as well. Similarly, the series of tests carried out with a rigid boundary (i.e. steel of the shear wall apparatus) indicated reasonable results. The above observations indicate that the front boundary in the small-scale tests has a very important role in the quality of the test results. The extent of its influence can vary with the soil type and test preparation method among other factors (e.g. moisture content, overburden pressure and shearing rate).

The soil was compacted in four 7 mm-thick layers. The total dry mass of soil was 159 g. A 20 mm-wide geotextile strip was placed in the machine direction (MD) on the top of the middle soil layer, similar to the large-scale pullout tests. The geotextile was clamped to a custom-made clamp mounted on the test box. A 20 mm × 40 mm (width × length) area of the geotextile was embedded within the soil in tests carried out with a flexible front boundary. In tests with a rigid boundary, the embedded section of the geotextile was 20 mm × 50 mm.

Figure 33 shows the small-scale pullout test setup. The materials used as front boundaries were wrapped in plastic tape to prevent the moisture exchange with the soil. No contact between the geotextile specimen and the front boundaries was allowed.

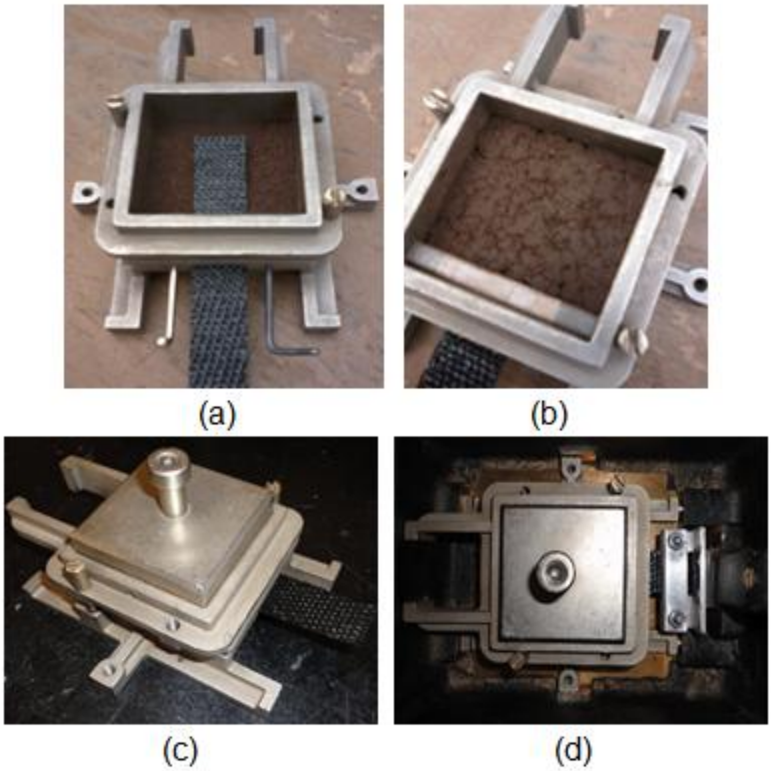

Figure 33. Small-scale pullout test setup: (a) geotextile specimen placed at the middle of the test cell, (b) upper half of the soil with front boundary and geotextile detail, (c) test cell and (d) customized clamp mounted on the test apparatus for pullout tests

The sidewall friction effect in the test cell during soil placement and compaction was minimized by using a thin layer of grease during the tests performed with rigid boundary. This effect was minimized in some preliminary tests by lining plastic tape on the walls of the box. However, plastic tape tended to tear during compaction and needed to be replaced very often. It is believed that grease facilitates the compaction process and an adequate distribution of the vertical stress over the soil.

3.3.1.3 Small-Scale Interface Tests

Small-scale interface shear tests (IST) were performed to evaluate the effect of matric suction on the soil-geotextile interface strength. The tests were carried out in overall conformance with the ASTM D 5321 test protocol (ASTM 2008) with the difference that the available small-scale DST machine with the 60 × 60 mm test cell was used instead of the 300 × 300 mm shear box recommended by the test protocol. Since both the soil particle size and the asperities of the geotextile used were orders of magnitude smaller than the dimensions of the test cell, the test results are not believed to be negatively impacted by scale effects. In addition, the use of small test cells has been deemed acceptable for evaluating soil-reinforcement interface shear properties when sands and finer soils are used together with geotextiles (Koerner 2005). Soil-geotextile interface parameters such as interface friction angle and adhesion intercept can be obtained from these tests.

A 60 mm-square piece of geotextile was attached to a metal plate and placed in the bottom half of the shear cell. In the upper half, the soil was compacted on top of the geotextile in two 6 mm-high layers of soil mixed at OMC-2%, OMC and OMC+2%. The total dry mass of soils was 78 g. Tests were carried out at 10, 20 and 50 kPa of overburden pressure and sheared at a constant displacement rate 1.0 mm/min. **Figure 34** shows different stages of specimen preparation. **Figure 34d** illustrates the imprint of the geotextile in the soil which indicates a desirable frictional contact between the two materials.

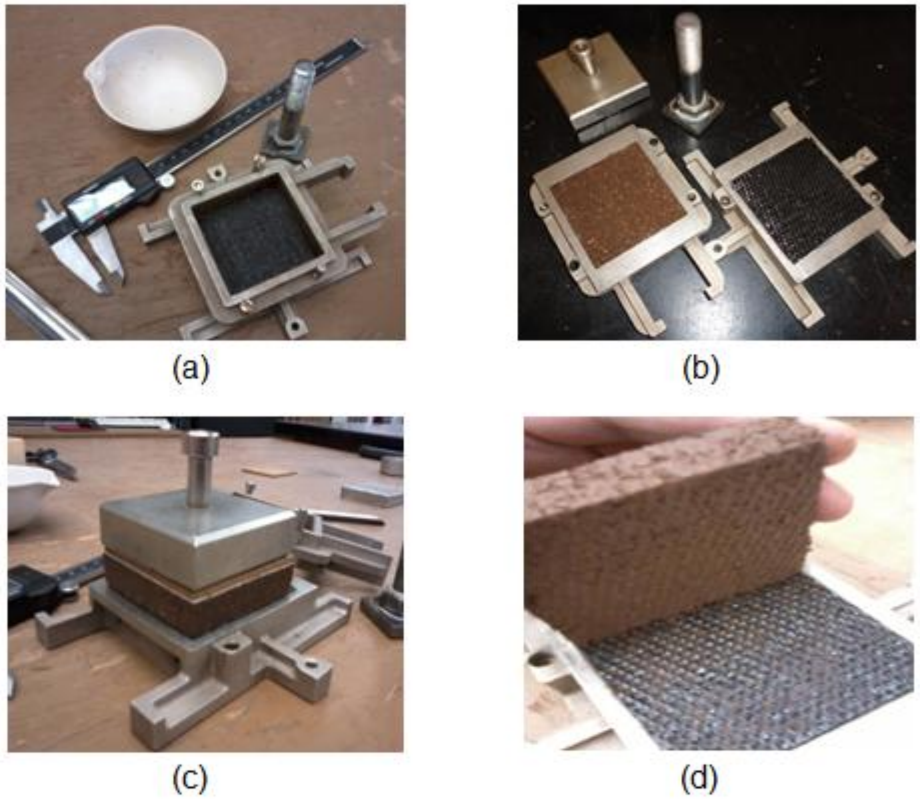

Figure 34. Small-scale interface shear test

3.3.2 Soil Water Characteristic Curve

The Soil Water Characteristic Curve (SWCC) of the OUM-NCMA marginal soil was determined using three different methods: (1) from values measured using small-tip tensiometers in large-scale pullout tests, “on-site”, (2) from the soil moisture and suction data from the same small-tip tensiometers used in the large-scale pullout tests, “off-site” and (3) using a Pressure Plate Extractor (PPE or Pressure Plate test), “off-site”. The soil matric suction was determined as a function of the moisture content. The results obtained from these different methods were overall consistent but showed some differences as discussed in **Section** 4.

The soil samples used to obtain the SWCC using tensiometers were mixed and compacted at target moisture content values (**Figure 35**). The 2100F model tensiometers were inserted in 76-mm-diameter and 48-mm-thick soil samples that were compacted in three layers. A hole was made in the soil using a drill. The 25-mm-long 2100F probes (tensiometer cups) were inserted at the mid-height of the soil specimens and subsequently sealed using plastic wrap to maintain a constant soil moisture content during the period of the tests (**Figure 36a**). The soil samples were prepared at moisture contents within the range from OMC-4% (8.6%) to approximately OMC+4% (16.5%). The OMC+4% case represented an essentially fully saturated condition for the OUM-NCMA soil with negligible suction in the soil. The moisture content of the soil was calculated before compaction and at the end of the test as per ASTM D2216 test protocol (ASTM 2010).

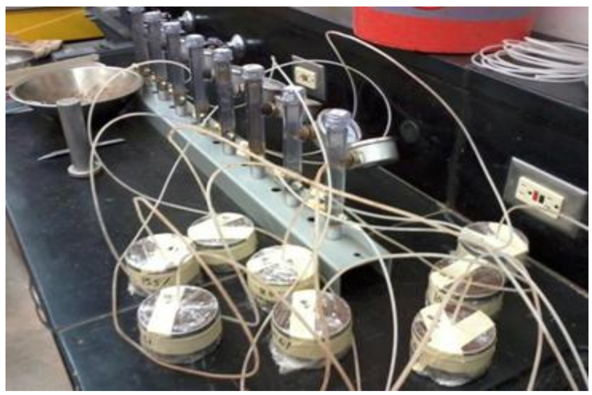

Figure 35. 2100F tensiometers used to determine the soil matric suction at small-scale

The response of the 2100F tensiometers was verified using a pressure transducer tensiometer (PTT-T5). A PTT-T5 and two 2100F tensiometers were inserted in a small-scale (102-mm-diameter, 116-mm-high) soil sample which was prepared in a Proctor mold at OMC-2% with no overburden pressure applied to the sample (**Figure 36b**). The PTT readings in both large-scale pullout and small-scale suction tests were in close agreement with the mean suction values measured with the 2100F probes. However, measured suction values from both the 2100F and PTT devices in small-scale tests were greater than the corresponding values in large-scale tests.

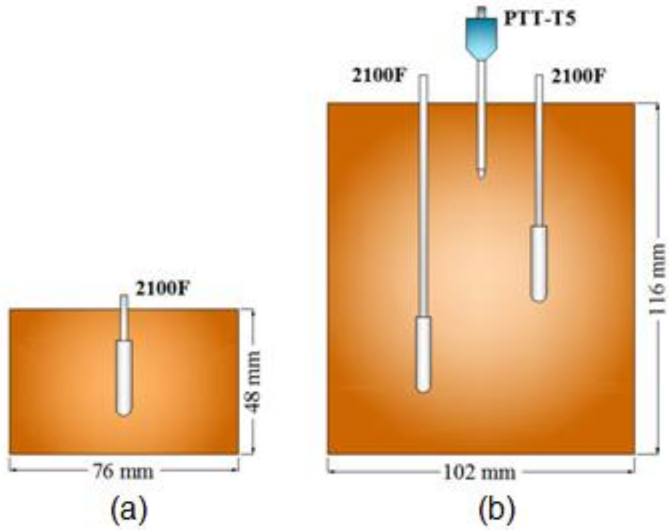

Figure 36. Determination of the SWCC for the OUM-NCMA marginal soil: (a) using 2100F tensiometers tests and (b) verification of 2100F tensiometer readings using a calibrated PTT-T5 device

The Pressure Plate Extractor (PPE) was also used to obtain the SWCC from small samples compacted at OMC-2% and OMC (e.g. 10.6% and 12.6%, respectively) and trimmed into a 51 mm diameter and 10 mm-high ring. Fully saturated soil samples were placed over a 1-bar high air-entry porous disk to generate the primary drying curve of the SWCC. This disk was replaced by a 3-bar high air entry porous disk when the suction values were close to its 1imiting capacity (i.e. 100 kPa). The suction was controlled by applying air pressure into a sealed chamber which was connected to the atmospheric pressure through a burette (**Figure 37**). After each increment of air pressure (i.e. matric suction) and once the water level in the burette achieved equilibrium, the samples were extracted from the chamber and weighed to determine their moisture content. The PPE works based on the axis translation technique, which allows the matric suction (i.e. $u_a - u_w$) to increase beyond 100 kPa without cavitation. The air pressure (i.e. u_a) can be increased up to approximately 1500 kPa while water is maintained at the atmospheric pressure (i.e. $u_w = 0$). **Figure 38** shows the sample preparation for the pressure plate test. Further description of the test can be found in the ASTM D6836 (ASTM 2008).

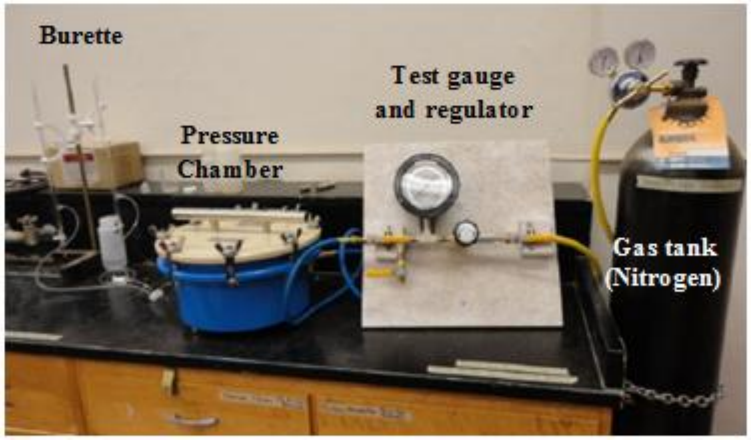

Figure 37. General view of the Pressure Plate Extractor system used in this study

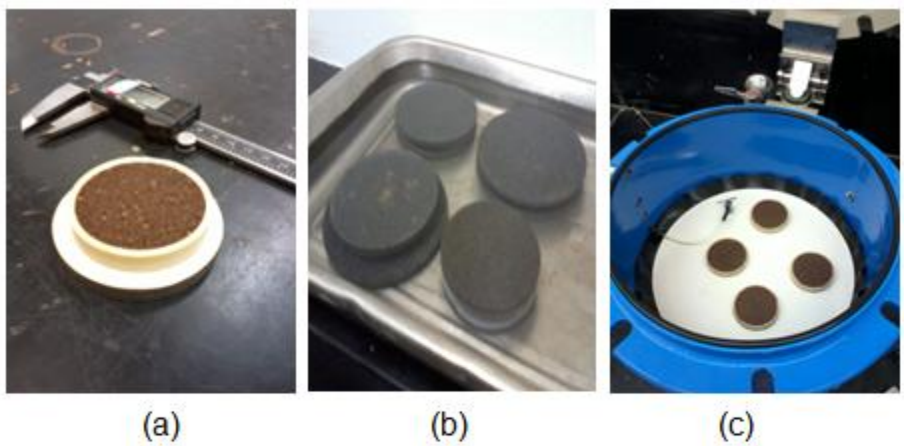

Figure 38. Pressure Plate Extractor sample preparation (a) soil trimmed or compacted into a 51 mm-diameter rubber ring, (b) samples submerged in water for several days and (c) saturated samples placed on the high-air entry porous disk

3.4 Triaxial Tests

In order to predict the pullout response of the geotextile using a numerical model, soil strength parameters such as internal friction angle, cohesion, Young's Modulus, Poisson's ratio, bulk modulus, and shear modulus were required in the program FLAC (Version 7.0, Itasca 2011). Triaxial tests on unsaturated (and saturated) samples were performed to obtain the soil strength parameters required for the model. The test specimens were prepared at initial moisture content values of 10.6% and 12.6%, which correspond to OMC-2% and OMC, respectively.

Using a 0.30 mm-thick rubber membrane, a vacuum pump (**Figure 39a**) and a 144 mm-height and 71 mm-diameter mold (**Figure 39b**), the soil was prepared and compacted at the target moisture content in five (5) layers at 95% of its maximum dry density (i.e. 17.8 kN/m^3). The soil was placed in the moist room for 24 hours before compaction and 24 extra hours after compaction to promote moisture equilibrium. Samples were placed in a triaxial chamber as shown in **Figure 39c** and the system was connected to a control panel depending on the type of test. The sample preparation for both the saturated and unsaturated specimens was similar.

(a) (b) (c)

Figure 39. Triaxial test preparation: (a) membrane subjected to vacuum in the compaction mold, (b) soil compacted in the mold and (c) sample placed in the triaxial chamber

3.4.1 Triaxial Tests on Saturated Samples (CIUC Tests)

The Consolidated Isotropically Undrained Compression (CIUC) test is used to determine the strength and stress-strain relationships of saturated specimens. Specimens are isotropically consolidated and sheared at a constant rate of axial deformation without allowing drainage. Effective stresses, pore-water pressures, and deformation are measured or calculated based on the results. Mohr-Coulomb envelope and Elastic Modulus (Young´s Modulus) can be obtained from tests prepared at different confining pressures. CIUC tests were performed on soil samples compacted at a target moisture content of 10.6% (OMC-2%). The confining pressures (i.e. cell pressure minus back pressure) were set up at 14.0 kPa (2 psi), 27.9 kPa (4 psi) and 55.6 kPa (8 psi).

The test procedure was carried out following the ASTM D4767 (ASTM 2011) and consisted of three phases: 1) saturation, 2) consolidation and 3) shearing. De-air water was pumped into the sample at high pressures until the soil sample was saturated. The back pressure was slowly increased in small increments up to 420 (60 psi) until the Skempton's B-value reached at least 0.94. The saturation stage typically took two weeks. The confining pressure throughout the saturation phase was kept at ≈ 14 kPa (2 psi). In the consolidation stage, the cell pressure was increased to reach the target confining pressure and then allowed to consolidate for two days until the burettes indicated that the water flow had stopped. The cell pressure was applied using water as a confinement medium. The shearing phase consisted of applying vertical deformation at a constant strain rate (4%/hour) and recording the corresponding deformation, vertical load and increment of pore pressure until failure was reached (10 – 15 % strain). In-valves were closed during shearing. Area and membrane corrections were included in the calculations.

Figure 40 shows the triaxial system during a CIUC test. The gauges in the triaxial panel are in psi units and its accuracy is limited to 1 psi. Therefore, it was not possible to set up the confining pressures at 10, 20 or 50 kPa exactly. The minimum accurate confining pressure for the system was ≈ 14 kPa (2 psi), which also corresponds to the confining pressure during the saturation stage.

Figure 40. Triaxial test equipment

3.4.2 Triaxial Tests on Unsaturated Samples

Six triaxial tests were performed on unsaturated samples during this research. Air was used as the medium to confine the sample. A 0.1 psi-accuracy gauge was implemented for this series of tests. The specimens were prepared at OMC-2% (10.6%) and OMC (12.6%). The confining stresses were set up at 10, 20 and 50 kPa. The cell pressure valve was connected to an air regulator to achieve the target confining stress and was also used to adjust the pressure during the test if necessary. The pedestal and cap valves were open to atmospheric pressure (i.e. $u_a = 0$).

Figure 41 shows the triaxial chamber connected to the air system during the test. Confining pressure was achieved by increasing the cell pressure (i.e. air pressure) in small increments of 10 kPa. The vertical load was applied at 4%/hour, which can be considered a relatively slow rate of strain for a sandy material. Similar tests on a finer soil (i.e. Minco Silt) were carried out at similar strain rates with fairly good results (Hatami et al. 2010).

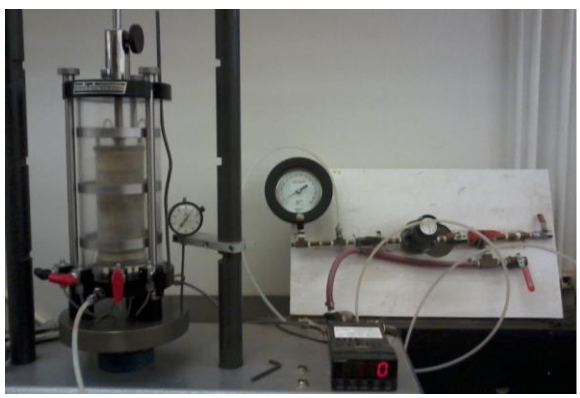

Figure 41. Unsaturated triaxial test

It should be noted that these series of triaxial tests were not performed under suction-controlled conditions. Therefore, the resulting parameters could have been affected by suction changes during shearing and could not represent completely the conditions encountered during the large-scale pullout tests. Although the conditions near the soil-geotextile interface in the pullout tests were not suction controlled, suction variations during the course of the pullout tests were expected to be significantly low due to the predominant coarse size of the soil particles and the relatively short period of time required to complete the tests.

4. LARGE-SCALE PULLOUT TEST RESULTS

4.1 Pullout Capacity of the Geotextile Reinforcement

The pullout capacity of the geotextile (P_r) is the maximum pullout force that the reinforcement can resist before being completely mobilized. Pullout capacity values are expressed in units of force per unit width, i.e. the pullout force (F_p) is divided by the width of the geotextile (W_g). The geotextile width was 305 mm (≈1 ft) for all testing conditions in this study. The corrected pullout force was determined by subtracting from the total applied horizontal force (as measured by the load cell) a small amount of frictional resistance inherent in the pullout rig assembly. The total amount of force correction was calculated as the summation of the friction between the roller clamp and the mounting frame and the elastic force generated by the extensometers during the tests. The mean value of force correction was calculated as 0.16 kN. This value was considered small since it only corresponded to approximately 0.5% of the lowest magnitude of pullout capacity developed during the testing program (i.e. for a test set up at OMC+2% and 10 kPa of overburden pressure).

Figure 42 through **Figure 44** show the pullout capacity of the geotextile reinforcement as a function of the actuator displacement and overburden pressures for the tests compacted at OMC-2%, OMC and OMC+2%, respectively. The pullout curves show the maximum pullout capacity of the geotextile followed by a strength softening in the soil-geotextile shear strength interface. As expected, results showed that pullout resistance of the geotextile increased at higher overburden pressures.

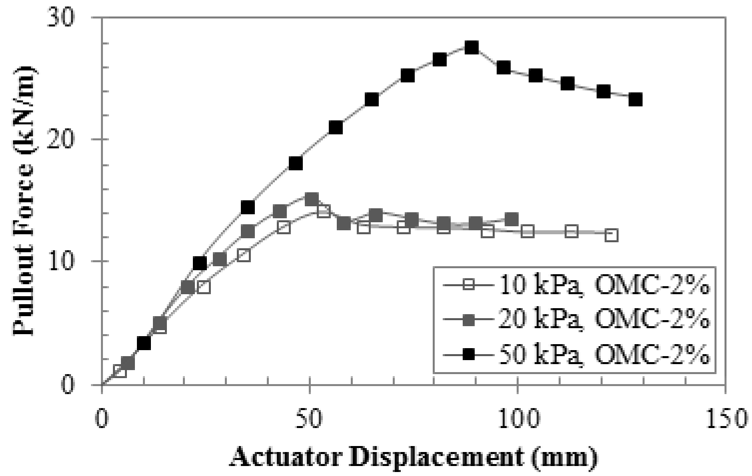

Figure 42. Pullout capacity of the geotextile at OMC-2%

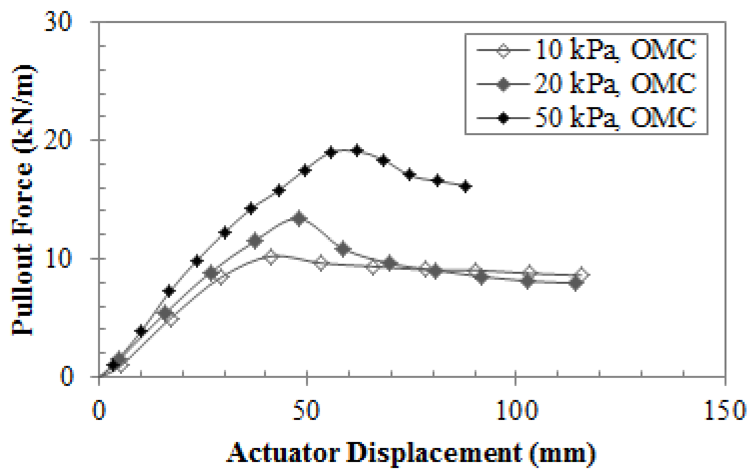

Figure 43. Pullout capacity of the geotextile at OMC

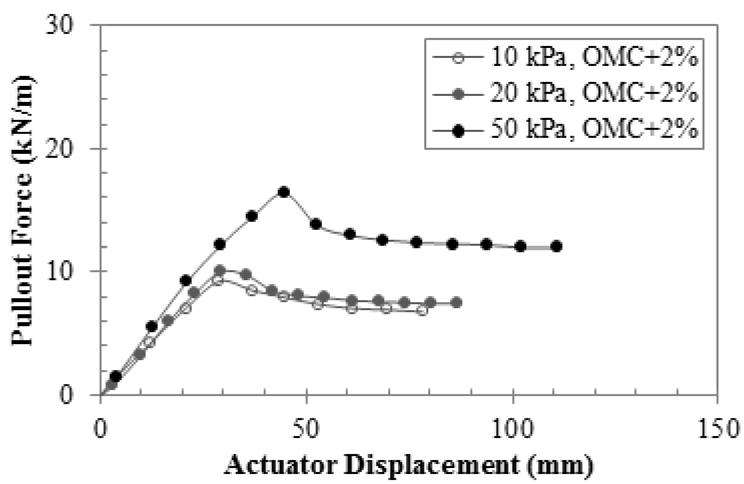

Figure 44. Pullout capacity of the geotextile at OMC+2%

Figure 45 through **Figure 47** show the pullout force-displacement data for different moisture content and overburden pressure values tested in this study. The results are plotted for the same overburden pressure in each figure to compare the effect of the soil moisture content and matric suction on the pullout capacity of the geotextile reinforcement. The peak pullout values in each test typically coincided with the mobilization of the geotextile tail-end.

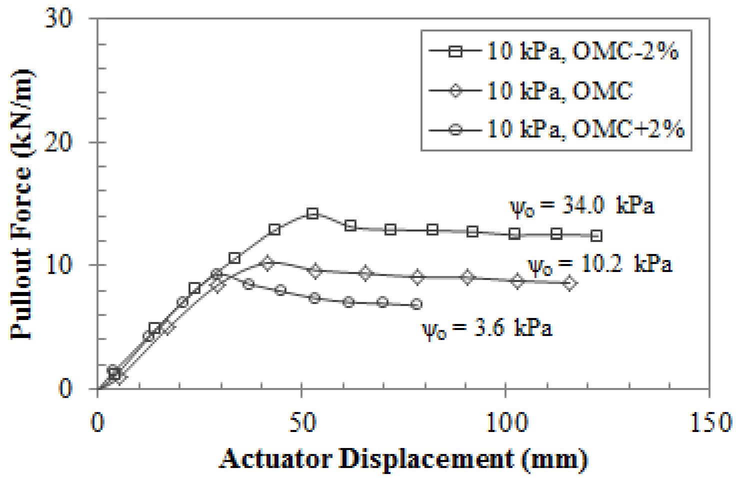

Figure 45. Pullout capacity of the geotextile at 10 kPa and different moisture contents

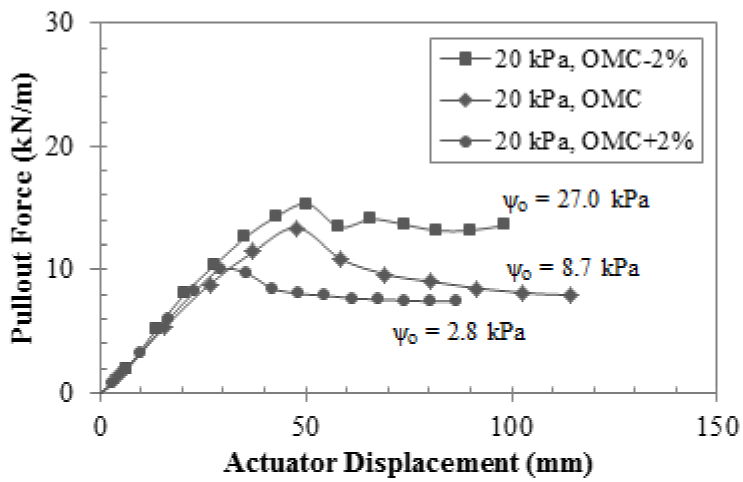

Figure 46. Pullout capacity of the geotextile at 20 kPa and different moisture contents

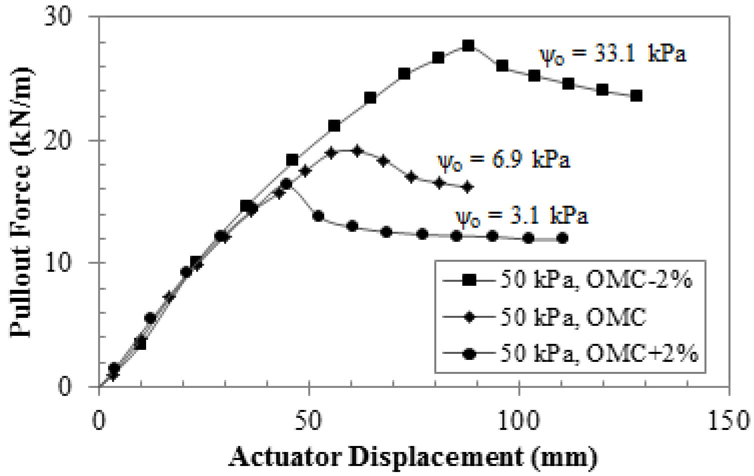

Figure 47. Pullout capacity of the geotextile at 50 kPa and different moisture contents

Figure 48 shows the pullout capacity envelopes on the frontal (**a**) and lateral (**b**) planes of the extended Mohr-Coulomb envelope as a function of overburden pressure and matric suction, respectively. These results indicate that the geotextile pullout resistance is greater for greater overburden pressures and suction values. The subscript “p” in the strength parameters in this figure indicates that they correspond to pullout parameters as opposed to interface shear parameters in **Equation** 3.

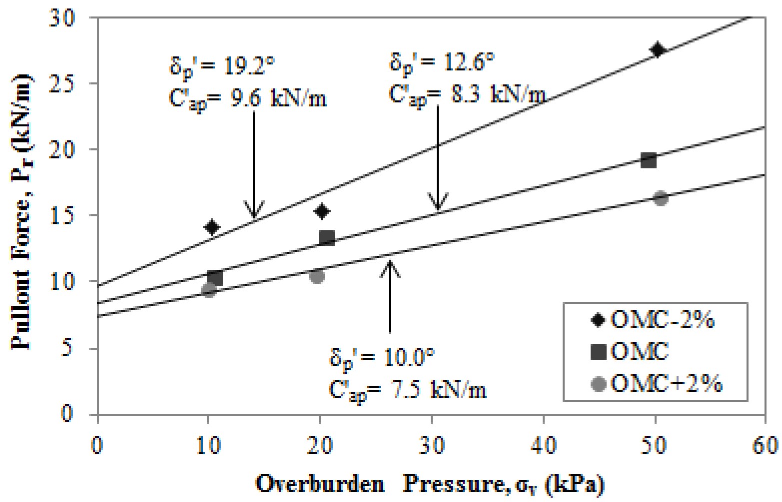

(a)

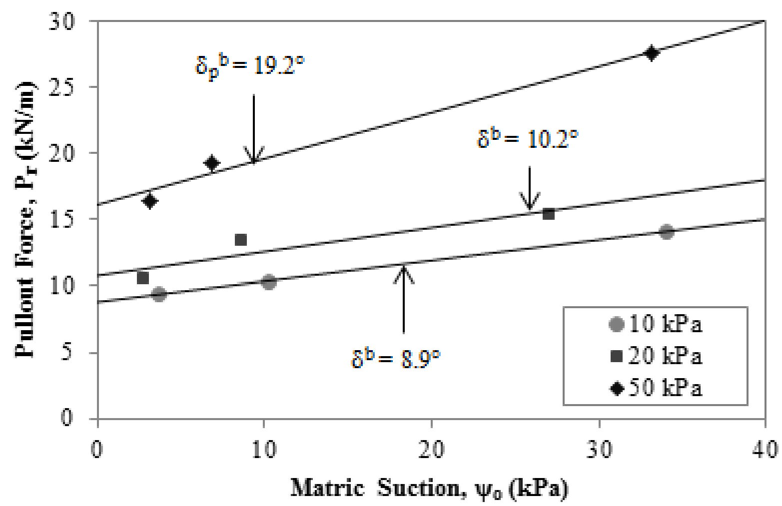

(b)

Figure 48. Maximum pullout capacity envelopes of the geotextile at a) different moisture contents and b) different overburden pressures

According to the results shown in **Figure 48**, the geotextile pullout capacity of the soil compacted at OMC+2% (with a mean matric suction value equal to 3.2 kPa) can be up to 40% (for the case of 50 kPa overburden pressure) lower than that for the soil compacted at OMC-2% (with a mean matric suction value equal to 31.4 kPa). The corresponding magnitudes of reduction for the 10 kPa and 20 kPa overburden pressure cases were calculated as 33% and 32%, respectively. This important reduction of the pullout capacity was attributed mainly to the loss of matric suction in the soil.

Selected tests were repeated during the large-scale testing program to evaluate the repeatability of the results and the performance of the equipment. The results presented in this chapter correspond to those in which the components of the pullout system (e.g. EPC, actuator, displacement rate, extensometers, load cell, etc) showed the best performance.

4.2 Pullout Resistance (F*) and Scale Correction (α) Design Parameters

The pullout resistance (F*) and scale correction (α) design parameters used by Berg et al. (2009) in the FHWA guidelines to predict the pullout capacity of the geotextile reinforcement (**Equation** 5) were calculated based on the deformation of the geotextile within the soil.

Figure 49 summarizes the procedure to calculate the pullout design factors (i.e. F* and α) as indicated in the FHWA guidelines. The example shown is for a test carried out at OMC-2% and 50 kPa overburden pressure.

$$P_r = F^* \alpha \, \sigma'_v \, L_e \, C \qquad [5]$$

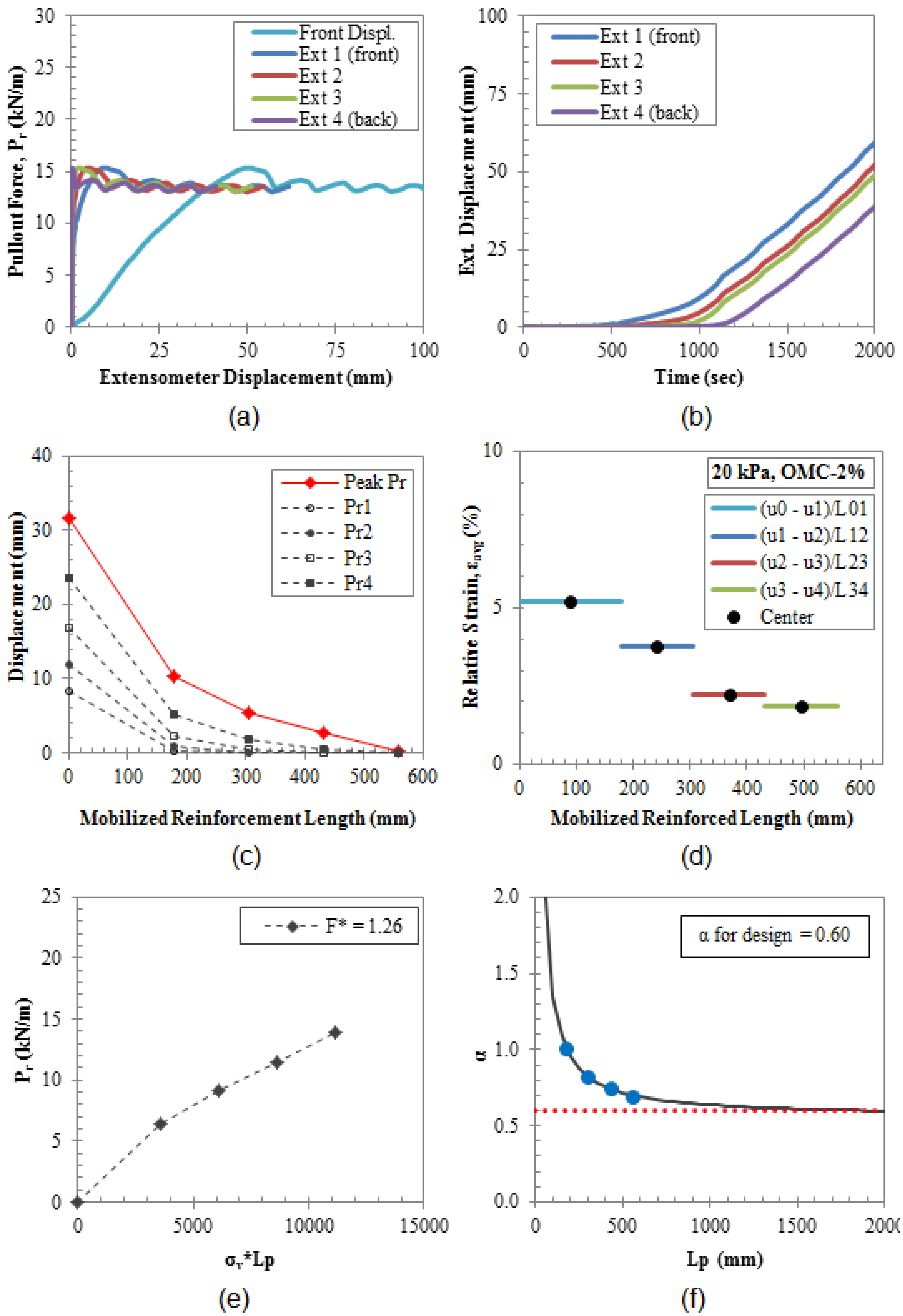

Figure 49. Calculation of F* and α parameters from pullout test at OMC-2% and 20 kPa

Figure 49a shows the pullout force-displacement data for the front end of the geotextile and the extensometers attached to different locations along the geotextile length. **Figure 49b** shows the deformation of each extensometer as a function of the time during the test. **Figure 49a** and **Figure 49b** are compared and combined into **Figure 49c** to plot the pullout force as a function of the mobilized reinforcement length. The mobilized reinforcement length refers to the length of that geotextile which was mobilized as the pullout force (P_i) increased. The relative strains within the geotextile are plotted in **Figure 49d** to identify deformation patterns at the moment of pullout.

In **Figure 49e**, the pullout force (P_r) required to mobilized each extensometer is plotted as a function of the mobilized reinforcement length and overburden pressure (σ_v*L_p). The pullout resistance design parameter (F*) is calculated as the secant for the mobilized reinforcement length at pullout. In **Figure 49f**, the scale correction factor (α) is calculated as the asymptotic value of the normalized pullout resistant factor (F*), i.e., F^*_m/F^*_{peak}, calculated for each mobilized reinforcement length. A hyperbolic trend was obtained using the GraphSight V.2.0.1 software (2004) and extended asymptotically to cover the total length of the geotextile specimen. The scale correction design parameter (α) is calculated as the intercept of the asymptote with the vertical axis.

Table 6 summarizes the large-scale testing conditions, the range of measured matric suction, peak pullout forces and pullout design parameters used in **Equation** 5 to calculate the design pullout capacity. The mean matric suction values presented in **Table 6** were measured using the 2100F Tensiometers.

Table 6. Summary of large-scale pullout results

Target Conditions		Actual Conditions		Range of Measured Suction	Mean Matric Suction	Peak Pullout Force	Resistance Factor	Scale Correction Factor
ω (%)	σ_v (kPa)	ω (%)	σ_v (kPa)	ψ (kPa)	ψ (kPa)	P_{rmax} (kN/m)	F*	α
10.6 (OMC-2%)	10	10.5	10.29	31 – 35	34.0	14.18	2.26	0.63
	20	10.7	20.10	24 – 30	27.0	15.38	1.26	0.60
	50	10.3	50.30	30 – 36	33.1	27.50	0.90	0.55
12.6 (OMC)	10	12.6	10.42	9 – 11	10.2	10.29	1.62	0.64
	20	12.5	20.44	7 – 10	8.7	13.37	1.07	0.64
	50	12.8	49.42	6 – 9	6.9	19.27	0.64	0.61
14.6 (OMC+2%)	10	14.4	9.84	3 – 4	3.6	9.53	1.59	0.65
	20	14.9	19.64	2 – 4	2.8	10.50	0.88	0.72
	50	14.5	50.35	2 – 4	3.1	16.46	0.54	0.71

Higher values of the pullout resistance factor F* and α, are expected for lower moisture contents (i.e. higher suction values), indicating greater soil-reinforcement shear strength values. Results for both factors F* and α in **Table 6** show consistent variations with the soil moisture content and confining pressure. The only exception is the results for the factor α at OMC+2%, which could be attributed to factors such as compaction method and variations in the soil density and moisture content in the vicinity of the soil-geotextile interface.

4.3 Soil-Geotextile Interface Shear Strength

In this section, mean interface shear stress values are calculated for the OUM-NCMA marginal soil and the woven geotextile. A preliminary discussion on the soil-geotextile maximum interface shear stress is also given. Interface shear strength parameters obtained from large-scale pullout tests are compared with interface shear test parameters obtained from small-scale test results in the next chapter.

4.3.1 Interface Shear Parameters

Several authors have proposed the use of pullout tests to compute soil-reinforcement interface parameters such as interface friction angle and intercept adhesion (Zhai et al. 1996, Alobaidi et al. 2005, Koerner 2005, Hatami et al. 2010, 2011a, b). This is due to the frictional interaction between the soil and the reinforcement during pullout. However, the standard to evaluate the geosynthetic pullout capacity (ASTM D6706) does not include the calculation of shear stress values in its scope. Soil-geosynthetic interface shear tests (IST - ASTM D5321) are commonly accepted to evaluate these parameters. The extensibility of geotextile reinforcement typically leads to large and non-uniform deformations during the pullout mechanism whereas the deformation of the geosynthetic is restrained in the IST. Pullout tests represent the actual pullout mechanism and represent the actual distribution of the interface shear stress along the reinforcement length.

For comparatively inextensible materials such as metal strips and grouted soil nails, the pullout mechanism consists of linear friction with small or no deformation along the reinforcement length. In this case, the use of either the interface shear or pullout testing methodologies could be used to obtain comparable interface shear strength parameters. Nevertheless, some researchers have found significant differences between pullout and interface shear tests, which have been attributed to scale effects, moisture content and soil type (e.g. Pradhan 2003, Chu 2005, Gurpersaud et. al 2010).

4.3.1.1 Mean interface shear stress

The authors that use pullout test results to evaluate shear interface parameters usually determine the stress as mean stress values which do not depend on the reinforcement deformation (Zhai et al. 1996, Alobaidi et al. 2005, Koerner 2005, Hatami et al. 2011b). Therefore, the area reduction factor is not needed in the computation of the shear resistance as shown in **Equation** 6. However, it could result in underestimation of the reinforcement resistance.

Figure 50 shows the Mohr-Coulomb envelopes on the frontal and lateral planes, as calculated using **Equation** 6. **Table 7** summarizes the target and actual testing conditions, maximum pullout capacity and shear stresses on the geotextile.

$$\tau_{mean} = \frac{F_{p-\max}}{A_g} \qquad [6]$$

Where,

τ_{mean} = mean shear stress on reinforcement in kPa

$F_{p\text{-}max}$ = maximum pullout force in kN

A_g = total area of geotextile embedded in the soil, i.e. 2 times width × length

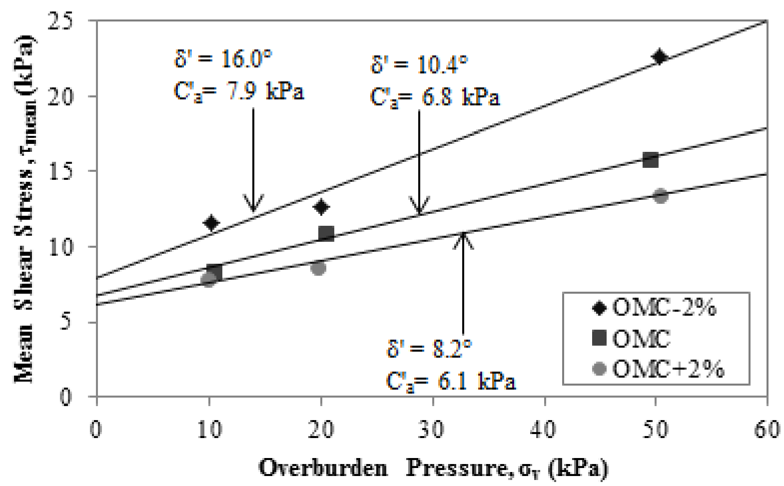

(a)

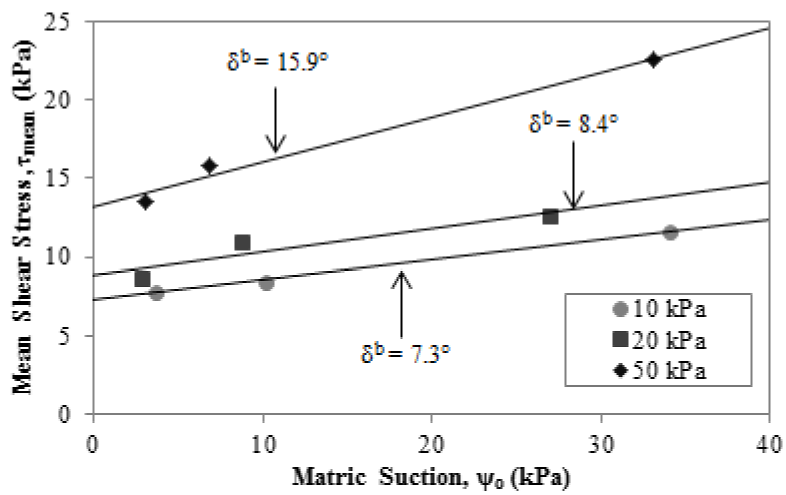

(b)

Figure 50. Mohr-Coulomb envelopes for the mean shear stresses at pullout at different overburden pressures on the a) frontal plane and b) lateral plane

Table 7. Large-scale pullout results including shear strength

Target conditions		Actual conditions		Matric Suction	Peak Pullout	Mean Shear Stress
ω (%)	σ_v (kPa)	ω (%)	σ_v (kPa)	ψ_o (kPa)	$P_{r\,max}$ (kN/m)	τ_{mean} (kPa)
10.6 (OMC-2%)	10	10.5	10.3	34	14.2	11.6
	20	10.7	20.1	27	15.4	12.6
	50	10.3	50.3	33.1	27.5	22.6
12.6 (OMC)	10	12.6	10.4	10.2	10.3	8.4
	20	12.5	20.4	8.7	13.4	11.0
	50	12.8	49.4	6.9	19.3	15.8
14.6 (OMC+2%)	10	14.4	9.8	3.6	9.5	7.8
	20	14.9	19.6	2.8	10.5	8.6
	50	14.5	50.4	3.1	16.5	13.5

Results given in **Figure 50** and **Table 7** clearly show the influence of the moisture content and suction on the pullout capacity of the geotextile. As the moisture content increases from OMC-2% (10.6%) to OMC (12.6%) and OMC+2% (14.6), the matric suction decreases from mean values of 31.4 kPa to 8.6 kPa and 3.2 kPa, respectively. Pullout resistances at low matric suction values (e.g. 3.2 kPa) are up to 40% lower than values at high suction values (e.g. 31.4 kPa) for the same overburden pressure.

The Mohr-Coulomb envelopes in **Figure 50** indicate that both the soil-geotextile adhesion and interface friction angle obtained from pullout tests are functions of the matric suction. Reduction in the adhesion is in agreement with the theory of unsaturated soils, which states that cohesion of the soil is expected to decrease as the matric suction decreases. The soil internal friction angle is expected to be unaffected by the change in suction, which based on the results from small-scale tests is not the case. Pullout test results on Minco silt and Chickasha clay by Hatami et al. (2010, 2011a,b) indicated that suction affected the soil-geotextile adhesion but had little influence on the measured interface friction angle. Nevertheless, there are several possible reasons that support the current findings. Recent studies have found that interface friction angle may be affected by changes in moisture content depending on the soil and reinforcement materials used (e.g. Pradhan 2003, Chu 2005, Gurpersaud et. al 2010).

The results found in the present study also indicate that the effect of the clay portion on the soil-geotextile interface strength is especially important for high moisture content values. This is believed to be due to the structure that the clay exhibits depending on the state of moisture content, i.e. clays present a flocculated structure on the dry side of OMC and a disperse structure on the wet side.

4.4 Average Strain of the Geotextile within the Soil

The deformation of the geotextile within the soil was measured using four (4) extensometers attached to the geotextile specimens at different positions (**Figure 20**). The displacement measured at each extensometer position at pullout was used to calculate the average displacement (ε_{avg}) over the span between two consecutive extensometers.

Figure 51 shows the results for a test carried out at OMC-2% and 20 kPa overburden pressure. Results shown in **Figure 51** and similar results on other test cases confirmed that geotextile deformation at the front end was significantly larger than its deformation at the tail end.

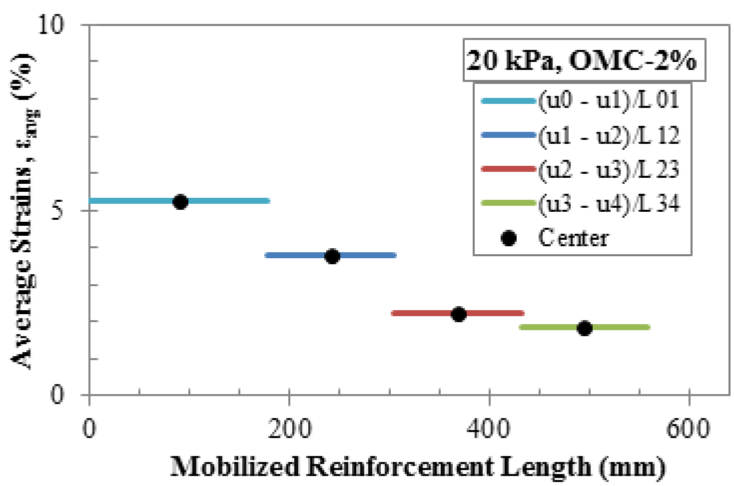

Figure 51. Geotextile average strains at OMC-2% and 20 kPa

4.5 Quality Control Program

4.5.1 Moisture Content and Matric Suction

The OUM-NCMA marginal soil was prepared at target moisture contents of OMC-2%, OMC and OMC+2%. **Figure 52** through **Figure 54** show the target moisture contents and variations for three different overburden pressures, i.e. 10, 20 and 50 kPa, respectively. Results are grouped for the same level of overburden pressure. The moisture content was monitored at eight different levels within the soil. The continuous lines are the range bars for the soil moisture content, and the bullets represent the actual mean water contents before testing (B.T.) and after testing (A.T.). Samples were taken during compaction (B.T.) and during the excavation (A.T.). The dashed lines indicate the corresponding target moisture content values, i.e. OMC-2%, OMC and OMC+2%.

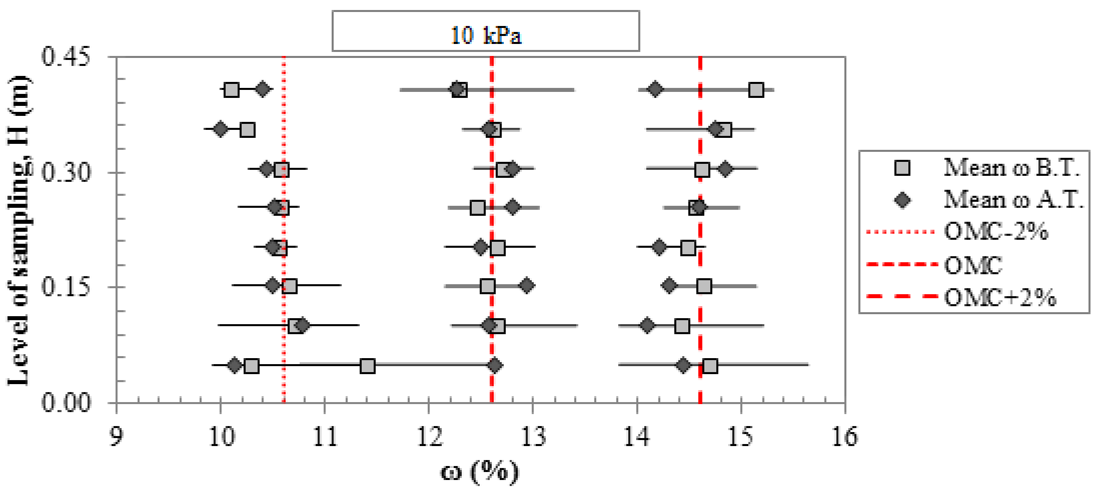

Figure 52. Results of mean moisture content and its variation for tests carried out at 10 kPa

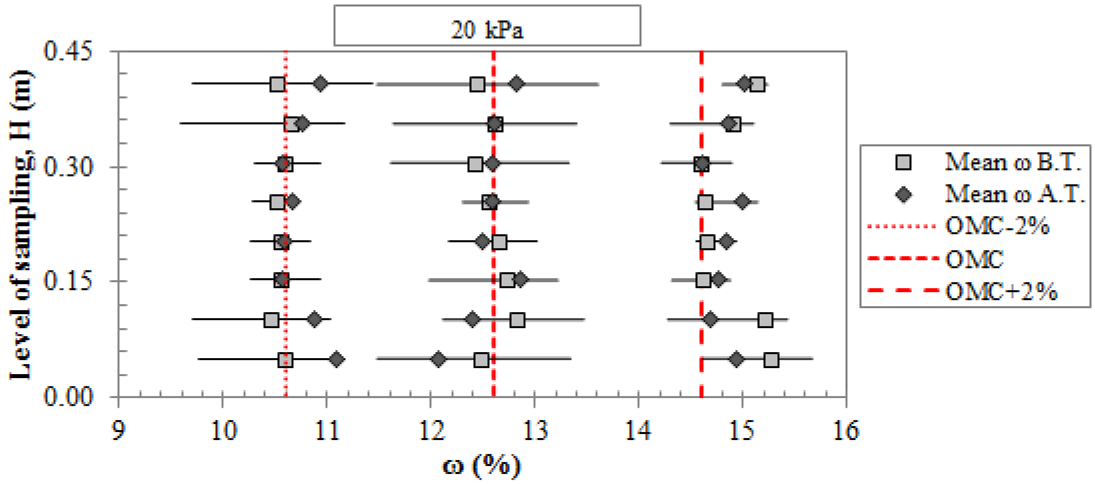

Figure 53. Results of mean moisture content and its variation for tests carried out at 20 kPa

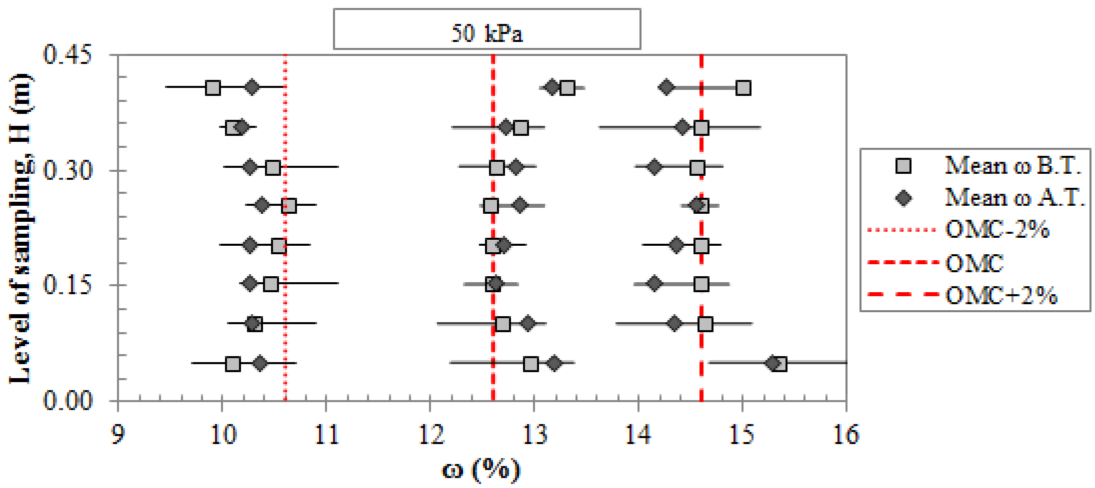

Figure 54. Results of mean moisture content and its variation for tests carried out at 50 kPa

In general, **Figure 52** through **Figure 54** show small variations of the moisture content near the soil-geotextile interface. **Table 8** summarizes the moisture content results and shows the variations measured between the soil compaction and excavation stages, i.e. before and after testing. In the table, the total moisture content refers to the moisture content of the soil mass and was calculated based on at least 24 samples taken from different levels in the pullout box for each test. The interface moisture content was calculated based on at least 16 samples taken from the vicinity of the soil-geotextile interface, i.e. 100 mm above and 100 mm beneath the geotextile specimen.

Table 8. Summary and variations of moisture contents

Target conditions		Total Moisture Content				Interface Moisture Content			
ω (%)	σ_v (kPa)	Before test (%)	After test (%)	Variation Δ (%)	Mean value (%)	Before test (%)	After test (%)	Variation Δ (%)	Mean value (%)
10.6 (OMC-2%)	10	10.5	10.4	0.1	10.5	10.6	10.5	0.1	10.6
	20	10.5	10.7	-0.2	10.6	10.6	10.6	0.0	10.6
	50	10.3	10.3	0.0	10.3	10.5	10.3	0.2	10.4
12.6 (OMC)	10	12.5	12.6	-0.1	12.6	12.6	12.6	0.0	12.6
	20	12.6	12.5	0.1	12.6	12.6	12.5	0.1	12.6
	50	12.8	12.8	0.0	12.8	12.6	12.7	-0.1	12.7
14.6 (OMC+2 %)	10	14.7	14.4	0.3	14.6	14.6	14.4	0.2	14.5
	20	14.9	14.9	0.0	14.9	14.6	14.9	-0.3	14.8
	50	14.8	14.5	0.3	14.7	14.6	14.4	0.2	14.5

Table 9 summarizes the matric suction measured with the 2100F tensiometers as a function of the mean moisture contents and overburden pressures. For OMC-2% and 20 kPa, the measured suction value seems too low when compared to similar moisture content conditions. This result could be attributed to clogging of the ceramic cups due to high contents of clay in the soil. The ceramic cups were sandpapered occasionally to mitigate the clogging. However, chemical products were not used to mitigate the storage of clay particles in the porous cups.

Table 9. Summary of matric suction as a function of moisture content and target overburden pressures

Target conditions		Mean values		
ω (%)	σ_v (kPa)	ω (%)	σ_v (kPa)	ψ_o (kPa)
10.6 (OMC-2%)	10	10.6	10.3	34.0
	20	10.6	20.1	27.0
	50	10.4	50.3	33.1
12.6 (OMC)	10	12.6	10.4	10.2
	20	12.6	20.4	8.7
	50	12.7	49.4	6.9
14.6 (OMC+2%)	10	14.5	9.8	3.6
	20	14.8	19.6	2.8
	50	14.5	50.4	3.1

Figure 55 shows the soil water characteristic curve (SWCC) obtained using the large-scale test results presented in **Table 9**. The figure shows that matric suction decreases as the soil moisture content increases from OMC-2% (10.6%) to OMC+2% (14.6%). The reduction in matric suction is especially significant when moisture content increases from OMC-2% to OMC (12.6%).

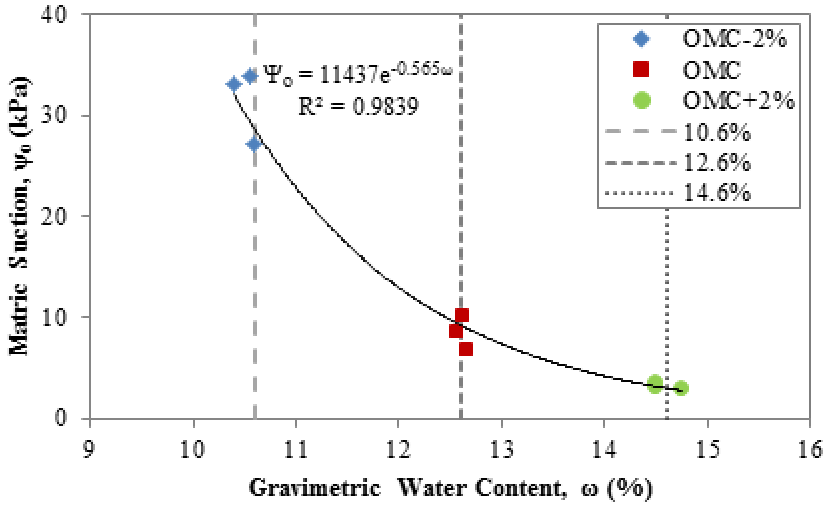

Figure 55. Large-scale SWCC of the OUM-NCMA marginal soil

4.5.2 Overburden Pressure

Table 10 summarizes the overburden pressures measured at the beginning of the test and the value projected for the time of pullout. The overburden pressure value projected for the time of pullout was calculated as the average between the overburden pressure measured before and after the test. Overburden pressures were set at 10, 20 and 50 kPa as described in the Experimental Program. The ASTM test protocol for measuring geosynthetics pullout capacity (ASTM D6706) recommends the use of normal stress–loading devices such as flexible pneumatic, e.g. air-bags, or hydraulic diaphragm-loading device capable of maintaining the vertical stress within ±2% (ASTM 2007). Results obtained during this study using an air-bag were found to be satisfactory based on the above criteria.

Table 10. Summary and variation of overburden

Target conditions		Overburden pressure			
ω (%)	σ_v (kPa)	Before testing (kPa)	At pullout (kPa)	Total change (kPa)	Variation (%)
10.6 (OMC-2%)	10	10.5	10.3	0.2	1.9
	20	20.2	20.1	0.1	0.5
	50	50.2	50.3	-0.1	-0.2
12.6 (OMC)	10	10.4	10.4	-0.0	0.0
	20	20.6	20.4	0.2	0.7
	50	50.3	49.4	0.9	1.0
14.6 (OMC+2%)	10	9.9	9.8	0.1	0.9
	20	20.0	19.6	0.4	1.0
	50	50.4	50.4	0.0	0.0

4.5.3 Pullout Displacement Rate

Figure 56 shows the actuator displacement rate data for a test at OMC and 50 kPa overburden pressure. The displacement rate measured is that of the actuator (and the clamp). The date terminates at the moment of pullout. The ASTM D6706 test protocol recommends the use of a system capable of applying a pullout force at a constant rate of displacement of 1 mm/min ±10% when no pore pressure excess is anticipated.

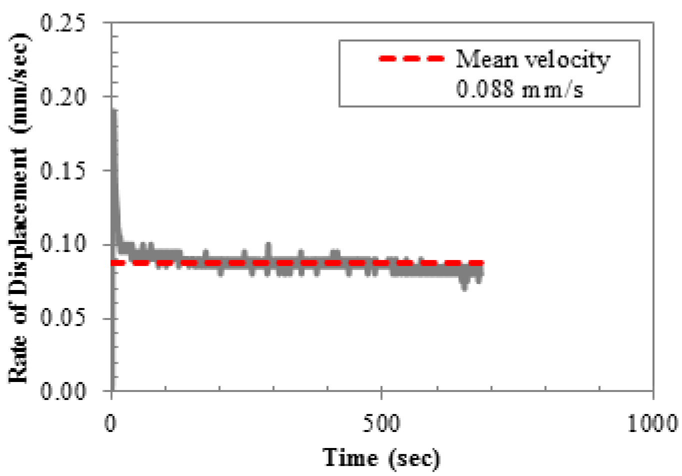

Figure 56. Actuator displacement rate for the pullout test at OMC and 50 kPa overburden pressure

Table 11 shows the actuator displacement rates measured during each test, together with values of the standard deviation (S) and coefficient of variation (CV). The calculated displacement rate of the geotextile at the location of the first extensometer inside the soil (near the front end) is also reported. The mean value for this latter in-soil displacement rate over all the large-scale pullout tests in this study was calculated as 1.1 mm/min with a standard deviation of 0.3 mm/min.

Table 11. Calculated displacement rates for the actuator and the front end of the geotextile in pullout tests

Target conditions		**Actuator Displacement Rate**			
ω (%)	σ_v (kPa)	Average Speed (mm/min)	Standard Deviation, S (mm/min)	Coefficient of Variation, CV (%)	Geotextile* (mm/min)
10.6 (OMC-2%)	10	7.9	0.28	3.5	1.2
	20	3.1	0.21	6.6	1.0
	50	3.8	0.86	21.1	1.0
12.6 (OMC)	10	9.8	0.27	2.8	1.7
	20	8.8	0.30	3.4	1.0
	50	5.3	0.28	5.3	0.7
14.6 (OMC+2%)	10	6.7	0.21	3.1	0.8
	20	5.2	0.31	5.8	1.2
	50	6.6	0.31	4.6	1.4

* Calculated at the location of the first extensometer (front end) on the geotextile in soil

Although the displacement rates of the clamp were higher than the target value (i.e. 1 mm/min), the values in the last column of **Table 11** indicate that the geotextile displacement rates inside the soil were in close agreement with the recommended rate in the ASTM D6706 test protocol. This was due to the presence of an in-air geotextile segment in between the clamp and its in-soil portion in the test box. It is important to note that the displacement rate along the length of the geotextile was variable as it was mobilized during the test.

4.5.4 Soil Properties

Atterberg limits and sieve analysis tests were performed after some selected large-scale pullout tests to compare the soils properties against the NCMA recommendations and indentify any possible variations with respect to their initial values. **Table 12** summarizes the results of these tests. In general, the results indicate that the variations of the properties throughout the study very fairly small. The maximum values of standard deviation for the Atterberg limits and the sieve analyses were 0.7 and 2.5%, respectively.

Table 12. Summary of Atterberg limit and gradation test results on samples taken from large-scale pullout tests

	Atterberg Limits Values				**Gradation (% passing)**		
Test	LL	PL	PI	PI*	#4	#40	#200
NCMA**	**N/A**	**N/A**	**20**	**20**	**100**	**60**	**35**
1	35.6	16.0	19.6	20	100	48	33
2	35.9	15.8	20.1	20	100	48	32
3	37.1	16.1	21.0	21	100	49	32
4	36.9	16.8	20.1	20	100	50	33
5	36.3	15.9	20.4	20	100	49	32
6	36.2	15.9	20.3	20	100	52	33
7	35.7	15.6	20.1	20	100	53	34

* Rounded to the nearest whole number
** Limits required by the NCMA
N/A: Not applicable

5. SMALL-SCALE TESTING PROGRAM RESULTS

5.1 Small-Scale Direct Shear Tests

The OUM-NCMA marginal soil was prepared and compacted at target moisture contents of OMC-2%, OMC and OMC+2%. Because the recommended strain rate in pullout tests is approximately 1 mm/min, this speed was selected for a first set of direct shear tests. An additional series of tests was carried out at a much slower displacement rate, i.e. 0.083 mm/min, to investigate if the pore water pressure had influenced the preliminary results at 1 mm/min. This displacement rate is recommended by the ASMT D3080 test protocol for dense sands with more than 5% percent of fines and assuming failure at approximately 10% strain.

5.1.1 Small-Scale Direct Shear Tests at 1mm/min

Figure 57 through **Figure 59** show the shear stress of the OUM-NCMA marginal soil as a function of the horizontal displacement. Tests were performed at 10, 20, 35 and 50 kPa of overburden pressure and 1 mm/min.

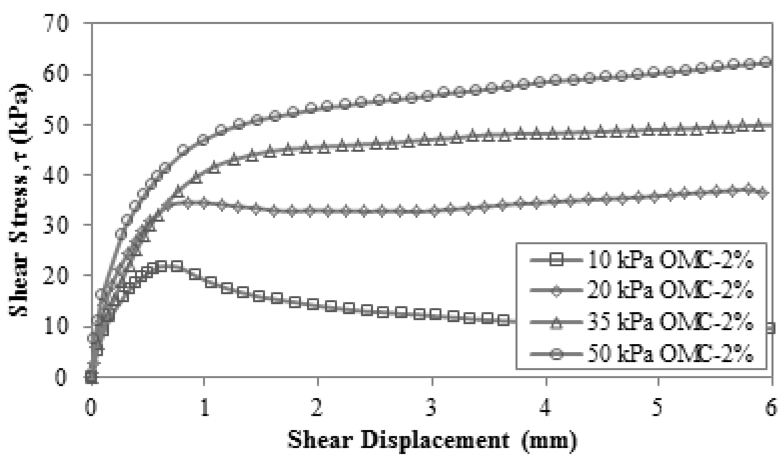

Figure 57. Shear stress of the OUM-NCMA soil at OMC-2% and 1 mm/min

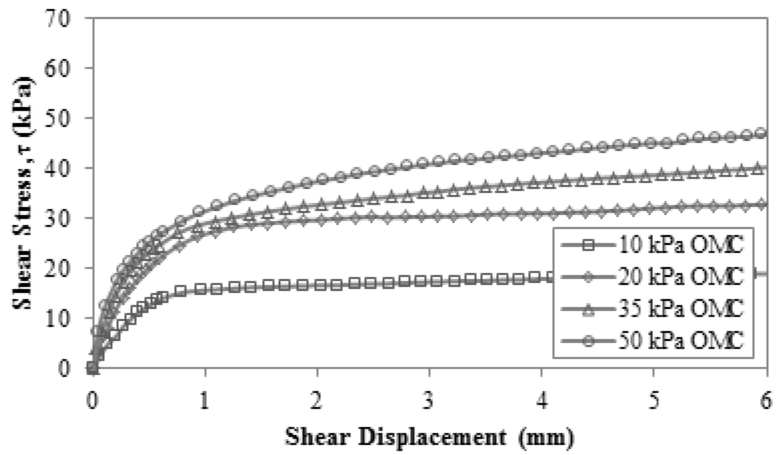

Figure 58. Shear stress of the OUM-NCMA soil at OMC and 1 mm/min

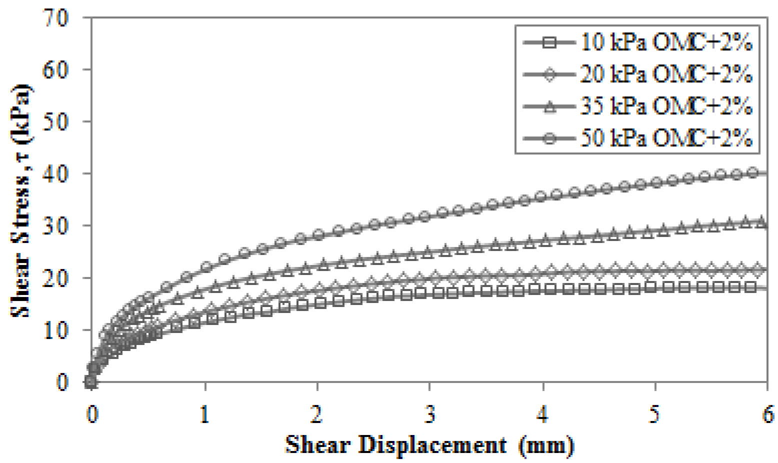

Figure 59. Shear stress of the OUM-NCMA soil at OMC+2% and 1 mm/min

Results show that the shear strength of the soil is reduced as the moisture content of the soil increases. **Figure 57** through **Figure 59** show that the peak shear stress tends to disappear as the overburden pressure increases. This behavior can be expected for dense sands and overconsolidated clays (Budhu 2000). The ASTM D3080 test protocol (ASTM 2004) recommends a failure strain between 10% and 20% strain in the absence of peak. Determination of soil friction angle and cohesion in the absence of peak relies on the assumptions and considerations stated. Several soil properties and conditions such as soil type, stress history, consolidation state, void ratio, among other parameters, are responsible for the soil shear behavior and therefore, influence the determination of these shear strength parameters.

Data points to construct the Mohr-Coulomb envelopes in **Figure 60** were determined at 10% strain, i.e. 6 mm of shear displacement. The test results for the soil compacted at OMC-2% and an overburden pressure of 10 kPa exhibited a strain-softening behavior. Including this result would have led to very high friction angles and low cohesion values, i.e. 44.5° and 14.3 kPa. This friction angle is not consistent with the type of soil tested (i.e. a clayey sand). Because this was an isolated result, this test was not included in the shear strength calculations shown in the figure.

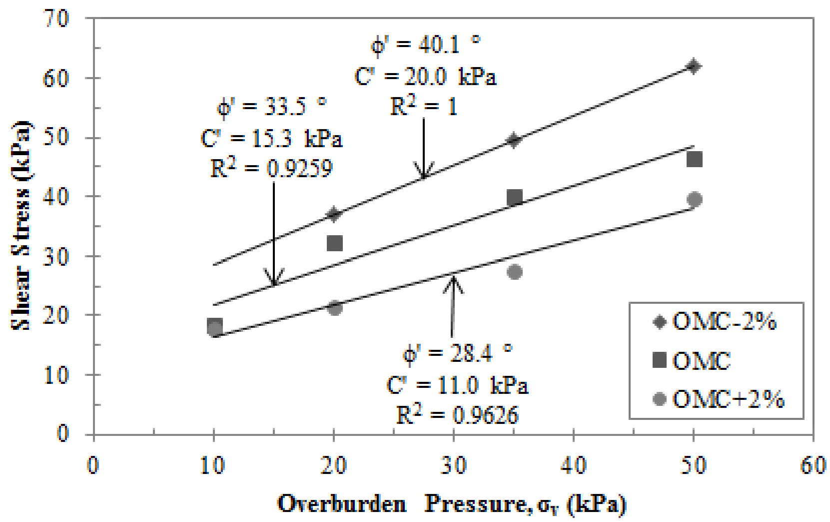

Figure 60. Mohr-Coulomb envelope of the OUM-NCMA marginal soil determined at 10% strain for different moisture contents and 1 mm/min displacement rate

5.1.2 Small-Scale Direct Shear Tests at 0.083 mm/min

An additional series of small-scale direct shear tests (DST) was carried out on the OUM-NCMA soil at a slower displacement rate of 0.083 mm/min at three different moisture contents to evaluate the influence of the shearing speed on the measured shear strength. This displacement rate was calculated based on the recommendations given in the ASTM D3080 for dense sands with more than 5% of fines (ASTM 2004). These tests were carried out at 10, 20 and 50 kPa of overburden pressure. **Figure 61** through **Figure 63** shows the measured strain-stress results. **Figure 64** shows the corresponding Mohr-Coulomb envelopes at peak or 10%.

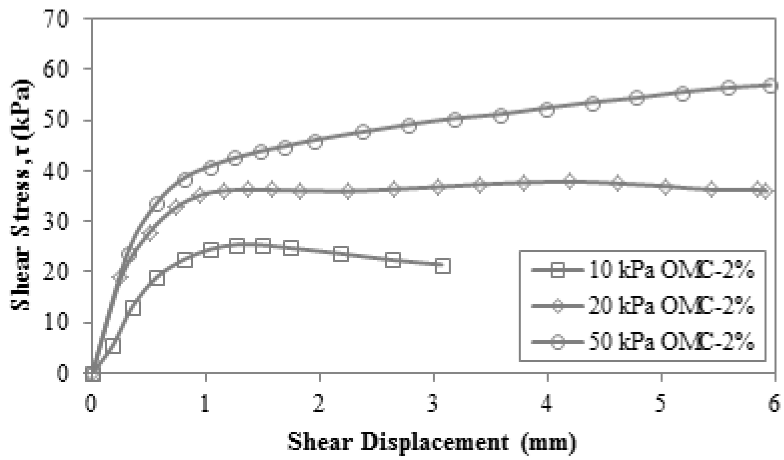

Figure 61. Shear stress at OMC-2% and 0.083 mm/min

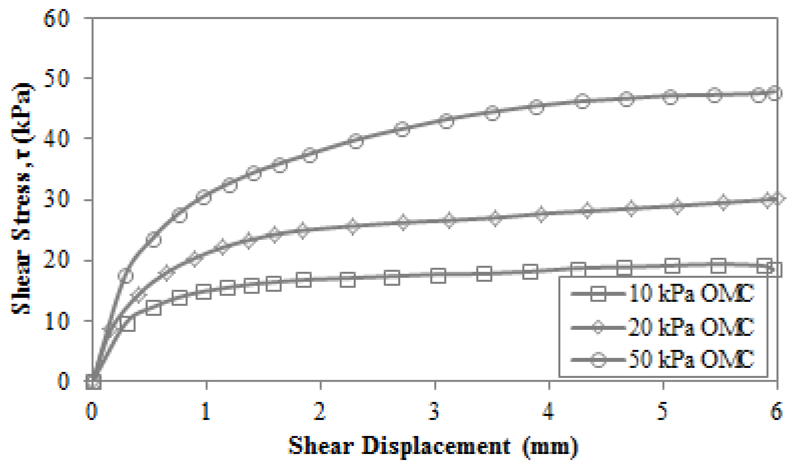

Figure 62. Shear stress at OMC and 0.083 mm/min

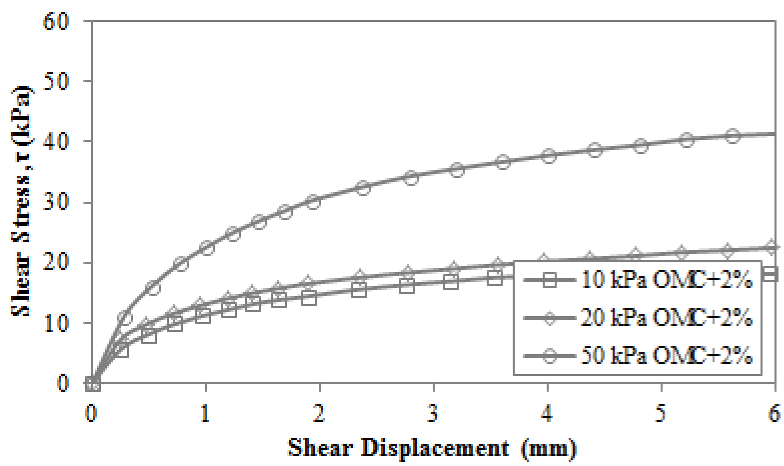

Figure 63. Shear stress at OMC+2% and 0.083 mm/min

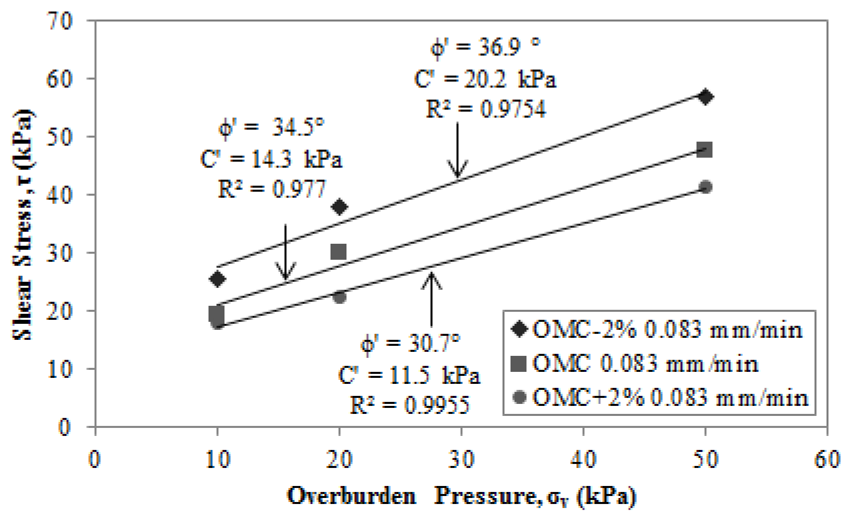

Figure 64. Mohr-Coulomb envelope of the OUM-NCMA marginal soil determined at 10% strain for different moisture contents and 0.083 mm/sec displacement rate

Figure 60 and **Figure 64** indicate that the results from the tests performed at different displacement rates are in general agreement with each other. The greatest variations among the test results were observed for the friction angle while the cohesion remained approximately constant. The DST results showed that shear the strength of the OUM-NCMA marginal soil decreased as the moisture content increased. This is attributed to the loss of matric suction at higher moisture content values. The greatest variations in the friction angle and soil cohesion were approximately 5° and 1 kPa at OMC-2%. For OMC and OMC+2%, these variations were approximately 2° and less than 1 kPa, respectively.

Results summarized in **Table 13** show the variations of the soil internal friction angle and cohesion as function of moisture content and strain. Since the soil tested is mostly sand (i.e. contains approximately 67% sand particles), some differences among the results may be attributed to sample preparation rather than strain rate or development of pore water pressure. The strength parameters are presented as effective values based on the assumption that no pore pressure was developed during shearing. Moisture content results before compaction and after the tests indicated variation within a range of ±0.4% of the target values. No significant variations of the moisture contents were measured between the beginning and end of the tests. These small variations occurred mostly during sample preparation.

Table 13. Measured friction angle and cohesion of the OUM-NCMA marginal soil at 10% strain and different moisture contents

	1 mm/min			0.083 mm/min		
	OMC-2%	**OMC**	**OMC+2%**	**OMC-2%**	**OMC**	**OMC+2%**
ϕ' (°)	40.1	33.5	28.4	36.9	34.5	30.7
C'(kPa)	20.0	15.3	11.0	20.2	14.3	11.5

Suction-controlled tests on unsaturated specimens have been conducted in several studies using triaxial and direct shear devices (e.g. Satija 1978, Escario 1980, Ho and Fredlund 1982, Gan et al. 1988, Hatami et al. 2010, Khoury et al. 2011). In these studies, it was found that variation in the soil suction primarily influences the soil cohesion and the friction angle remained fairly constant. As mentioned before, other studies have found that interface friction angle may be affected by changes in moisture content depending on the soil and reinforcement materials used (e.g. Pradhan 2003, Chu 2005, Gurpersaud et. al 2010).

The variation of the friction angle with moisture content observed in the present study could be attributed to testing conditions, scale effects and sample preparation. It is very important to recall that soils compacted at different moisture contents cannot be compared as if they were identical samples. For compacted soils, Fredlund (1993) pointed out that samples must be considered as "identical" only if the soil is compacted at the same initial water content and using the same compaction effort. Samples compacted at different moisture contents must be considered different. The compaction effort required to achieve the same dry unit weight decreased as the moisture content increased. Besides, these tests were not carried out in a suction-controlled environment and hence, matric suction might have changed during shearing, especially at relatively high suction values (i.e. low moisture contents).

Soils with a significant amount of fine particles such as the OUM-NCMA (which has approximately 33% of fines) develop a different structure depending on the water content at which they are compacted. Soils compacted on the dry side of OMC present a flocculated structure while soils compacted on the wet side of OMC exhibit a dispersed structure. Therefore, different results of friction angle and cohesion as presented here are deemed reasonable and explain the different behavior of the soil when compacted at different moisture contents.

5.2 Small-Scale Pullout Tests

As described in the **Section** 3, small-scale pullout tests were carried out using different materials as front boundaries including a rigid boundary, Styrofoam, cardboard and rubber. The shear stress on the geotextile was calculated as an average value as given in **Equation** 6. Due to the small size of the geotextile strip, it was assumed that the deformation of the specimen within the soil during small-scale pullout tests was negligible and hence the area of geotextile in contact with the soil, remained constant throughout the test.

A challenge during the testing program was to obtain repeatable results for small-scale pullout tests that were performed under the same conditions of moisture content and vertical stress. The challenge was due to the small size of the test specimens and the amount of the materials used. To verify the level of repeatability at this scale, duplicate tests were carried out to determine the soil-reinforcement interface shear strength. The results presented in this study arethose with the smallest variability in the data.

Small-scale pullout tests were initially performed at a strain rate of 1 mm/min as recommended by the ASTM D6706. Results obtained using Styrofoam at this speed were not reasonable and did not show well defined trends. These results are not presented here. Results obtained using cardboard were also discarded because this material is very compressible and hence, the target soil density could have been inaccurate. A new series of tests using Styrofoam was carried at a strain rate of 0.074 mm/min, which corresponds to the mean speed at large-scale pullout tests (i.e. 1.11 mm/min) scaled down by a factor of 15. No duplicate tests were carried out during this last series of tests.

5.2.1 Small-Scale Pullout Tests at 1.0 mm/min

Figure 65 shows the mean strength values calculated using a rigid front boundary, i.e. the front wall of the shear box, and the maximum variation bars for each moisture content. The maximum Deviation Standard (S) and Coefficient of Variation (CV) were 3.8 kPa and 11%, respectively. These values corresponded to the test prepared at OMC-2% and 50 kPa overburden pressure. **Figure 66** shows the mean strength values calculated using rubber obtained from papermate© eraser as a front boundary. The maximum Deviation Standard (S) and Coefficient of Variation (CV) were 5.1 kPa and 31%, respectively. These values corresponded to OMC and 10 kPa. However, the mean S and CV values for all the tests performed at 1 mm/min using a rubber were calculated as 1.95 kPa and 10%.

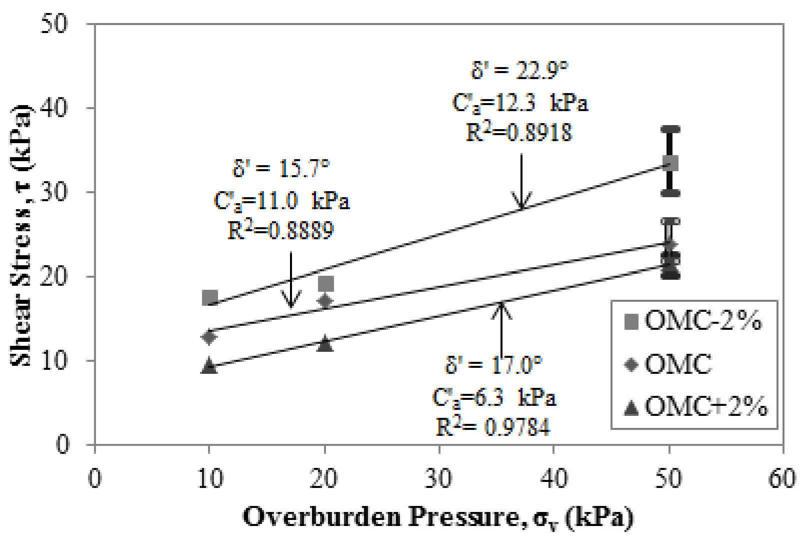

Figure 65. Mohr-Coulomb envelopes at different moisture contents from small-scale pullout tests using a rigid front boundary at 1 mm/min

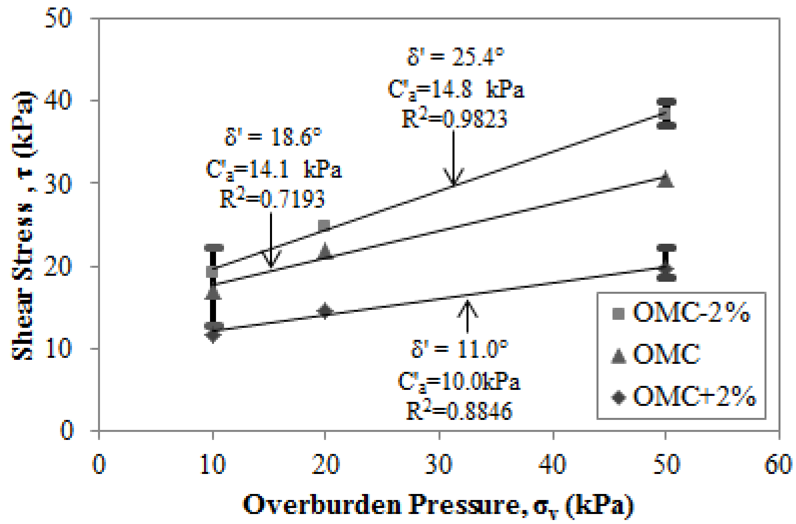

Figure 66. Mohr-Coulomb envelopes at different moisture contents from small-scale pullout tests using a rubber as a front boundary at 1 mm/min

Table 14 compares the mean shear strength values obtained from large-scale tests and small-scale tests with rubber and steel as front boundary. Large-scale pullout resistance values are represented by calculated mean shear stresses. **Table 15** shows the ratio among the test results after normalizing them with respect to the large-scale pullout resistance values. **Table 16** summarizes the interface shear strength parameters calculated from mean shear stresses.

Table 14. Summary of large and small scale mean shear strengths

	Mean Interface Shear Strength, τ_{mean} (kPa)								
	Large-Scale			Small-Scale (rigid boundary)			Small-Scale (rubber boundary)		
σ_v (kPa)	**OMC-2%**	**OMC**	**OMC+2%**	**OMC-2%**	**OMC**	**OMC+2%**	**OMC-2%**	**OMC**	**OMC+2%**
10	11.63	8.44	7.82	17.67	12.81	9.47	19.19	17.04	11.62
20	12.61	10.97	8.61	19.24	17.09	12.17	24.84	21.81	14.45
50	22.56	15.81	13.50	33.59	24.64	21.53	38.40	30.70	19.72

Table 15. Summary of ratios between large and small scale shear strengths

	Large-Scale			Small-Scale (rigid boundary)			Small-Scale (rubber boundary)		
σ_v (kPa)	**OMC-2%**	**OMC**	**OMC+2%**	**OMC-2%**	**OMC**	**OMC+2%**	**OMC-2%**	**OMC**	**OMC+2%**
10	1.00	1.00	1.00	1.52	1.52	1.21	1.65	2.02	1.49
20	1.00	1.00	1.00	1.53	1.56	1.41	1.97	1.99	1.68
50	1.00	1.00	1.00	1.49	1.56	1.59	1.70	1.94	1.46

Table 16. Summary of soil-geotextile interface parameters from mean shear strengths

	Large-Scale			Small-Scale (rigid boundary)			Small-Scale (rubber boundary)		
	OMC-2%	**OMC**	**OMC+2%**	**OMC-2%**	**OMC**	**OMC+2%**	**OMC-2%**	**OMC**	**OMC+2%**
δ´ (°)	16.0	10.4	8.2	22.9	15.7	17.0	25.4	18.6	11.0
C'_a (kPa)	7.9	6.8	6.1	12.3	11.0	6.3	14.8	14.1	10.0
$\mathbf{R^2}$	0.980	0.991	0.990	0.892	0.889	0.978	0.982	0.719	0.885

The average ratio of the small-scale to large-scale pullout test results for the 1.0 mm/min pullout rate using a rigid front boundary was 1.49. This means that the calculated average shear strength from pullout tests at small-scale was approximately 50% greater than that at large-scale. The standard deviation (S) and maximum coefficient of variation (CV) for the small-scale results were calculated as 0.12 and 0.10 (10%), respectively. These preliminary results are overall satisfactory and indicate that large-scale and small-scale pullout tests can be compared and small-scale tests could be used as an alternative to evaluate soil-reinforcement interaction for marginal soils.

5.2.2 Small-Scale Pullout Tests at 0.074 mm/min

Figure 67 shows the mean soil-geotextile interface shear strength calculated using Styrofoam as a front boundary at a strain rate of 0.074 mm/min. Similar to the results shown previously, these test data show greater pullout capacity for the soil tested at lower moisture contents. Only one test was performed per each testing condition.

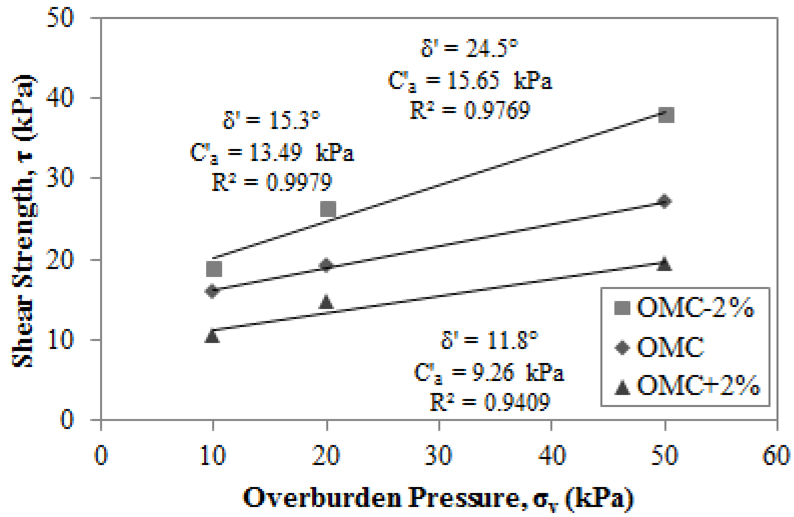

Figure 67. Mohr-Coulomb envelopes at different moisture contents from small-scale pullout tests using Styrofoam as a front boundary at 0.074 mm/min

Table 17 through **Table 19** show a summary of the mean soil-reinforcement interface shear strength, the ratios of shear strength values calculated from large-scale and small-scale test data and the interface shear parameters calculated from pullout tests, respectively.

Table 17. Summary of large-scale and small-scale mean shear strength values at the soil-geotextile interface

	Mean Interface Shear Strength, τ_{mean} (kPa)					
	Large-Scale			Small-Scale (Styrofoam boundary)		
σ_v (kPa)	**OMC-2%**	**OMC**	**OMC+2%**	**OMC-2%**	**OMC**	**OMC+2%**
10	11.63	8.44	7.82	18.99	16.01	10.45
20	12.61	10.97	8.61	26.38	19.26	14.67
50	22.56	15.81	13.50	38.02	27.12	19.44

Table 18. Summary of ratios of shear strength values calculated from large-scale and small-scale test data

	Large-Scale			Small-Scale (Styrofoam boundary)		
σ_v (kPa)	**OMC-2%**	**OMC**	**OMC+2%**	**OMC-2%**	**OMC**	**OMC+2%**
10	1.00	1.00	1.00	1.63	1.90	1.34
20	1.00	1.00	1.00	2.09	1.76	1.70
50	1.00	1.00	1.00	1.69	1.72	1.44

Table 19. Summary of soil-geotextile interface parameters using mean shear strength values at the soil-geotextile interface

	Large-Scale			Small-Scale (Styrofoam boundary)		
	OMC-2%	**OMC**	**OMC+2%**	**OMC-2%**	**OMC**	**OMC+2%**
δ′ (°)	16.0	10.4	8.2	24.5	15.3	11.8
C'_a (kPa)	7.9	6.8	6.1	15.7	13.5	9.3
R^2	0.9759	0.9911	0.9891	0.9769	0.9979	0.9409

The mean value for the ratios reported in

Table 18 over all test cases is 1.70. This means that the calculated shear stress from pullout tests was approximately 70% greater at small scale than at large scale. The corresponding values of standard deviation (S) and coefficient of variation (CV) were calculated as 0.22 and 0.17 (17%), respectively. These values are larger than the corresponding values for the case of rigid front boundary. This means that the rigid front boundary overall resulted in less scatter in data than the test series in which a Styrofoam block was used at the front boundary of the test cell.

Several factors could have influenced the small-scale pullout test results including moisture content, density, geotextile dimensions, and scale and boundary effects. However, the overall trends are reasonable and comparable to results obtained at large-scale with greater strength properties obtained for soil prepared at a drier condition (i.e. OMC-2% as compared to specimens prepared and tested at OMC and OMC+2%). The above results, for both 1.0 mm/min and 0.074 mm/min strain rates and different materials tested, showed that measured interface shear strength values at small-scale are between 1.2 and 2.0 times as great as those from large-scale pullout tests. Further investigation of this topic is required to fully understand the factors affecting the pullout resistance when small geotextile samples are used.

5.3 Soil-Geotextile Interface Shear Strength

Figure 68 through **Figure 70** show the interface shear strength developed between the OUM-NCMA marginal soil and the woven geotextile as a function of the lateral displacement. Tests were performed at target moisture contents of OMC-2%, OMC and

OMC+2%. The strain rate was set up at 1 mm/min as recommended by the ASTM D5321. Overburden pressures varied from 10 kPa to 20 kPa and 50 kPa as indicated. Similar to DST tests, the peak strengths tend to disappear as the overburden pressure and moisture content values increase.

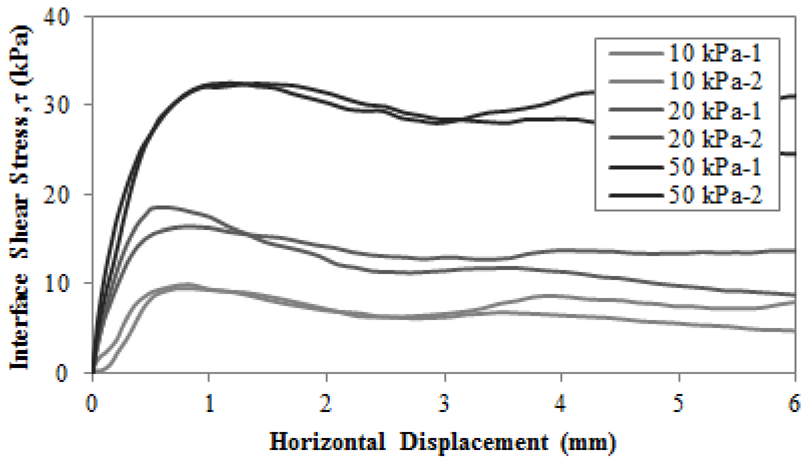

Figure 68. Soil-geotextile interface shear strength at OMC-2%

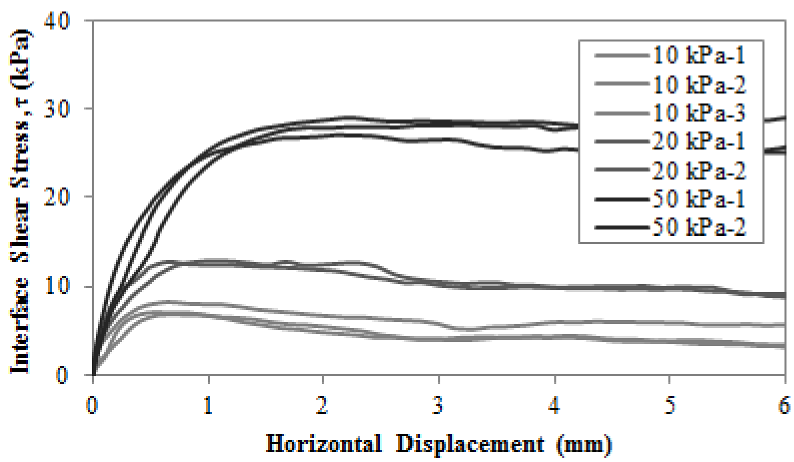

Figure 69. Soil-geotextile interface shear strength at OMC

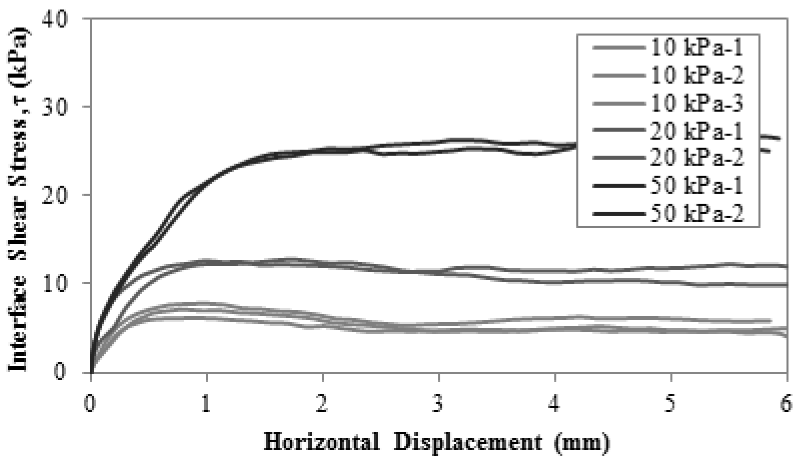

Figure 70. Soil-geotextile interface shear strength at OMC+2%

Mohr-Coulomb envelopes for the OUM-NCMA soil-geotextile interface from the Interface Shear Tests (IST) are shown in **Figure 71**. The data points shown in this figure correspond to the mean shear strength values of two or more nominally identical tests. The main purpose of running duplicate tests was to check their repeatability, which could be a concern for tests performed using shear test apparatus smaller than the size specified by the ASTM D5321. **Table 20** shows the soil-geotextile friction angles (δ'), adhesion intercept values (C_a') and coefficients of determination (R^2). The mean standard deviation (S) for all shear strength data points was calculated as 1.14 kPa, which corresponds to a mean coefficient of variation (CV) equal to 7.7%.

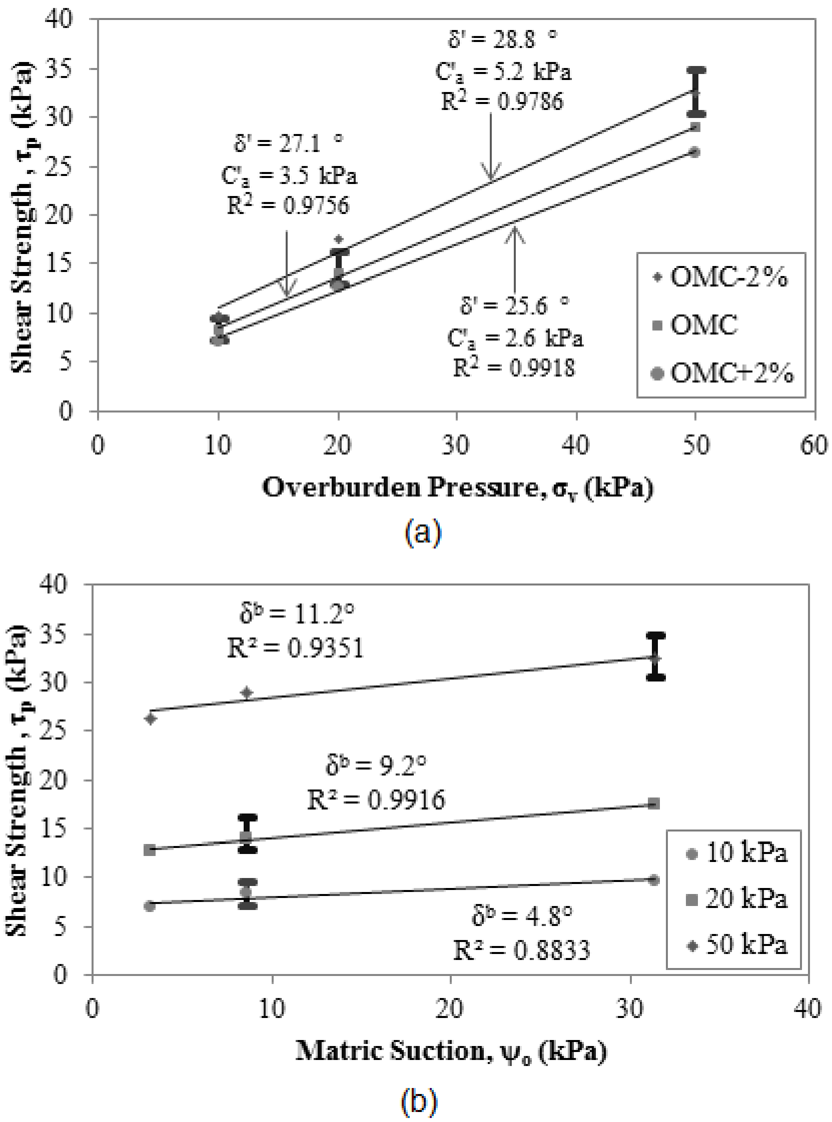

Figure 71. Mohr-Coulomb envelopes at different moisture contents from small-scale interface shear tests in (a) frontal plane and (b) lateral plane

Table 20. Soil-geotextile interface friction angle and adhesion intercept calculated from small-scale interface tests

	OMC-2%	**OMC**	**OMC+2%**
δ' (°)	28.8	27.1	25.6
C_a' (kPa)	5.21	3.49	2.56
R^2	0.9786	0.9756	0.9918

Failure envelopes in **Figure 71** indicate that both the interface friction angle and adhesion intercept of the soil-geotextile interface was lower when the soil was compacted on the wet side of OMC as compared to the dry side. The interface adhesion at OMC+2% was approximately 51% (2.65 kPa) smaller than its measured value at OMC+2%. The corresponding difference for the friction angle was approximately 11% or 3.2°. The above data indicate that the influence of matric suction was greater on the interface adhesion than on its friction angle. This observation is in agreement with previous studies on silts and clays involving suction-controlled interface shear tests and interface shear tests similar to those carried out in the present study (Hatami et al. 2010, 2011a,b).

The interface strength parameters presented in this section are also in agreement with those by Goodhue et al. (2001), who reported interface friction angle values for foundry sands (containing up to 13% of bentonite) and geotextiles between 29° and 32° at OMC. The undrained adhesion varied between 2 and 5 kPa for normal stresses of 10, 30 and 50 kPa. The matric suction varied between 25 and 38 kPa.

Even though 300 mm-square, standardized shear boxes are preferred for evaluating the soil-geosynthetic interface parameters, it has been suggested that smaller shear apparatuses could be acceptable for geotextiles and finer-grained soils (e.g. sand, silts and clays; Koerner 2005, Hatami et al. 2010, 2011a,b). The small-scale test results obtained in this study overall showed satisfactory CV and R^2 values. However, in terms of actual values obtained, the interface friction angle from large-scale pullout tests varied between 8.2° and 16.0° and the adhesion intercept between 6.1 and 7.9 kPa. The same parameters from small-scale interface shear tests varied between 25.6° and 28.8° for the interface friction angle and between 2.56 and 5.21 kPa for the adhesion intercept. Therefore, these results need to be validated using a larger shear test device as recommended by the ASTM D5321 to check their validity and whether or not smaller shear test cells would indeed be suitable to evaluate the shear interface of geotextiles in marginal soils and to determine a scale correction factor as applicable.

5.3.1 Efficiency of Soil-Geotextile Interface

The efficiency of the soil-geotextile interface indicates how effective a geosynthetic material is as compared to the soil properties. Soil-geotextile efficiency is measured for both the interface friction angle and adhesion using **Equation** 7 and **Equation** 8, respectively.

Table 21 shows the efficiency ratios calculated for each moisture content, shearing rate and the failure strain assumed in the analysis.

$$E_c = \left(\frac{c_a}{c}\right)100 \quad [7]$$

$$E_\phi = \left(\frac{\tan\delta}{\tan\phi}\right)100 \quad [8]$$

Table 21. Efficiency of soil-geotextile interface properties

	1 mm/min			0.083 mm/min		
	OMC-2%	**OMC**	**OMC+2%**	**OMC-2%**	**OMC**	**OMC+2%**
E_ϕ (%)	71.8	80.9	90.1	78.0	78.6	83.4
E_c (%)	26.0	22.8	23.3	25.8	24.4	22.2

Results in

Table 21 are in agreement with those by Martin et al. (1984) on efficiency of sandy soils in woven and nonwoven geotextiles, who found the efficiency of the geotextile to be between 77% and 100%. Woven geotextiles showed lower efficiencies (i.e. 77% to 87%) as compared to nonwoven geotextiles (i.e. 84% to 100%).

5.4 Comparison of Interface Parameters

Table 22 shows the soil-geotextile interface shear parameters as function of the moisture content and test type. In general, it is observed that the interface friction angle obtained from large-scale pullout tests is much lower as compared to the same parameter obtained from interface shear tests. The interface friction angle obtained from small-scale pullout tests is in between these two values. This behavior can be attributed to the differences between the failure mechanisms. The geotextile is subjected to a non-linear deformation during large-scale pullout tests whereas there is no deformation during interface shear tests. These results show that the interface friction angle is a function of the deformation of the reinforcement. Koerner (2005) highlighted the re-orientation of soil particles during pullout as a result of the large deformations, which reduces the shear strength interface. Regarding the soil-geotextile adhesion, the trend is not as clear as for the friction angle trend. Adhesion values obtained from small-scale pullout tests were the greatest, followed by the ones obtained from large-scale pullout tests and interface shear tests.

Table 22. Shear strength parameters of the soil-geotextile interface

		LS-PT	**SS-PT**			**IST**
Displacement rate (mm/min)		1.1	1.0	1.0	0.074	1.0
Front Boundary		Styrofoam	Rigid	Rubber	Styrofoam	N/A
δ' (°)	OMC-2%	16.0	22.9	25.4	24.5	28.8
	OMC	10.4	15.7	18.6	15.3	27.1
	OMC+2%	8.2	17.0	11.0	11.8	25.6
Ca' (kPa)	OMC-2%	7.9	12.3	14.8	15.7	5.2
	OMC	6.8	11.0	14.1	13.5	3.5
	OMC+2%	6.1	6.3	10.0	9.3	2.6

5.5 Soil Water Characteristic Curve (SWCC)

The Soil Water Characteristic Curve (SWCC) of the OUM-NCMA soil was obtained using a Pressure Plate Extractor (PPE), the 2100F Soilmoisture probes (tensiometers) and the Pressure Transducer Tensiometers (PTT, models T4 and T5). **Figure 72** shows the SWCC of the OUM-NCMA soil from the PPE tests compacted at two different moisture contents, i.e. PPE/OMC-2% and PPE/OMC, together with the mean suction values from the 2100F small-tip tensiometers that were used in the large-scale pullout tests (2100F/LS) and small-scale suction tests (2100F/SS). Suction values from the PTT from the large-scale tests (PTT/LS) are also shown in the figure. The horizontal dotted line in the figure indicates the actual limiting capacity of the tensiometers to measure the soil suction (i.e. approximately 85 kPa). A full description on the methodologies to determine the soil suction is given in **Section** 3.

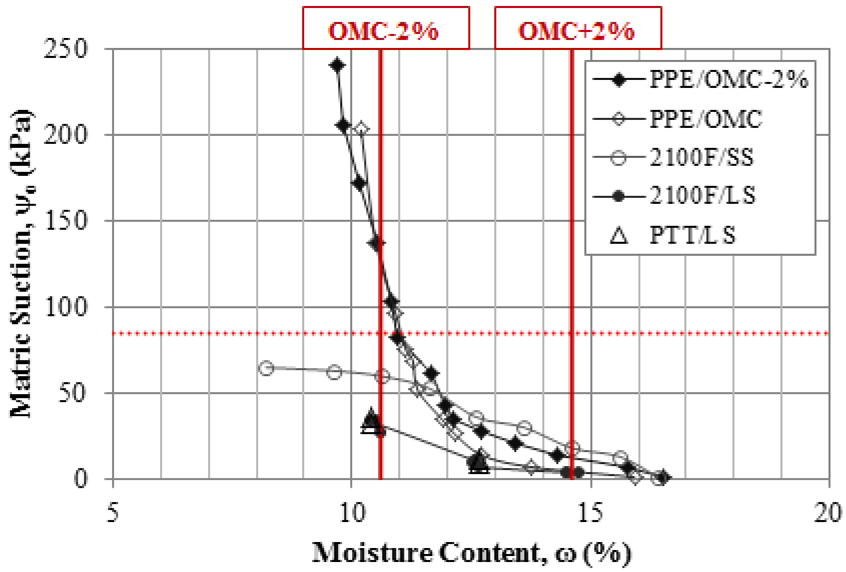

Figure 72. SWCC of the OUM-NCMA marginal soil at large and small scale using different techniques

Results shown in **Figure 72** indicate that the matric suction values from small-scale tests were measurably greater than those at large-scale. The measured suction in small samples using tensiometers (2100F/SS) was found to be especially greater than the values obtained at large scale (i.e. greater than 100% difference at some moisture content values). Pressure plate and tensiometers results on small-scale specimens were found to be comparable over a range of moisture content values (i.e. OMC-1% to practically complete saturation). In contrast, under drier conditions the SWCC increased exponentially up to a suction value equal to 138 kPa at OMC-2%, while the mean suction values from tensiometers in small-scale and large-scale specimens were found to be 60 kPa and 35 kPa, respectively.

Differences among these results may be attributed to the size of the samples, vertical stress, void ratio and soil hysteresis due to wetting and drying paths. Samples at large scale are subjected to overburden pressures from 10 to 50 kPa while no vertical stress was applied on samples at small scale. Vertical stress on the soil induced some amount of settlement, resulting in a reduction in the soil void ratio. This might have contributed in a change in the volumetric water content of the soil and the measured suction. In addition, the soil hysteresis could have affected more significantly the matric suction results obtained from large-scale pullout tests than small-scale tests. This was because in order to achieve the target moisture content, the soil used to perform the large-scale pullout tests was subjected to several wetting and drying cycles while small-scale samples were wetted only once for the tests.

It is believed that drying and wetting paths (i.e. soil hysteresis) might have contributed to the observed differences in **Figure 72**. For instance, in the pressure plate tests, the samples started a drying path from full saturation while tensiometers measured the actual matric suction at a given moisture content and confining pressure.

The T4 and T5 Pressure Transducer Tensiometers (PTT, UMS 2012) were used in selected small-scale and large-scale tests to verify the reliability of the small-tip tensiometers and the pressure plate method. Results shown in **Figure 72** indicate that the measured data from PTT probes were in overall agreement with those using small-tip tensiometers. However, suction results from PPE and PTT methods were different. This finding indicates that differences in instrumentation and methodology could lead to considerably different suction results.

According to **Figure 72**, the PPE and 2100F/SS results are in overall agreement within the range between OMC-2% and OMC+2%. The 2100F/SS results deviate from the overall trend for samples at OMC-2% and drier due to the limitation of tensiometers to measure suction beyond approximately 85 kPa. The suction readings from pullout tests at large-scale using 2100F tensiometers (2100F/LS) and PPT sensors (PPT/LS) are in close agreement with each other. However, factors such as application of overburden pressure, compaction process, small variations of moisture content over a larger soil model, among others, may have contributed to lower suction values in the large-scale pullout tests as compared to those from the small-scale test data. Nevertheless, these data indicate that the matric suction in the OUM-NCMA soil is significantly lower at OMC+2% as compared to OMC-2%. The consequence of this difference in the soil suction as related to the soil-reinforcement interface strength is discussed in the following sections.

Sreedeep and Singh (2011) reviewed several methodologies to measure matric suction in three fine-grained soils using tensiometers, the pressure plate test and the dew-point potentiometer. They concluded that factors such as the operating range and precision of each method/instrument, soil type and the equilibration time lead to different suction measurements and SWCC results.

On a more general note, there are several factors that can influence the measured value of matric suction in a soil including instrumentation technique, compaction process, soil texture, structure, stress history and density, in addition to any variations in the soil water contents. Considering all the above factors, variations in the measured matric suction and the SWCC using different methods in this study is to be expected. **Figure 72** shows that the range of matric suction values in the OUM-NCMA soil in this study varied between 0 and 200 kPa. This range is consistent with the range of suctions reported in literature for sands, sands with fines, silts and low plasticity clays have been (e.g. Fredlund 2005).

This page is intentionally blank

6. MOISTURE REDUCTION FACTOR

6.1 Development of a Moisture Reduction Factor

Moisture Reduction Factors (MRFs) were calculated to account for the change in the reinforcement interface strength and soil internal shear strength as a function of the soil moisture content. The MRFs were developed using the measured reductions in the maximum pullout capacity, interface shear strength and the soil internal shear strength at different moisture contents as compared to the corresponding values at OMC-2% (i.e. 10.6%). The OMC-2% value was taken in this study as a recommended value for the compaction of the backfill in reinforced soil structures in the field (Berg et al. 2009). The MRF is a mathematically expressed as $\mu(\omega)$, which is a function of the moisture content ω(%) in percent units.

Figure 73 through **Figure 76** show the MRFs for Large-Scale Pullout Test (LS-PT), Small-Scale Pullout Test (SS-PT), Direct Shear Test (DST) and Interface Shear Test (IST) results, respectively. The MRFs were calculated as the best fit lines for all the overburden pressure values in each test type. The MRF for SS-PT was calculated based on the tests using Styrofoam at the front boundary of the test cell at a strain rate at 0.074 mm/min. In the case of the DST, the MRF was calculated based on the test results at a strain rate of 0.083 mm/min. **Figure 77** compiles the MRFs for LS-PT, SS-PT, DST and IST.

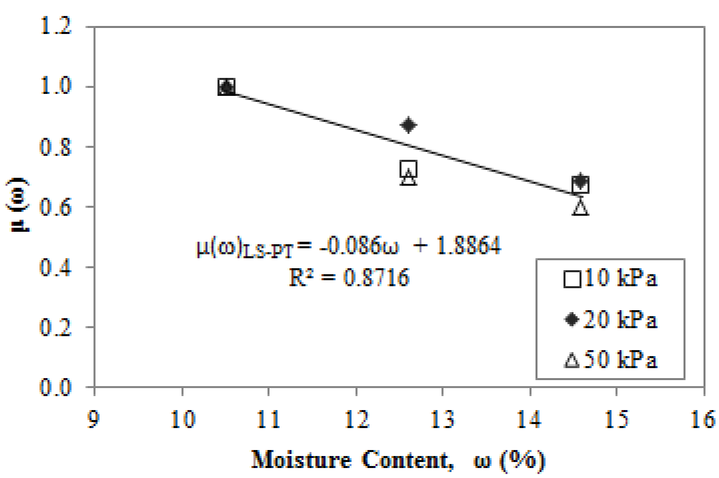

Figure 73. Moisture reduction factor (MRF) for large-scale pullout tests (LS-PT)

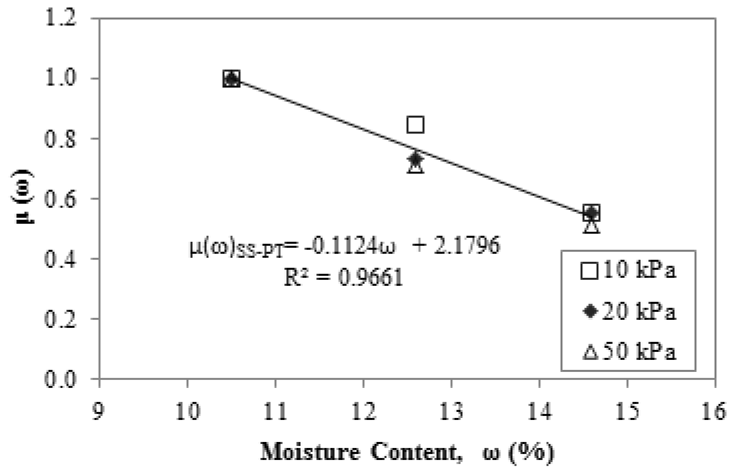

Figure 74. Moisture reduction factor (MRF) for small-scale pullout tests (SS-PT)

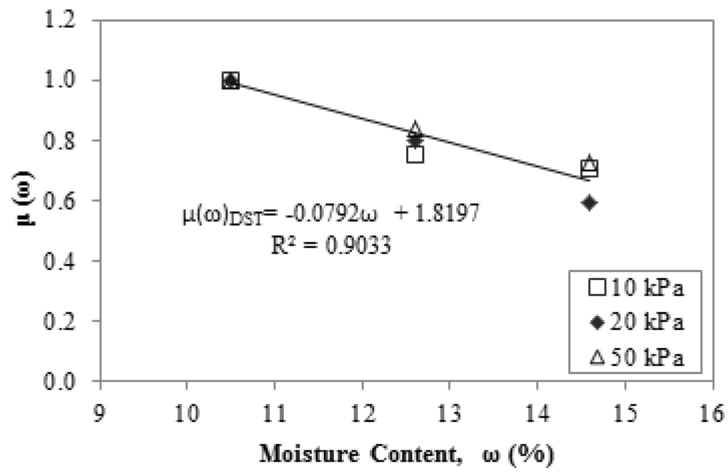

Figure 75. Moisture reduction factor (MRF) for direct shear tests (DST)

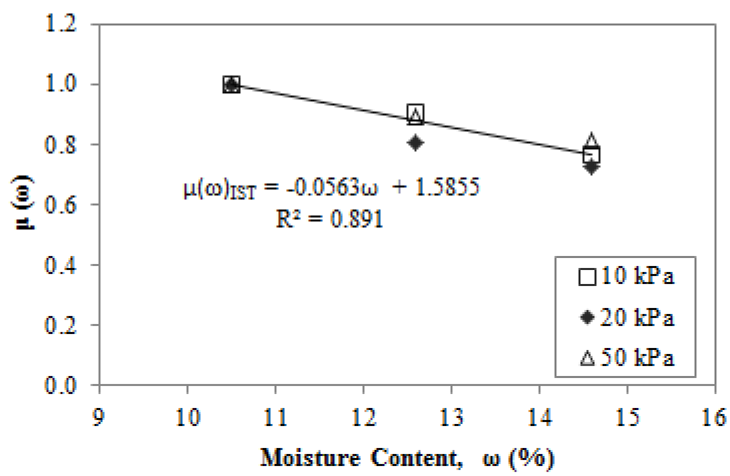

Figure 76. Moisture reduction factor (MRF) for interface shear tests (IST)

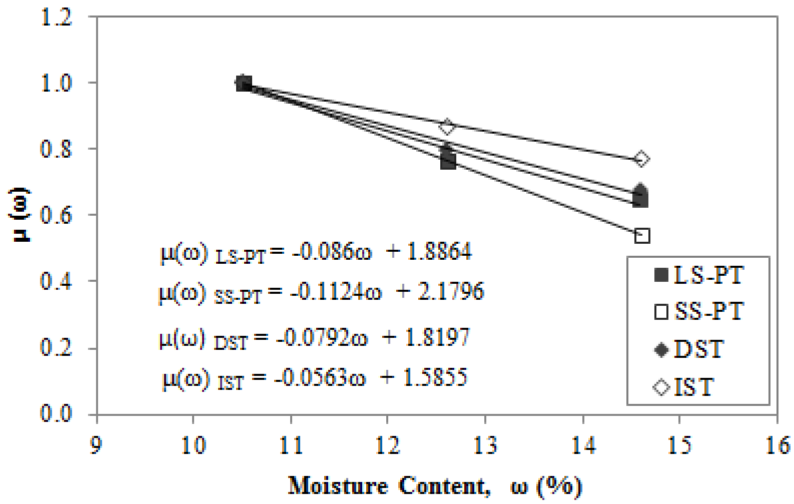

Figure 77. Comparison of moisture reduction factors (MRF)

The MRF values shown in **Figure 77**, i.e. μ(ω), were the calculated mean values of the reduction in pullout capacity (LS-PT, SS-PT) or shear strength (DST, IST) for different overburden pressures tested. According to the IST results shown in **Figure 77**, the soil-reinforcement interface strength was nearly 23.6% lower for the soil at OMC+2% as compared to the same soil placed at OMC-2%. The corresponding difference based on the large-scale pullout test data was 36.9%. At small-scale, the pullout reduction was 46.1%. The shear strength of the soil was reduced 33.7% from OMC-2% to OMC+2%.

Differences in the nature of the interaction between the soil and the reinforcement (including the extensibility of the reinforcement) between the interface and pullout tests in addition to factors such as perceivably greater boundary effects, and greater sensitivity to the soil placement and accuracy of measuring the soil density and moisture content in the small-scale interface tests can explain the difference between the LS-PT and IST results in **Figure 77**. Nevertheless, these data shown in the figure consistently indicate that the reinforcement pullout capacity (or equivalently, the soil-reinforcement interface strength) could significantly decrease as a result of an increase in the moisture content of the SRW marginal backfill. These data quantify the expected variation in the soil-reinforcement interface strength for the case of a geotextile reinforcement material and a limiting NCMA marginal soil.

It should be noted that the behavior of a marginal soil which is initially placed and compacted at OMC-2% (with a flocculated structure) and is wetted to OMC+2% is different from the same marginal soil placed and compacted at OMC+2% (with a dispersed structure) (Fredlund et al. 1998). Consequently, the values of $\mu(\omega)$ for the latter case are expected to be somewhat different from those given in **Figure 77**. Nevertheless, the broader conclusions of the study and their implications to the design of MSE walls with marginal soils are believed to remain valid.

Hatami et al. (2010, 2011a,b) developed pullout moisture reduction factors for two marginal soils, i.e. Minco silt and Chickasha clay, based on large-scale pullout tests. These factors were reported as the expressions given in **Equation** 9 and **Equation 10**, for the Minco silt and Chickasha clay, respectively. **Equation 11** represents the MRF for the OUM-NCMA marginal soil. The greater the slope of the MRF, the higher the influence of moisture change on the pullout capacity of the geotextile. The intercept value depends on the soil type and its optimum moisture content. According to these results, the magnitude of reduction in the reinforcement pullout capacity in the OUM-NCMA soil as a result of wetting over the range between OMC-2% and OMC+2% is comparable to that in the Chickasha soil.

$$\mu(\omega) = -0.0395\omega + 1.4311 \quad \text{Minco silt} \quad [9]$$

$$\mu(\omega) = -0.0862\omega + 2.36 \quad \text{Chickasha Clay} \quad [10]$$

$$\mu(\omega) = -0.086\omega + 1.8864 \quad \text{OUM-NCMA} \quad [11]$$

6.2 Pullout Capacity for Design

6.2.1 Incorporation of a MRF in the FHWA Pullout Equation

Figure 78 shows the design pullout failure envelopes, which were calculated using the modified FHWA equation. The moisture reduction factor (MRF) determined in this study was introduced in the FHWA pullout equation to account for the loss of matric suction on the OUM-NCMA marginal soil as presented in **Equation 12**. The pullout envelopes at OMC and OMC+2% were calculated by applying the corresponding MRF values to the OMC-2% pullout data. These results are in close agreement with the experimental data as shown in **Figure 79**. Hatami et al. (2010) found similar results using the same type of reinforcement tested in Minco Silt.

$$P_r = F^* \alpha \, \sigma'_v \, L_e \, C \, \mu(\omega) \qquad [12]$$

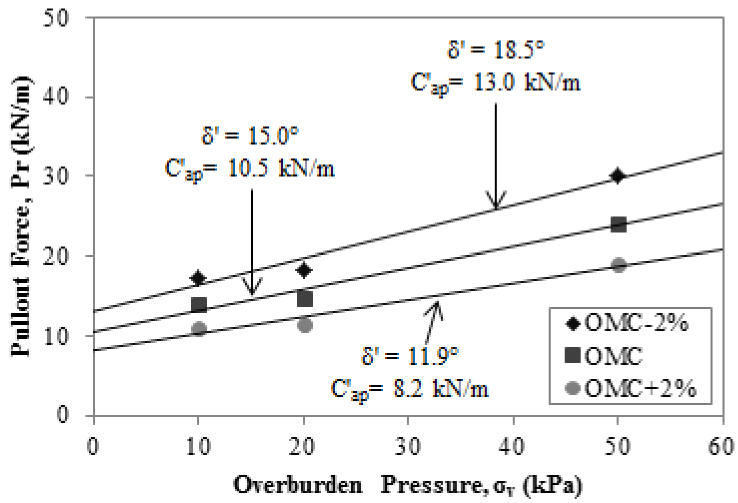

Figure 78. Pullout failure envelopes calculated using the modified pullout equation

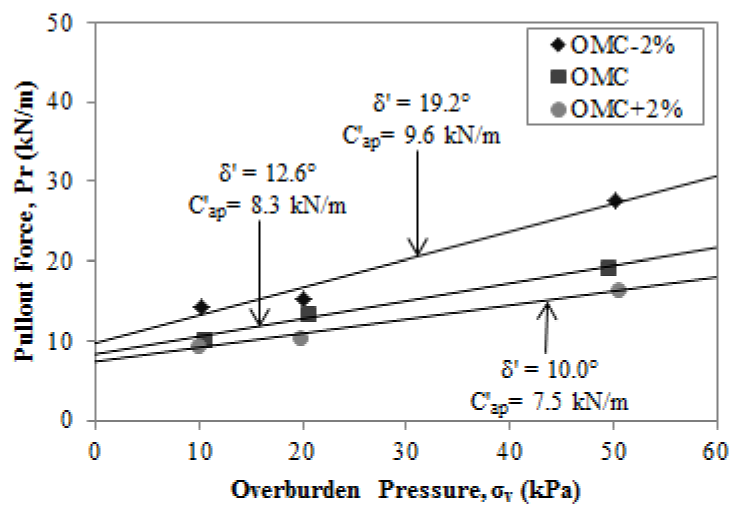

Figure 79. Large-scale experimental pullout results in the front plane

The pullout resistance factor (F*) in **Equation 12** can be estimated from Interface Shear Tests (IST) as *tan*(δ'_{peak}) or from Direct Shear Tests (DST) as *tan*(2/3ϕ'). The scale correction factor (α) may be assumed as 0.6 for geotextiles (Berg et. al 2009). However, it should be noted that the actual distribution of shear stresses along the length of the geotextile specimen is not well represented by the IST. Furthermore, a scale correction factor (α) of 0.6 may not be adequate for all types of soil-geotextile interfaces. This study shows that both F* and α factors are functions of the soil moisture content and overburden pressure which could be accounted for explicitly using the MRF from laboratory tests similar to the methodology presented in this study. The mean scale correction factor (α) was calculated as 0.64 with a standard deviation (S) of 0.05 and a Coefficient of Variation of 8%. The pullout resistance factor (F*) varied from 0.54 to 2.24 and it was found to be greater at lower suction values and lower overburden pressures.

6.2.2 Effective Stress in Unsaturated Soils

It is important to note that **Equation 12** shows the pullout capacity for design as a function of the effective vertical stress. Bishop (1959) proposed the following expression to represent the effective stress in unsaturated soils:

$$\sigma' = (\sigma - u_a) + \chi(u_a - u_w) \qquad [13]$$

Where,

σ' = effective stress

σ = total stress

u_a = pore-air pressure

χ = a parameter related to the degree of saturation of the soil (0 for dry conditions and 1 for saturated conditions)

In this expression, the term (u_a-u_w) corresponds to the matric suction. The pore-air pressure (u_a) is assumed to be in equilibrium with the atmospheric pressure (i.e. zero gauge pressure). The effective stress on the interface can be calculated using **Equation 13** if suction values are known.

Although the χ parameter depends on soil type (Bishop and Henkel 1962), for simplicity it can be assumed to be similar to the degree of saturation of the soil. The degree of saturation of the OUM-NCMA soil was calculated as 64%, 76% and 89% for moisture contents at OMC-2%, OMC and OMC+2%, respectively. These values were calculated assuming that the range of overburden pressures (i.e. 10 kPa to 50 kPa) has a minimum impact on the soil void ratio among all test cases. However, the void ratio is a function of both overburden pressure and matric suction (Fredlund and Rahardjo 1993).

Table 23 shows the experimental pullout tests results (i.e. $P_{r\text{-}EXP}$) as compared to those obtained using the pullout capacity equation for design (**Equation** 4) for both total and effective stress (i.e. $P_{r\text{-}D1}$ and $P_{r\text{-}D2}$). The factor F* was calculated for the total vertical stress as the slope of the P_r – σ_v*L_p curve at pullout (**Figure 6**). The second pullout resistance factor ($F^*_{(2)}$) was recalculated for the effective vertical stress on the soil-geotextile interface (i.e. P_r – σ'_v*L_p curve). The scale correction factor (α) remained constant because it only depends on the deformation of the reinforcement.

Table 23. Comparison between experimental and design pullout capacity results

	Total Stress	Matric Suction	Effective Stress	Peak Pullout	$P_r = F^*\alpha\ \sigma_v L_e C$			$P_r = F^*\alpha\ \sigma'_v L_e C$		
ω (%)	**σ_v** (kPa)	**$(u_a\text{-}u_w)$** (kPa)	**σ'_v** (kPa)	**$P_{r\text{-}EXP}$** (kN/m)	**F***	**α**	**$P_{r\text{-}D1}$** (kN/m)	**$F^*_{(2)}$**	**α**	**$P_{r\text{-}D2}$** (kN/m)
10.6	10.3	34.0	32.2	14.2	2.26	0.63	17.9	0.72	0.63	17.8
	20.1	27.0	37.5	15.4	1.26	0.60	18.5	0.67	0.60	18.4
	50.3	33.1	71.6	27.5	0.9	0.55	30.4	0.63	0.55	30.2
12.6	10.4	10.2	18.2	10.3	1.62	0.64	13.2	0.92	0.64	13.1
	20.4	8.7	27.1	13.4	1.07	0.64	17.1	0.81	0.64	17.1
	49.4	6.9	54.7	19.3	0.64	0.61	23.5	0.58	0.61	23.6
14.6	9.8	3.6	13.0	9.5	1.59	0.65	12.4	1.20	0.65	12.4
	19.6	2.8	22.1	10.5	0.88	0.72	15.2	0.77	0.72	15.0
	50.4	3.1	53.1	16.5	0.54	0.71	23.5	0.51	0.71	23.4

$F^*_{(2)}$: Calculated using **Equation 13** with $\chi \approx S$ (degree of saturation)

Results in **Table 23** indicate that pullout values for design remain constant if either total or effective stress is used because the product of $F^*\sigma'_v$ is equal to the product of $F^*\sigma_v$ if F* is calculated at pullout as indicated in **Figure 6**. **Figure 80** shows the envelope for the pullout capacity for design when effective vertical stress is used. This figure confirms the important relationship between the pullout capacity of the reinforcement and the moisture content of the backfill. The moisture reduction factor accounts for the loss of matric suction as the moisture content increases.

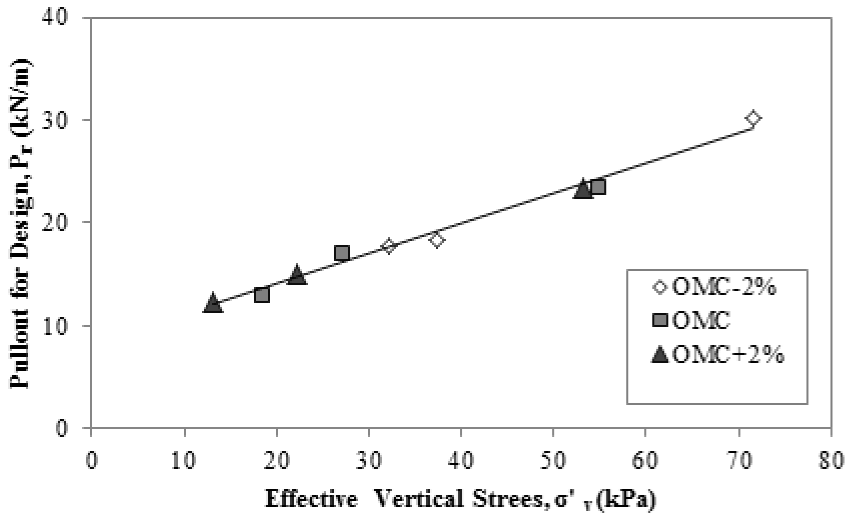

Figure 80. Large-scale pullout results for design as function of the effective vertical stress

7. NUMERICAL MODEL

7.1 Pullout Model in FLAC

The finite difference method (FDM)-based computer program Fast Lagrangian Analysis of Continua (FLAC, Itasca 2011) was used to develop the numerical model. FLAC is a two-dimensional explicit finite difference program for engineering mechanics computation. The program can be used to simulate the response of soil structures to various static and dynamic loading conditions including their yielding and collapse behavior. Dr. Peter Cundall initially developed FLAC in 1986 for to solve a wide range of complex problems in mechanics with an emphasis on the geotechnical and mining engineering applications (Itasca 2011).

One of the first reinforcement strip models was developed by Itasca Consulting Group, Inc. in collaboration with Terre Armée/Reinforced Earth Company, Soiltech R&D Division, Nozay, France. This model which was originally developed to represent the behavior of the Terre Armée reinforcement strips was used in this study as a starting point. The model was modified accordingly to represent the behavior of the soil-geotextile interface in the OUM-NCMA marginal soil.

In the FLAC model in this study, a strip of geotextile is embedded in the soil and confined under a given magnitude of vertical stress. The specimen is pulled at its front node out of a box (which is modeled using a continuum finite difference grid) at a constant displacement rate. Dimensions, properties and loading conditions of the interacting materials are defined by the user. In this study, the soil, geotextile and their interface properties were obtained from laboratory test data. The pullout force is monitored and plotted versus the horizontal displacement of the geotextile at selected nodes.

FLAC provides the user with a wide range of constitutive models and programming tools to design new models for different applications. The elastic model was used in the present study. **Figure 81** shows a screenshot of the pullout box modeled with FLAC. The geotextile reinforcement is placed in the middle of the gap without any contact with the sleeves.

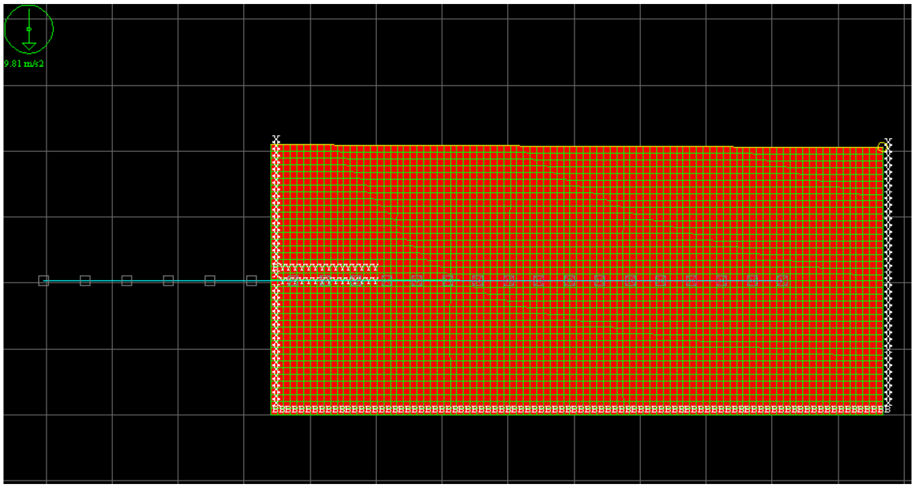

Figure 81. Screenshot of the pullout box model

7.2 Strength Properties of the OUM-NCMA Soil

7.2.1 CIUC Triaxial Test Results

Figure 82 shows the total deviator stresses as a function of the vertical strain for each initial confining stress. **Figure 83** shows the Total Stress Paths (TSP), Total Stress Paths minus Pore Pressure (TSP – Ub) and Effective Stress Paths (EST) for the three confining pressures in the *p* – *q* diagram (*p* – *q* diagrams represent the state of stress at a point with respect to the principal stresses).

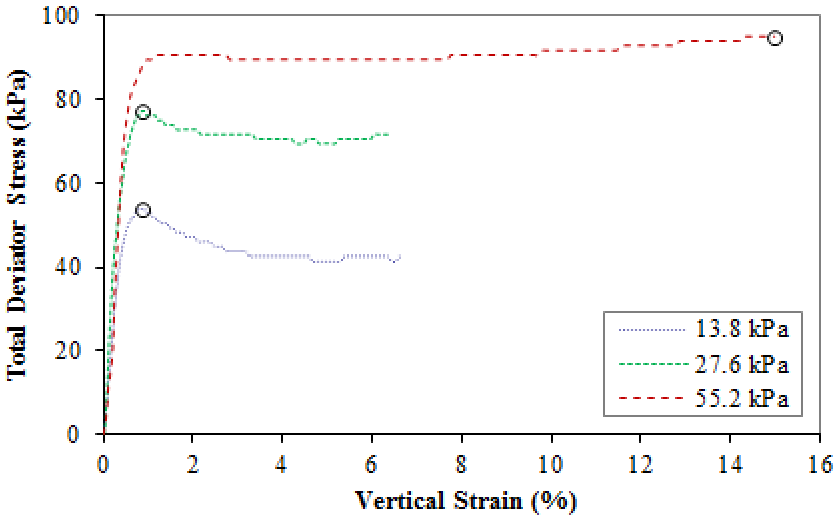

Figure 82. Total stress-strain curves obtained from CIUC triaxial tests

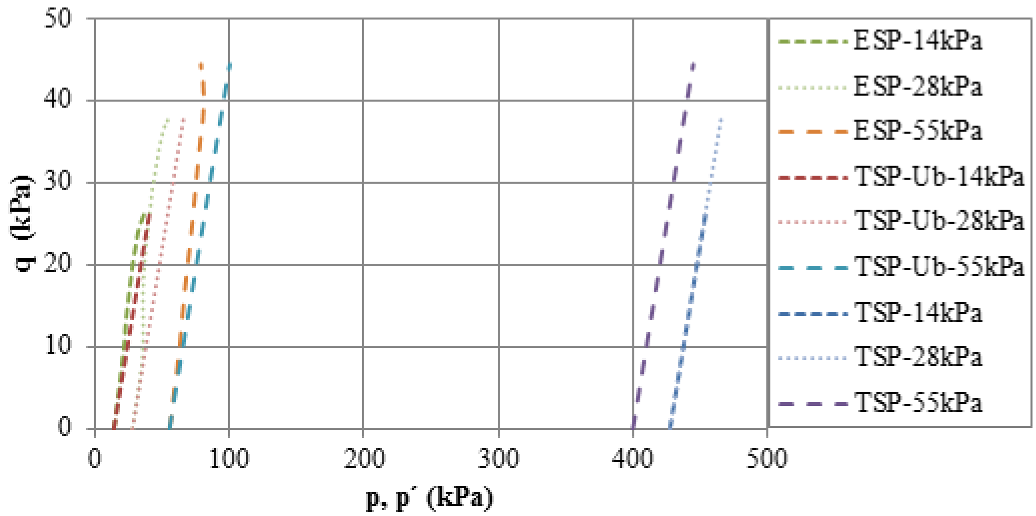

Figure 83. Total and Effective Stress Paths in the p' – q diagram

Figure 84 shows in further detail the Effective Stress Paths (ESP) for each confining stress, i.e. ≈ 7 kPa, 14 kPa and 55 kPa. The best fit envelope represents **Equation 14**, which is used to calculate the effective friction angle and cohesion of the soil as described in **Equation 15** and **Equation 16**.

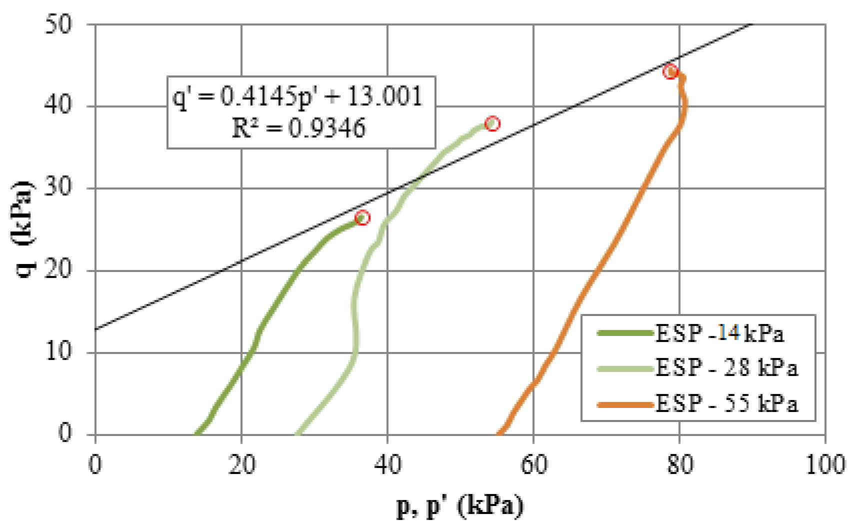

Figure 84. Effective stress paths (ESP) in p' - q diagram

$$q' = p' \tan \alpha + m \qquad [14]$$

$$\phi' = \sin^{-1}(\tan \alpha) \qquad [15]$$

$$c' = \frac{m}{\cos\phi'} \qquad [16]$$

Table 24 summarizes the strength properties of the OUM-NCMA marginal soil from CIUC tests. The undrained elastic modulus (E_u) is given as a function of the confining pressure (σ_o). Effective friction angle (ϕ') and cohesion (C') are also presented.

Table 24. Soil strength parameters obtained from CIUC tests

σ_o (kPa)	**14**	**28**	**55**
E_u (MPa)	5.68	7.46	9.45
ϕ´ (°)		24.5	
C´ (kPa)		14.3	

7.2.2 Unsaturated Triaxial Test Results

Figure 85 and **Figure 86** show the stress – strain curves for different confining pressure values at OMC-2% and OMC. In absence of a peak shear strength value, the maximum shear was determined as 15% axial strain as recommended in the ASTM D4767 test protocol (ASMT 2011). The Young's modulus of the soil was calculated as the maximum tangent value of each curve. **Figure 87** and **Figure 88** show the Mohr-Coulomb envelope for the OUM-NCMA marginal soil at OMC-2% and OMC, respectively. As compared to direct shear test results, the soil shear strength decreased as the soil was compacted at higher moisture contents.

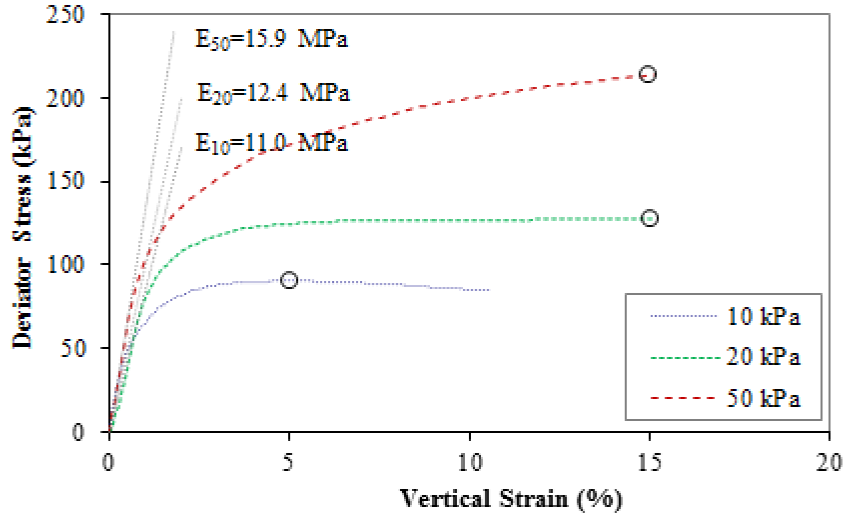

Figure 85. Stress-strain curves obtained from unsaturated triaxial tests at OMC-2%

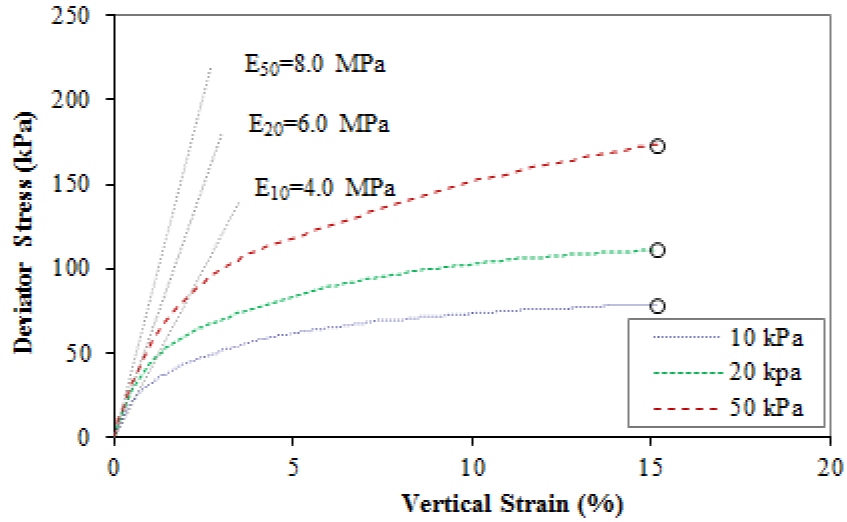

Figure 86. Stress-strain curves obtained from unsaturated triaxial tests at OMC

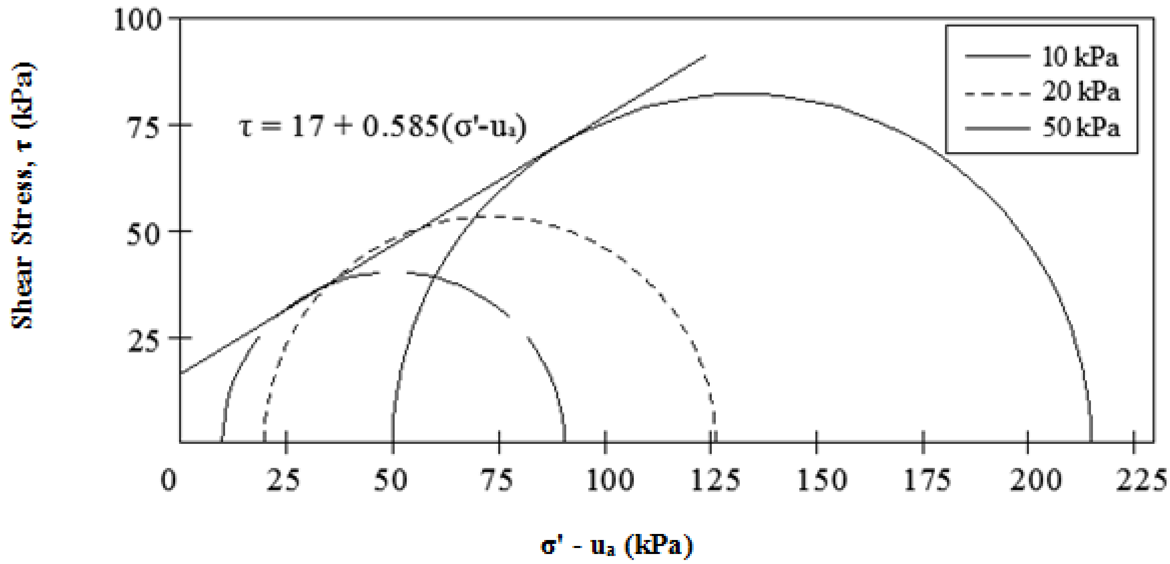

Figure 87. Mohr-Coulomb envelope for the OUM-NCMA soil from triaxial tests at OMC-2%

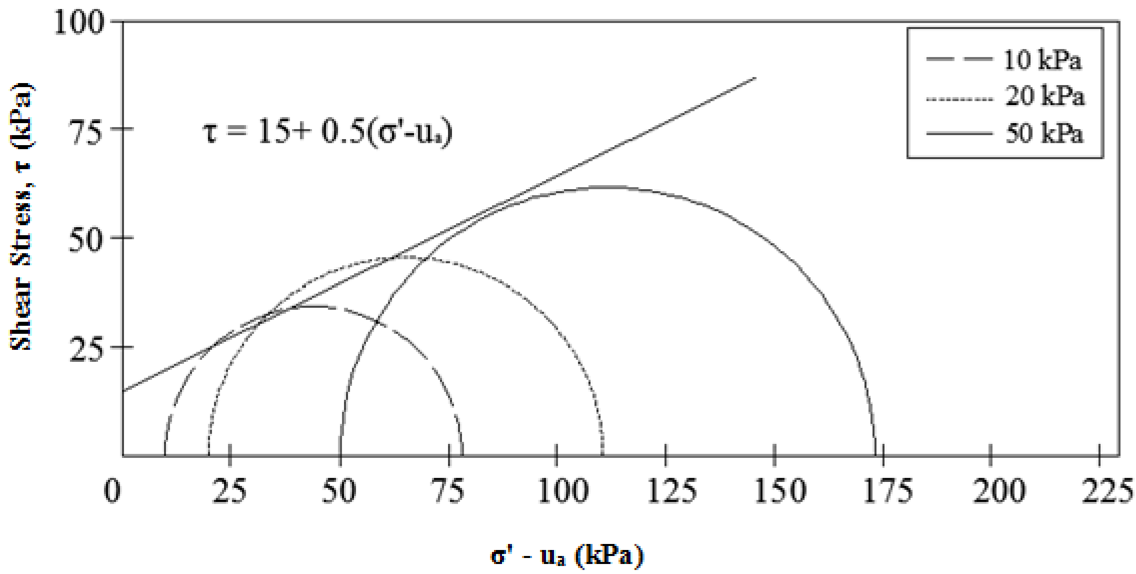

Figure 88. Mohr-Coulomb envelope for the OUM-NCMA soil from triaxial tests at OMC

7.3 Pullout Model

The input properties for the FLAC model included the soil unit weight and elastic properties (i.e. bulk modulus, shear modulus). Soil strength properties such as friction angle and cohesion were also included. A Poisson's ratio of 0.35 was considered appropriate for this soil type and is commonly used for illustrative purposes (Fredlund et al. 1993). Additionally, geotextile reinforcement properties, overburden pressure and interface strength properties were needed to run the model. **Table 25** and **Table 26** summarize the most important properties used in FLAC for OMC-2% and OMC. The properties of the Mirafi HP 370 geotextile were obtained from an earlier study (Hatami et al. 2010). The interface shear stiffness (k) was calculated based on large-scale pullout test results.

Table 25. Summary of model properties used in FLAC simulations for OMC-2%

Parameters	**Overburden Pressure, σ_v (kPa)**		
	10	**20**	**50**
Dry Unit Weight (kN/m^3)	17.8	17.8	17.8
Bulk Unit Weight (kN/m^3)	19.7	19.7	19.7
Poisson's ratio, v	0.35	0.35	0.35
Young's Modulus, E_{tan} (MPa)	11.03	12.41	15.87
Bulk Modulus, K (MPa)	12.26	13.79	17.63
Shear Modulus, G (MPa)	4.09	4.6	5.88
Soil friction angle, φ (°)	30.5	30.5	30.5
Cohesion, C (kPa)	17.7	17.7	17.7
Young's Modulus of Geotextile, E (kPa)	396	396	396
Strip yield or Sbond of Geotextile, (s) kN/m	47.3	47.3	47.3
Interface Shear Stiffness, K_{bond} (k) kN/m^3	447.3	504.6	513.6
FLAC Model Type (soil)	Linear Elastic-Plastic (Mohr-Coulomb)		

Table 26. Summary of model properties used in FLAC simulations for OMC

Parameters	**Overburden Pressure, σ_v (kPa)**		
	10	**20**	**50**
Dry Unit Weight (kN/m^3)	17.8	17.8	17.8
Bulk Unit Weight (kN/m^3)	20.0	20.0	20.0
Poisson's ratio, v	0.35	0.35	0.35
Young's Modulus, E_{tan} (MPa)	5.0	6.0	8.0
Bulk Modulus, K (MPa)	5.56	6.67	4.7
Shear Modulus, G (MPa)	1.85	2.22	2.96
Soil friction angle, φ (°)	26.6	26.6	26.6
Cohesion, C (kPa)	15.0	15.0	15.0
Young's Modulus of Geotextile, E (kPa)	396	396	396
Strip yield or Sbond of Geotextile, (s) kN/m	47.3	47.3	47.3
Interface Shear Stiffness, K_{bond} (k) kN/m^3	422.0	447.6	526.8
FLAC Model Type (soil)	Linear Elastic-Plastic (Mohr-Coulomb)		

For saturated conditions (i.e. ≈ OMC+4%, CIUC tests), elastic parameters corresponded to undrained values. In this case, the soil Poisson's ratio approaches 0.5 for undrained conditions because there is no volumetric change during the test. This makes the calculation of the bulk modulus (K) meaningless because it would become an infinitely large value. The pullout model developed in this study only included the OMC-2% and OMC testing conditions.

Figure 89 through **Figure 91** show a comparison of the predicted and measured large-scale pullout test results using the soil properties obtained at OMC-2% for 10 kPa, 20 kPa and 50 kPa overburden pressure.

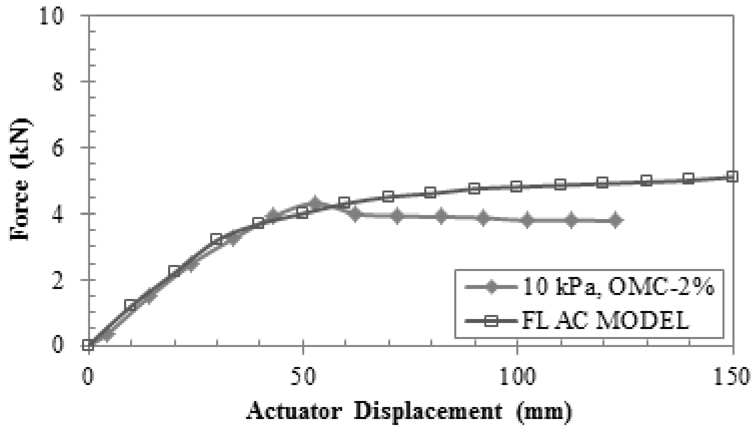

Figure 89. Experimental results vs. FLAC model at OMC-2% and 10 kPa

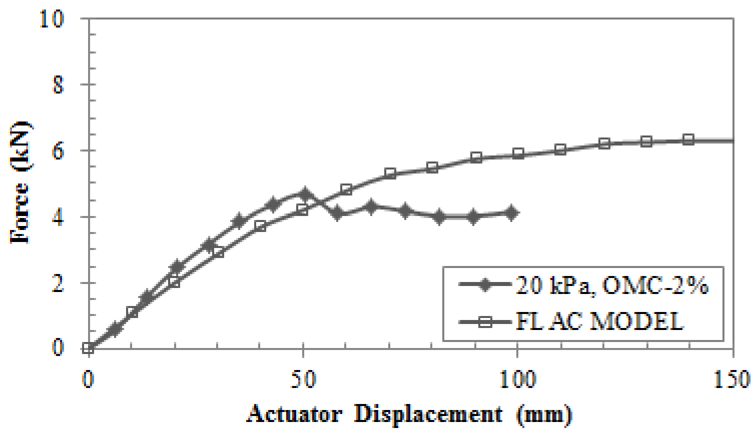

Figure 90. Experimental results vs. FLAC model at OMC-2% and 20 kPa

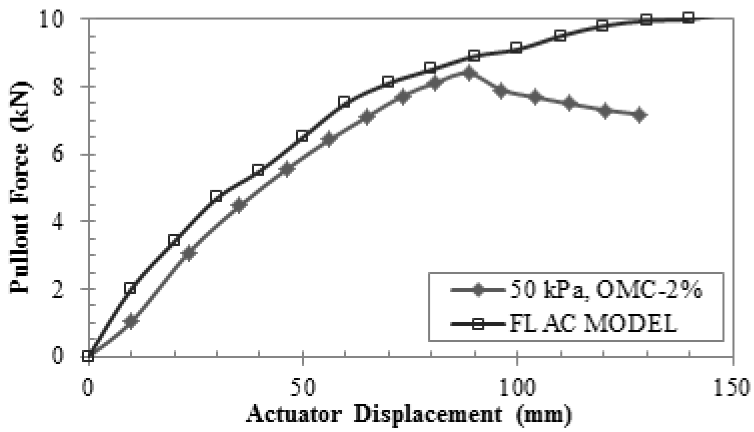

Figure 91. Experimental results vs. FLAC model at OMC-2% and 50 kPa

Figure 92 through **Figure 94** show a comparison of the predicted and measured pullout results at OMC. The FLAC predictions show a fairly satisfactory agreement with the measured data for the model response prior to the peak value. However, it fails to capture the post-peak strain-softening response observed in the measured data.

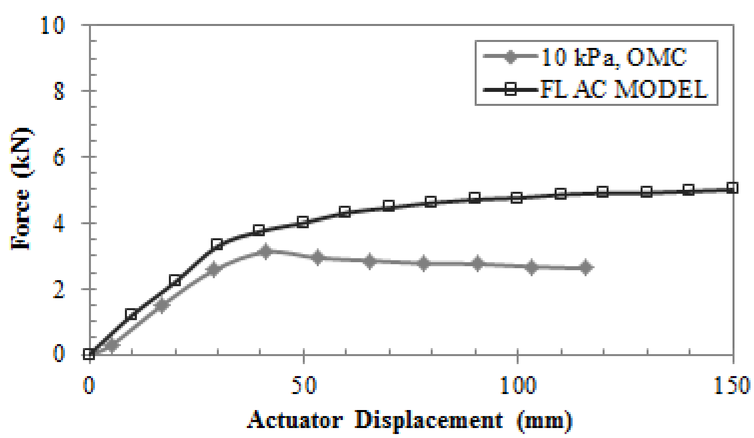

Figure 92. Experimental results vs. FLAC model at OMC and 10 kPa

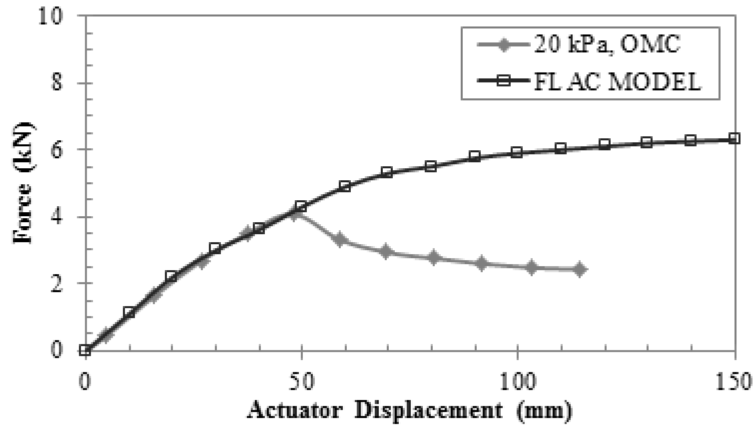

Figure 93. Experimental results vs. FLAC model at OMC and 20 kPa

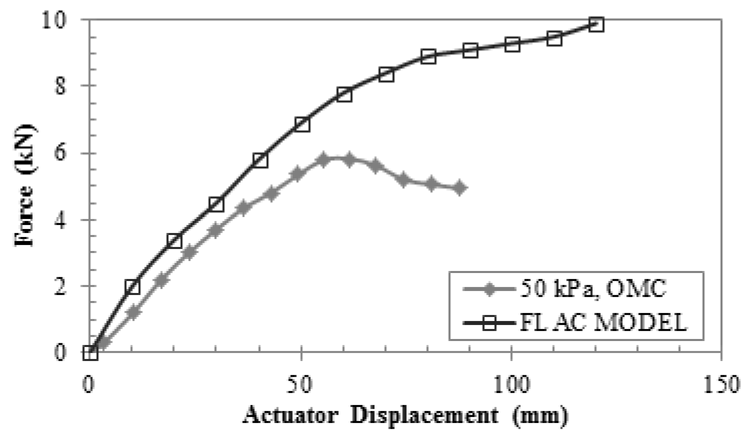

Figure 94. Experimental results vs. FLAC model at OMC and 50 kPa

Even though the soil properties from the unsaturated triaxial tests overall led to satisfactory results, it is worth nothing that these tests are not suction controlled. Garcia (2010) and Hatami et al. (2010) developed a model with satisfactory results for different soil moisture contents after running similar unsaturated triaxial tests on Minco silt samples.

In general, the predicted results were in close agreement with the experimental data. Except the case of OMC and 50 kPa overburden pressure, which notably over-predicted the pullout capacity of the geotextile (especially post-peak), the model predicted the pullout response of the reinforcement at small displacements fairly well. Pre-peak reinforcement load and displacements are more representative of the structural response under service conditions and therefore are more important in the design and satisfactory performance of the structure than post-failure values. During the above simulation exercise it was found that it is important to determine the soil elastic properties with the greatest accuracy possible. The predicted data is expected to improve by including the soil dilation angle and the use of the strain softening model in FLAC.

This pullout model was developed as a preliminary attempt to compare the predicted response of the geotextile and the experimental data. While a fairly satisfactory agreement was found between the predicted and measured pullout response prior peak values, a more advanced model would be required to better simulate the soil, geotextile and their interface response. The stress-softening of the interface could be represented using a model could better predict its peak and post-peak behavior as a function of the shear strain.

This page is intentionally blank

8. CONCLUSIONS

A. A marginal quality soil was produced by blending a natural Oklahoma soil and commercially available sand to meet the limiting requirements of the NCMA (2002) for the backfill of MSE walls with respect to fines content, plasticity and gradation. The blended soil was called the OUM-NCMA marginal soil throughout this study. Its PI was calculated as 20 and the soil passing No. 40 and No. 200 sieves was 49% and 33%, respectively.

B. A series of large-scale pullout tests were carried out to measure the pullout resistance of a woven geotextile in the OUM-NCMA marginal soil over a range of moisture contents from dry (OMC-2%) to wet (OMC+2%) side of the soil Optimum Moisture Content (OMC). Overburden pressures varied from 10 kPa to 20 kPa and 50 kPa. In addition, this study included a multi-scale testing program in which Interface Shear Tests (IST), Small-scale Pullout Tests (SSPT) and Direct Shear Tests (DST) were performed on the soil and soil-geotextile reinforcement over the same range of moisture contents and overburden pressures to determine the influence of the soil moisture content increase and the loss of matric suction on the shear strength of the soil/interface.

C. The Soil Water Characteristic Curve (SWCC) was determined using several methods including the use of tensiometers in the pullout tests and in small-scale (76-mm-diameter and 48-mm-thick) cylindrical soil samples, pressure transducer tensiometers (PTT) in Proctor mold-size soil samples and a Pressure Plate Extractor (PPE) device. It was found that the PTT readings in both large-scale pullout and small-scale suction tests were in close agreement with the mean suction values measured with the 2100F probes. However, measured suction values from both the 2100F and PTT devices in small-scale tests were greater than the corresponding values in large-scale tests. This was attributed to differences in instrumentation, sample preparation and application of overburden pressure between the two series of tests at different scales.

D. Suction values as measured from large-scale pullout tests using the 2100F tensiometers varied from mean values of 3.2 kPa at OMC+2% to 31.4 kPa at OMC-2%. Suction as measured from small-scale pullout tests using the PPE varied from 0 at saturation (≈ OMC+4%) to approximately 250 kPa at 9.6% (OMC-3%).

E. The test data from the pullout and interface shear tests were used to calculate Moisture Reduction Factors (MRF) to account for the reduction in the soil-reinforcement interface strength in the SRW marginal backfill due to the loss of matric suction at higher moisture content values.

F. The mean values of reduction in the reinforcement pullout capacity for the soil samples compacted at OMC+2% as compared to those compacted at OMC-2% were approximately 37% and 46%, for both large-scale and small-scale tests, respectively. The same reduction for the interface shear strength and the soil shear strength was calculated as 23% and 32%, respectively. These results, while obtained from soil models with different as-compacted moisture content values, indicate that the loss of reinforcement pullout capacity in MSE structures with marginal backfills (i.e. those which nonetheless, meet the NCMA requirements) could be significant and deserve proper attention in the design of these systems. This reduction of the pullout capacity of the geotextile reinforcement and the shear strength of the soil is attributed to the loss of soil matric suction due to an increase in its moisture content.

G. Strength parameters obtained from IST, DST and Triaxial tests indicated that both interface friction angle and adhesion or soil friction angle and cohesion are function of the matric suction and moisture content. This was mainly attributed to variations on the soil structure as the samples were compacted at different moisture contents.

H. Results of the simulation using FLAC yielded to overall satisfactory results. Small changes were necessary in some test cases to fit the experimental data. This was due to the sensitivity of the model and the quality of the experimental results (i.e. pullout tests, interface shear tests, unsaturated triaxial tests). The pullout response of the geotextile prior to the peak was simulated fairly well. However, the model was not capable to capture the strain-softening responses which were observed during the measure data.

This page is intentionally blank

9. RECOMMENDATIONS FOR FUTURE WORK

A. This study evaluated the soil-reinforcement interface for the soil compacted at three different moisture contents. A new approach may consist of compacting the soil at OMC-2% and increasing the moisture content to the target values prior testing. This approach includes several challenges related to the low permeability of marginal quality soils and the physical components of the pullout box. If this is not feasible for large-scale pullout tests, small-scale tests can be considered as an alternative.

B. Large-scale interface shear tests are recommended to be performed on the OUM-NCMA marginal soil and the woven geotextile interface to validate the preliminary data results presented in this study.

C. The model needs to be revised to account for the strain-softening of the soil and soil-reinforcement interface.

This page is intentionally blank

10. REFERENCES

Abu-Farsakh, A., Coronel, J., and Tao, M. Effect of Soil Moisture Content and Dry Density on Cohesive Soil-Geosynthetic Interactions Using Large Direct Shear Tests. *Journal of Materials in Civil Engineering, ASCE*, Vol. 19, No. 7, 2007, pp 540-549.

Agus, S.S., Schanz, T., and Fredlund, D.G. Measurements of Suction versus Water Content for Bentonite-Sand Mixtures. *Canadian Geotechnical Journal*, Vol. 47, 2010, pp 583-594.

Alobaidi, I.M., Hoare, D.J. and Ghataora, G.S. Load Transfer Mechanism in Pullout Tests. *Geosynthetics International*. Vol. 4, No. 5, 1997, pp 509-521.

American Association of State Highway and Transportation Officials, AASHTO. Guide Specifications for Design and Construction of Segmental Concrete Bridges, Second Edition, Washington, DC, 2003, Link to American Association of State Highway and Transportation Officials (AASHTO) Website.

American Society for Testing and Materials, ASTM International, West Conshohocken, PA, 1998 – 2011, Link to American Society for Testing and Materials (ASTM) Website.

Bathurst, R.J., Hatami, K., Walters, D.L. Taleb, B. and Simac, M.R. Geosynthetic Reinforced Soil Segmental Retaining Walls: A New Thechnology. *Jubilee Volume, 75th Anniversary of K. Terzaghi's "Erdbaumechanick" ("Soil Mechanics"),* Vienna Technical University. Vienna, Austria: 5, 2001, pp 175-204.

Berg, R.R., Christopher, B.R.C., and Samtani, N.C. Design of Mechanically Stabilized Earth Walls and Reinforced Soil Slopes, Volume I and II. FHWA-NHI-10-024, FHWA, U.S. Department of Transportation. Woodbury, MN. 2009.

Bishop, A.W. and Henkel, D.J. The Measurement of Soil Properties in the Triaxial Test. Edward Arnold Publishers Ltd. London, England, 2nd Edition, 1962, 227p.

Budhu, M. Soil Mechanics and Foundations. John Wiley & Sons, Inc. Hoboken, NJ, 1st Edition, 2000, 616p.

Carroll, R.G. and Richardson, G.N. Geosynthetic Reinforced Retaining Walls. In *Proceedings of the Third International Conference on Geotextiles*, Vienna, Austria, Vol. 2, 1986, pp 389-394.

Cerato, A. and Lutenegger, A.J. Specimen Size and Scale Effects of Direct Shear Box Tests of Sands. *Geotechnical Testing Journal, ASTM*, Vol. 29, No. 6, 2006, 10p.

Chandrakaran, S., Subaida, E.A. and Sankar, N. Prediction of Pullout Strength of Woven Coir Geotextiles from Yarn Pullout Resistances. In *Proceedings of the 12th International Association for Computer Methods and Advances in Geomechanics (IACMAG).* Goa, India, October 1-6, 2008, pp 3735-3742.

Christopher, B.R. and Stulgis, R.P. Low Permeable Backfill Soils in Geosynthetic Reinforced Soil Walls: State-of-the-Practice in North America. In *Proceedings of the NAGS / GRI-19 Cooperative Conference*, Las Vegas, NV, December 14–16, 2005, 12p.

Chu, L.M. and Yin, J.H. Comparison of Interface Shear Strength of Soil Nails Measured by Both Direct Shear Box Tests and Pullout Tests. *Journal of Geotechnical and Geoenvironmental Engineering, ASCE.* Vol.131, No. 9, 2005, pp 1097-1107.

City of Norman. Website. Link to City of Norman Website

Das, B.M. Principles of Foundation Engineering. Thompson. Toronto, Canada, 6th Edition, 2007, 750p.

Escario, V. Suction Controlled Penetration and Shear Test. In *Proceedings of 4th International Conference, Expansive Soils*, *ASCE*, Denver, CO, Vol. 2, 1980, pp. 781-797.

Farrag, K. and Morvant, M. Evaluation of Interaction Properties of Geosynthetics in Cohesive Soils: LTRC Reinforced-Soil Test Wall. Publication No. FHWA-LA.03/379. Baton Rouge, LA, 2004, 136p.

Fredlund, D.G., Morgenstern, N.R., and Widger, R.A. The Shear Strength of Unsaturated Soils. *Canadian Geotechnical Journal*, Vol. 14, No. 3, 1978, pp 313-321.

Fredlund, D.G. and Rahardo, H. Soil Mechanics for Unsaturated Soils. John Wiley & Sons, Inc. Hoboken, NJ, 1st Edition, 1993, 517p.

Gan, J.K.M., Fredlund, D.G and Rahardo, H. Determination of the Shear Strength Parameters of an Unsaturated Soils Using the Direct Shear Test. *Canadian Geotechnical Journal*, Vol. 25, 1988, pp 500-510.

Garcia, L.M. Influence of Moisture Content on Pullout Resistance of Geotextiles in Marginal Quality Soils. M.Sc. thesis. CEES, University of Oklahoma, Norman, OK, 2010, 165p.

Goodhue, M., Edil, T., and Benson, C. Interaction of Foundry Sands with Geosynthetics. *Journal of Geotechnical and Geoenvironmental Engineering, ASCE*, Vol. 127, No. 4, 2001, pp 353-362.

Gurpersaud, N., Vanalli, S.K. and Sivathalayan, S. Influence of Suction on the Pullout Capacity of Grouted Nails. In *Proceedings of GeoAlberta Conference 2010.* Calgary, Alberta, Canada, May 10-12, 2010. pp. 1748-1755.

Hatami, K., Garcia, L.M. and Miller, G.A., Influence of Moisture Content on the Pullout Capacity of Geotextile Reinforcement in Marginal Soils. *61st Highway Geology Symposium,* Oklahoma City, OK., August, 2010.

Hatami, K., Garcia, L.M. and Miller G.A. A Moisture Reduction Factor for Pullout Resistance of Geotextile Reinforcement in Marginal Soils. *GeoFrontiers 2011*, Dallas, TX, 2011 (a), Paper #1210.

Hatami, K., Granados, J.E., Esmaili, D. and Miller G.A. Influence of Gravimetric Water Content on Geotextile Reinforcement Pullout Resistance in MSE Walls with Marginal Quality Soils. Paper No. 13-3836, *Transportation Research Board Annual Meeting*, Washington, D.C., 2013. *In press*.

Hatami, K., Esmaili, D. and Miller, G.A. Use of MSE Technology to Stabilized Highway Embankments and Slopes in Oklahoma. Publication No. FHWA-OK-11-04. 2011 (b). 77p.

Ho, D.Y.F and Fredlund, D.G. A Multi-stage Triaxial Test for Unsaturated Soils. *Goetechnical Testing Journal, ASTM,* Vol. 5, No. 1, 1982, pp 18-25.

Holtz, R.D. Geosynthetics for Soil Reinforcement. In *Proceedings of The Ninth Spencer J. Buchanan Lecture*, College Station, TX, November 9, 2001, 19p.

Itasca Consulting Group Inc. Fast Lagrangian Analysis of Continua: FLAC, Version 7.0. Minneapolis, MN, 2011.

Keller, G.R. Experiences with Mechanically Stabilized Structures and Native Soil Backfill. *Transportation Research Record*, Paper No. 1474, 1995, pp 30-38.

Khoury, C.N., Miller G.A., and Hatami, K. Unsaturated Soil-Geotextile Interface Behavior, *Geotextiles and Geomembranes*, Vol. 29, No 1, 2011, pp 17-28.

Koerner, R.M. Designing with Geosynthetics. Prentice Hall, Englewood Cliffs, NJ, 5th Edition, 2005, 816p.

Kramer, S.L. Geotechnical Earthquake Engineering. Prentice-Hall, Upper Saddle River, NY, 1st Edition, 1996, 653p.

Lambe, T.W. The Engineering Behavior of Compacted Clay. *Soil Mechanics Division, ASCE Journal,* Vol.84, SM2, Paper No. 1655, 1958, pp 1-35.

Lambe, T. W. and Whitman, R. V., Soil Mechanics. John Wiley & Sons, Inc. Hoboken, NJ, 1st Edition, 1969, 553p.

Lee H. and Bobet, A. Design of MSE Walls for Fully Saturated Conditions. Publication FHWA/IN/JTRP-2002/13. Joint Transportation Research Program. Indiana Department of Transportation and Purdue University, West Lafayette, IN, 2002, 163p.

Lopes, M.L. and Silvano, R. Soil/Geotextile Interface Behaviour in Direct Shear and Pullout Movements. *Geotechnical Geological Engineering*. Vol. 28, 2010, pp 791-804.

Lu, N. Is Matric Suction a Stress Variable? *Journal of Geotechnical and Geoenvironmental Engineering, ASCE*, Vol. 134, No. 7, 2008, pp 899-905.

Marr, W.A. Selecting Backfill Materials for MSE Retaining Walls. NHCRP 24-22, 2003 to present, RiP, *Transportation Research Board of the National Academics*, Washington, D.C., 2012. Link to Transportation Research Board (TRB)

Martin, J. P., Koerner, R. M., and Whitty, J. E. Experimental Friction Evaluation of Slippage between Geomembranes, Geotextiles and Soils. In *Proceedings of the International Conference on Geomembranes*. June 20-24, 1984, pp 191-196.

Miller, G.A., and Hamid, T.B. Direct Shear Testing of Interfaces in Unsaturated Soil. In *Proceedings of the International Symposium on Advanced Experimental Unsaturated Soil Mechanics*, Trento, Italy, 27–29 June 2005. Edited by A. Tarantino, E. Romero, and Y.J. Cui. Taylor & Francis Group, London, UK, 2005, pp 111–116.

Mitchell J.K., Hooper D.R., and Campanella R.G. Permeability of Compacted Clay. *Foundations Engineering Division, ASCE*, Vol. 91, No 4, 1965, pp 41-65.

National Concrete Masonry Association. Design Manual for Segmental Retaining Walls, 2nd Ed., NCMA, Herndon, VA, 2002, 289p.

Natural Resources Conservation Service (NRCS), United States Department of Agriculture. (USDA). Web Soil Survey (WSS) link

Pradhan, B., Tham, L.G., Yue, Z.Q., Junaideen, S.M. and Lee, C. Soil Nail Pullout Interaction in loose Fill Materials. *International Journal of Geomechanics*. Vol. 6, No. 4, 2006, pp 238-247.

Satija, B.S. Shear Behavior of Partly Saturated Soils. PhD Dissertation, Indian Institute of Technology, Delhi, 1978, 327p.

Sawangsuriya, A., Edil, T.B., and Bosscher, P.J. Modulus-Suction-Moisture Relationship for Compacted Soils. *Canadian Geotechnical Journal*. Vol.45, 2008, pp 973-983.

Soilmoisture Equipment Corp. 2100F Soilmoisture Probe, Operating Instructions. Santa Barbara, CA, 2009.

Sreedeep, S. and Singh, D.N. Critical Review of Methodologies Employed for Soil Suction Measurement. *International Journal of Geomechanics, ASCE*, Vol. 11, No. 2, 2011, pp 99-104.

Teerawattanasuk, C., Bergardo, D. and Kongkitkul, W. Analytical and Numerical Modeling of Pullout Capacity and Interaction between Hexagonal Wire Mesh and Silty Sand Backfill under an In-soil Pullout Test. *Canadian Geotechnical Testing Journal*, Vol. 40, 2003, pp 886-899.

TenCate. Mirafi® HP-Series Woven Polypropylene Geotextiles for Stabilization and Soil Reinforcement Applications. Pendergrass, GA. 2012.

http://www.tencate.com/TenCate/Geosynthetics/documents/HPSeries/TDS_HP370A.pdf. Accessed July 30, 2012

The Reinforced Earth Company, 2012. Link to The Reinforced Earth Company Website

Umwelt-Monitoring-System, UMS. Pressure Transducer Tensiometer, User Manual T4/T4x – T5/T5x. Munchen, Germany, 2009.

U.S. Department of Agriculture, Soil Survey Staff, Natural Resources Conservation Service, Official Soil Series Descriptions. Link to the U.S. Department of Agriculture Website for soil series description

Vanapalli, S.K. and Fredlund, D.G. Comparison of Different Procedures to Predict the Shear Strength of Unsaturated Soils. In *Proceedings of GeoDenver Conference: Advances in Unsaturated Geotechnics.* Denver, CO, August 3-8, 2000, pp 195-209.

Vanapalli, S.K., Fredlund, D.G. and Pufahl, D.E. The Relationship between the Soil-Water Characteristic Curve and the Unsaturated Shear Strength of a Compacted Glacial Till. *Geotechnical Testing Journal, ASCE*, Vol. 19, No. 3, 1996, pp 259-268.

Whitlow, R. Basic Soil Mechanics. Longman Group Limited - John Wiley & Sons, Inc. Hoboken, NJ,. 3rd Ed. 1995, 554p.

Yang, H., Rahardjo, H., Leon, E.C. and Fredlund, D.G. Factors Affecting Drying and Wetting Soil-Water Characteristic Curves of Sandy Soils. *Canadian Geotechnical Journal*. Vol.41, 2004, pp 908-920.

Yang, K.H., Zornberg, J.G. and Bathurst, R.J. Mobilization of Reinforcement Tension within Geosynthetic-Reinforced Soil Structures. In *Proceedings of Earth retention 2010 Conference, Geo-Institute, ASCE*, Bellevue, WA, August 1-4, 2010, pp 494-501.

Yoo, H., Kim, H. and Jeon, H. Evaluation of Pullout and Drainage Properties of Geosynthetic Reinforcements in Weathered Granite Backfill Soils. *Fiber and Polimers*. Vol.8, 2007, pp 635-641.

Zhai, H., Mallick, S.B., Elton, D. and Adanur, S. Performance Evaluation of Nonwoven Geotextile in Soil-Fabric Interaction. *Textile Research Journal*. Vol.66, No. 4, 1996, pp 269-276.

Zollinger, D., Lee, S., Puccinelli, J., and Jackson, N. Long Term Pavement Performance Computed Parameter: Moisture Content. Publication No. FHWA-HRT-08-035. Springfield, VA, 2008, 104p.

Zornberg, J.G. and Kang, Y. Pullout of Geosynthetic Reinforcement with In-Plane Drainage Capability. In *Proceedings of Geo-Frontiers Conference, ASCE,* Austin, TX, January 24-26, 2005, 6p.